WestminsterResearch

http://www.westminster.ac.uk/westminsterresearch

Exosomes and miRNAs in disease pathogenesis and opportunities for molecular targeting

Momen Heravi, F.

This is an electronic version of a PhD thesis awarded by the University of Westminster. © Dr Fatemeh Momen Heravi, 2016.

EXOSOMES AND MIRNAS IN DISEASE PATHOGENESIS AND OPPORTUNITIES FOR MOLECULAR TARGETING

FATEMEH MOMEN HERAVI

A thesis submitted in partial fulfillment of the requirements of the University of Westminster for the degree of Doctor of Philosophy

October 2016

Abstract

Exosomes/extracellular vesicles (EVs) are cell-derived mixed-populations of vesicles released by almost all cells into the intercellular microenvironment, ending up in the circulation. Exosomes contain proteins, RNAs and lipid molecules reflecting the status of the parental cell at the time of release, making them promising candidates for biomarker discovery. The contents of exosomes are protected by a lipid bilayer, leading to better stability of bio-macromolecules. Recent evidence suggests a novel role for exosomes as conveyors of information among cells and across tissues, through horizontal transfer of proteins, lipids, and nucleic acids. Exosomes have been the subject of numerous research in recent years; however, their roles still have to be identified in the pathogenesis of different diseases.

MicroRNAs (miRNAs) are small (18-25 nucleotide long) non-coding RNAs which play pivotal roles in the gene expression process and it is estimated that about one third of the human genome is controlled by miRNAs. miRNA regulatory processes have been found to influence many essential biological pathways, such as cellular development, proliferation, apoptosis, and cellular signaling. A great proportion of miRNAs has been reported to be associated with the exosome function of different biofluids.

The aim of this research was to elucidate the role of exosomes/EVs as well as miRNAs in the pathogenesis of different diseases, including alcoholic liver disease, hepatitis C, and cancer. This knowledge may lead to the development of novel molecular diagnostic approaches, as well as innovative drug delivery modalities for small RNA-targeted therapy. My research resulted in a) the establishment of new methods and approaches to the study of exosomes/EVs, as well as comparative literature on the efficacy of several isolation and characterization techniques. b) identification of the role of exosomes and miRNA-122 in the cross talk between hepatocytes and immune cells in alcoholic liver disease c) identification of the role of exosomes in HCV pathogenesis, including the potential of molecular therapies based on miRNA and exosome targeting *in vitro* and *in vivo* d) understanding the bio-distribution of exosomes and miRNA in an *in vivo* murine model and f) exploring the utility of miRNA and exosomes in biofluids in cancer biomarker discovery.

Contents

CONTENTS

CONTENTS

List of figures

List of tables

List of boxes

Publications submitted for the PhD

1. **Exosomes derived from alcohol-treated hepatocytes horizontally transfer liver specific miRNA-122 and sensitize monocytes to LPS**
    Momen-Heravi F.; Bala S.; Kodys K.; Szabo G. *Sci. Rep.* **2015**, *5*, 9991

2. **Biodistribution and function of extracellular miRNA-155 in mice**
    Bala, S.; Csak, T.; Momen-Heravi, F.; Lippai, D.; Kodys, K.; Catalano, D.; Satishchandran, A.; Ambros, V. *Sci. Rep.* **2015**, *5*, 10721

3. **Exosomes from hepatitis C infected patients transmit HCV infection and contain replication competent viral RNA in complex with Ago2-miR122-HSP90**
    Bukong, T.N.;* Momen-Heravi, F.;* Kodys, K.; Bala, S.; Szabo, G. *PLOS Pathogens*, **2014**, *10*, e1004424. [*equal contribution]

4. **Exosome-mediated delivery of functionally active miRNA-155 inhibitor to macrophages**
    Momen-Heravi, F.; Bala, S.; Bukong, T.; Szabo, G. *Nanomedicine*, **2014**, *10*, 1517-1527

5. **Genome-wide Study of Salivary microRNAs for Detection of Oral Cancer**
    Momen-Heravi, F.; Trachtenberg, A.J.; Kuo, W.P.; Cheng, Y.L. *J. Dent. Res.* **2014**, *93*, 86S-93S

6. **Emerging technologies in extracellular vesicle-based molecular diagnostics**
    Jia, S.; Zocco, D.; Samuels, M.L.; Chou, M.F.; Chammas, R.; Skog, J.; Zarovni, N.; Momen-Heravi, F.; Kuo, W.P. *Expert Rev. Mol. Diagn.* **2014**, *14*, 307-321

7. **Detection Of Human c-Myc and EGFR Amplifications in Circulating Extracellular Vesicles in Mouse Tumour Models**

Balaj, L;* Momen-Heravi,F.;* Chen, W.; Sivaraman, S.; Zhang, X.; Ludwig, N.; Meese, E.; Wurdinger, T.; Noske, D.; Charest, A.; Hochberg, F.H.; Vandertop, P.; Skog, J.; Kuo, W.P. *J. Circ. Biomark.* **2014**, doi:10.5772/59174 [*equal contribution]

8. **Current methods for the isolation of extracellular vesicles**

Momen-Heravi, F.; Balaj, L.; Alian, S.; Mantel, P.Y.; Halleck, A.E.; Trachtenberg, A.J.; Soria, C.E.; Oquin, S.; Bonebreak, C.M.; Saracoglu, E.; Skog, J.; Kuo, W.P. *Biol. Chem.* **2013**, *394*, 1253-1262

9. **Impact of biofluid viscosity on size and sedimentation efficiency of the isolated microvesicles**

Momen-Heravi, F.; Balaj, L.; Alian, S.; Trachtenberg, A.J.; Hochberg, F.H.; Skog, J.; Kuo, W.P. *Front. Physiol.* **2012**, *3*, 162

10. **Alternative methods for characterization of extracellular vesicles**

Momen-Heravi, F.; Balaj, L.; Alian, S.; Tigges, J.; Toxavidis, V.; Ericsson, M.; Distel R.J.; Ivanov, A.R.; Skog, J.; Kuo, W.P. *Front. Physiol.* **2012**, *3*, 354

Acknowledgements

First and foremost, I would like to thank my advisors Sterghios Moschos and Stephen Getting. It has been an honor to be their PhD student. Sterghios has taught me, both consciously and unconsciously, how details in molecular biology can be crucial. Stephen, by his knowledge and demeanor, was a good example of a devoted teacher and scientist for me.

I would like to thank Gyongyi Szabo, who mentored me in my scientific adventure and contributed her times, ideas and funding to make my scientific experience meaningful and stimulating. I am also thankful for the excellent example that she provided me as a successful woman professor. I also thank Shashi Bala, with whom I shared excitement and joy of science in a frequent basis. She was an example of a friend for all seasons for me. All my co-authors deserve to be acknowledged as well, especially Banishree Saha and Terence Bukong, as their joy and enthusiasm for research was contagious and working with them was very joyful and stimulating for me. I am grateful to our group's lab manager Karen Kodys, who was always ready to help. All of the other group members at UMass medical School have been a source of friendships as well as good advice and collaboration.

I would like to thank Winston Kuo and Alexander Trachtenberg from Harvard Catalyst, and William Luscinskas from Harvard Medical School, who contributed to my joyful time and meaningful experience at Harvard medical school. I would also like to thank Leonora Balaj for the pleasant collaboration and times at Massachusetts General Hospital and in Charlestown. I would like to acknowledge Lisa Cheng from Texas A&M and Curtis Deutsch from UMASS Medical School. I enjoyed every moment of working with them. The members of Harvard Medical School and Harvard School of Public health have contributed immensely to my personal and professional time at Harvard. Lastly, I would like to thank my family for all their tremendous support and encouragement that helped me to enable my various selves and enabled me to pursue my dreams. Thank you!

Author's declaration

I declare that all the material contained in this thesis is my own work.

List of abbreviations

α-SMA	Alpha-smooth muscle actin
AAV	Adeno-associated viruses
AAV8	Adeno-associated virus serotype 8
AAV8-hFIX	AAV8 vector expressing human factor IX hFIX
ADA	Adenosine deaminase
ADA-SCID	Severe combined immunodeficiency due to adenosine deaminase deficiency
Ago2	Argonaute 2
ALIX	ALG-2-interacting protein X
ALP	Alkaline phosphatase
ALT	Alanine aminotransferase
APOB	Apolipoprotein B
APOE	Apolipoprotein E
ARRDC1	Arrestin domain-containing protein 1
AST	Aspartate aminotransferase
AUC	Area under curve
BAFA1	Bafilomycin A1
CA19-9	Cancer antigen 19-9
CAF	Cancer-associated fibroblasts
cDNA	Complementary DNA
CEA	Carcinoembryonic antigen
ChIP	Chromatin immunoprecipitations
CMC	Chemistry and manufacturing controls
CME	Clathrin-mediated endocytosis
CSF	Cerebrospinal fluid
CXCR4	C-X-C chemokine receptor type 4
DMEM	Dulbecco's modified eagle medium
DMSO	Dimethyl sulfoxide
EBV	Epstein-Barr virus
EC	Endogenous control
EDTA	Ethylenediaminetetraacetic acid
EGFR	Epidermal growth factor receptor
ELISA	Enzyme-linked immunosorbent assay

LIST OF ABBREVIATIONS

EM	Electron Microscopy
ERK	Extracellular signal-regulated kinase
ESCRT	Endosomal sorting complexes required for transport
EV	Extracellular vesicle
FBS	Fetal bovine serum
GAPDH	Glyceraldehyde 3-phosphate dehydrogenase
GDV	Gene delivery vehicle
GGT	Gamma-glutamyl transpeptidase
H	Hour
HBSS	Hank's balanced salt solution
HCC	Hepatocellular carcinoma
HCV E1/E2	HCV glycoproteins E1 and E2
HCV	Hepatitis C virus
Hep par1	Hepatocyte paraffin 1
HIV	Human immunodeficiency virus
HO-1	Heme oxygenase 1
HSP90	Heat shock protein 90
HSPs	Heat shock proteins
i.p.	Intraperitoneal
IFN-α	Interferon alpha
IgG	Immunoglobulin G
IL-1β	Interleukin 1 beta
IL-4	Interleukin 4
IL-6	Interleukin 6
KC	Kupffer cell
KO	Knockout
LDH	Lactate dehydrogenase
LDL	Low density lipoprotein
LncRNA	Long non-coding RNAs
LPL	Lipoprotein lipase
LPLD	Lipoprotein lipase deficiency
LPS	Lipopolysaccharide
MAPK	Mitogen-activated protein kinases
MCP1	Monocyte chemoattractant protein-1
MFGE8	Milk fat globule-EGF factor 8 protein
Min	Minute

LIST OF ABBREVIATIONS

miRNA	MicroRNA
MMF	Mycophenolate mofetil
MNC	Mononuclear cell
MOI	Multiplicity of infection
MVBs	Multivesicular bodies
Nox2	NADPH oxidase 2
NS3	Hepatitis C virus non-structural protein 3
OLP	Oral lichen planus
OSCC	Oral squamous cell carcinoma
OSCC-r	Oral squamous cell carcinoma in remission
PBS	Phosphate-buffered saline
PDAC	Pancreatic ductal adenocarcinoma
PF	Pair-fed
PI3K	Phosphoinositide 3-kinase (PI3K)-AKT
qPCR	Real-time quantitative PCR
RES	Reticuloendothelial system
RISC	RNA-induced silencing complex
RNAi	RNA interference
RNase H	Ribonuclease H
ROC	Receiver operating characteristic
ROS	Reactive oxygen species
RPM	Revolutions per minute
RSV	Respiratory syncytial virus
S	Second
SDS	Sodium dodecyl sulfate
SEM	Scanning electron microscope
SIP	Surface immunogenic protein
siRNA	Small interfering RNA
SLC3A1	Solute carrier family 3 member 1
snoRNA202	Small nucleolar RNA MBII-202
SOCS1	Suppressor of cytokine signaling 1
sPTPRG	Soluble protein tyrosine phosphatase γ
SR-BI	Scavenger receptor class B member 1
STAU1	Staufen Double-Stranded RNA Binding Protein 1
STAU2	Staufen Double-Stranded RNA Binding Protein 2
TAK1	Transforming growth factor beta-activated kinase 1

LIST OF ABBREVIATIONS

TBS	Tris-buffered saline
TBST	Tris-buffered saline with Tween 20
TEM	Transmission electron microscope
TGF-β	Transforming growth factor-β
TLR	Toll-like receptor
TNFα	Tumor necrosis factor alpha
TSG101	Tumor susceptibility gene 101 protein
UTR	Untranslated region
V-ATPase	Vacuolar-type H+-ATPase
WT	Wild type

Chapter 1
Introduction

Exosomes/extracellular vesicles (EVs) are heterogeneous membrane-coated vesicles released from almost all cell types into the microenvironment (Raposo and Stoorvogel, 2013; Mulcahy et al., 2014). The first reports on exosomes did not appreciate their biological value and role in cellular communication (Chargaff and West, 1946; Yanez-Mo et al., 2015). In the past decade, however, exosomes have emerged as major signaling molecule conveyors, delivering cargo (Mulcahy et al., 2014) that can modify recipient cell functions (Valadi et al., 2007; Yanez-Mo et al., 2015; Quesenberry et al., 2015). Several mechanisms of exosome internalization have been proposed, including clathrin-mediated endocytosis (CME), phagocytosis, micropinocytosis, and plasma membrane fusion (Mulcahy et al., 2014). Lipid rafts and specific protein–protein interactions have also been shown to play roles in exosome uptake (Mulcahy et al., 2014). The biological actions of exosomes can be mediated by different bio-macromolecules including lipids, proteins, glycans, and nucleic acids (Lotvall et al., 2014), playing roles in both physiological processes and disease pathogenesis. Exosome-contained bioactive molecules are also quite stable and protected against proteases as well as RNases, due to the presence of a lipid bilayer in EV structures (Valadi et al., 2007; Lambertz et al., 2015). Furthermore, these structures are stable under adverse physical conditions such as long-term storage, multiple freeze-thaw cycles, and extreme pH (Nawaz et al., 2014). As such characteristics match the criteria for selecting clinically-relevant biomarkers and drug delivery systems; interest in exosome biology is growing apace.

Specifically, the absolute number of exosomes has been reported to increase in pathological conditions, and to be enriched with a specific set of biological markers (a biomarker signature) related to the cell of origin and disease status (Taylor and Gercel-Taylor, 2008; Jia et al., 2014). Notably, exosomes have been isolated from numerous biofluids, including serum, plasma, cerebrospinal fluid (CSF), urine, and saliva and utilized for biomarker discovery, monitoring of therapy, as well as potential platforms for personalized medicine (Zocco et al., 2014; Verma et al., 2015; Ogawa et al., 2008; Pisitkun et al., 2004; Street et al., 2012).

1.1 Classification and biogenesis

The terminology referring to exosomes and EVs has changed tremendously over the past decade, with the words "exosomes", "microvesicles", and "microparticles" used interchangeably in the literature (Momen-Heravi et al., 2013; van der Pol et al., 2012). Since the current understanding of EV biogenesis is incomplete, EV isolation protocols and vesicle characterization varies, this terminology is used interchangeably in this thesis.

The heterogeneous family of EVs that can be broadly classified based on morphological characteristics, mode of biogenesis, and molecular markers (Box 1.1) (van der Pol et al., 2012). Thus, exosomes are the smallest (50-150 nm) and most studied subpopulation of EVs derived from multivesicular bodies (MVBs) (Denzer et al., 2000; Barry et al., 1998). These particles are understood to arise from early endosomes that can undergo ubiquitin-dependent interactions with endosomal sorting complexes required for transport (ESCRT) (ESCRT-0, ESCRT-I and ESCRT-II) and be recycled. Alternatively, they can proceed towards a late endosomal pathway and initiate exosome biogenesis (Raiborg and Stenmark, 2009). Late endosomal pathways are dependent on multivesicular bodies, are ubiquitin-independent pathways, and lead to formation and sorting of exosomes (de Gassart et al., 2004). In these pathways, ALG-2-interacting protein X (ALIX) can bind directly to the exosomal cargo molecules, which differentiate between exosomal sorting pathways and lysosomal recycling pathways (Hurley and Odorizzi, 2012). Whilst the ESCRT proteins are clearly required for the lysosomal degradation of proteins, the function of ESCRT in formation of exosomes is less studied (Urbanelli et al., 2013). Furthermore, the Rab GTPase family regulates fusion of late-endosomal MVBs with the plasma membrane and exosome release (Ostrowski et al., 2010). Specifically, Rab5 and Rab7 regulate endocytic trafficking downstream of MVB biogenesis and cargo sequestration whereas Rab27a, Rab27b, and Rab35 control the secretion of exosomes (Hurley and Odorizzi, 2012; Ostrowski et al., 2010; Vanlandingham and Ceresa, 2009).

Box 1.1: Classification of extracellular vesicles

Historically, EV classification was based on cellular origin. However, EVs can be more accurately categorized on the basis of their biogenesis.

Oncosomes: tumor microvesicles that transmit signaling complexes between cells.
Ectosomes: vesicles secreted by human polymorphonuclear leukocytes
Microparticles: vesicles originated from platelets
Dexosomes: vesicles released from dendritic cells
Texosomes: vesicles derived from tumor cells

EV classification based on mode of biogenesis

Exosomes

- **Origin:** budding of inter luminal multivesicular bodies of endosomal pathways
- **Size:** 50-150 nm
- **Surface markers:** Tetraspanins (CD63, CD 81,CD82, CD9), ESCRT components, TSG101, Flotillin 1 and Flotillin 2, HSPs, ALIX, MFGE8

Microvesicles

- **Origin:** Outward budding of plasma membrane
- **Size:** 100-1000 nm
- **Surface markers:** AnnexinV, Integrins, CD40 ligand

Apoptotic bodies

- **Origin:** Outward budding of plasma membrane in apoptotic cells
- **Size:** 500-2000 nm
- **Surface Markers:** AnnexinV, particularly enriched in phosphatidylserin

*ESCRT: Endosomal sorting complex required for transport complex, MFGE8: milk fat globule-EGF factor 8 protein, TSG101: tumor susceptibility gene 101, HSPs: heat shock proteins

Microvesicles (also called shedding microvesicles, shedding vesicles, or microparticles) are approximately 100-1000 nm in diameter and originate from the outward budding of the plasma membrane (Momen-Heravi et al., 2013). Tumor susceptibility gene 101 protein (TSG101), which is also involved in exosomes biogenesis, interacts with arrestin domain-containing protein 1 (ARRDC1) in the stage of microvesicle budding (Nabhan et al., 2012). This protein interaction leads to relocation of TSG101 from endosomes to the plasma membrane and mediates the formation of microvesicles (Nabhan et al., 2012). Both exosome and microvesicle release are associated with a specific region of plasma membrane which is enriched in cholesterol, lipid rafts, and ceramide (Bianco et al., 2009; Nawaz et al., 2014). The small GTP-binding protein ADP-ribosylation factor 6 (ARF6), the Rho signaling pathway, actin motors, and the elements of cytoskeleton are involved in the formation of microvesicles (D'Souza-Schorey and Chavrier, 2006; Li et al., 2012a; Charras et al., 2006).

Apoptotic vesicles are a subpopulation of EVs that range from 100-2000 nm in diameter and are generated by the blebbing of the plasma membrane of cells undergoing apoptosis. Larger apoptotic vesicles (1000-5000 nm) are referred to as apoptotic bodies and contain fragmented nuclei as well as fragmented cytoplasmic organelles (Gyorgy et al., 2011; Buzas et al., 2014). Crucially, uptake of apoptotic bodies originating from tumor cells can transfer oncogenic contents to the recipient cells and showed tumorigenic activity (Bergsmedh et al., 2001).

As indicated herein, vesicles originating from different biogenesis pathways can have overlapping diameter ranges (Witwer et al., 2013), making particle size a poor approach to EV classification. Presently, as understanding of vesicle formation biomechanics improves, characterization and classification of EVs is migrating from particle size to mode of origin. However, identification of vesicle-specific molecular patterns is expected to expand the horizons of vesicle classification in the future.

1.2 Function of extracellular vesicles in physiology and pathology

Increasing evidence suggests that EVs have multiple functions in both physiological and pathological conditions. Thus, beyond cell signaling, exosomes can exert immune modulation by transporting ligands and receptors (Martinez et al., 2006; Martinez-Lorenzo et al., 1999), presenting antigens (van Niel et al., 2001; Van Niel et al., 2003), transferring cytokines (Vojtech et al., 2014) and signaling components (Njock et al., 2015), triggering inflammation (Bretz et al., 2013), transferring genetic information (Valadi et al., 2007; Momen-Heravi et al., 2015a), and contributing to the spread of infectious diseases (Narayanan et al., 2013; Bukong et al., 2014). In tumorigenesis, exosomes have been demonstrated to trigger cancer cell proliferation, induce angiogenesis, and ultimately promote tumor growth and metastasis (Tickner et al., 2014). Table 1.1 provides a summary of the key roles of EVs in different pathological conditions.

Table 1.1: Role of extracellular vesicles in pathogenesis of different diseases

Disease	Vesicle type	Reference
Infectious disease		
Parasitic trematodes/nematodes: immunomodulation	Exosomes	(Marcilla et al., 2012)
Spongiform encephalopathies: spread of transmissible prions via the blood	Exosomes	(Saa et al., 2014)
HIV: miRNAs transport involved in HIV-associated neuronal dysfunction, trans-infection of CD4+ T-cells	Exosomes	(Hu et al., 2012),(Wiley and Gummuluru, 2006)
Malaria: Cellular communication within the parasite population/ immunomodulation of host innate immune system for parasite survival	Exosomes	(Mantel et al., 2013)
Epstein–Barr virus: viral biogenesis and egress, exosome-dependent immune suppression in EBV-associated lymphomas	Exosomes	(Meckes et al., 2013), (Pegtel et al., 2010)
Cancer		
Promote thrombosis, cell proliferation, and angiogenesis	Exosomes, Microvesicles	(Kucharzewska et al., 2013), (Webber et al., 2010), (Liu et al., 2015), (Millimaggi et al., 2007)
Prepare a tumor friendly environment to accept metastatic niches, formation of pre-metastatic niche in different organs	Exosomes, Microvesicles	(Rana et al., 2013), (Costa-Silva et al., 2015)
Inducing pro-vascular phenotype by modulating bone marrow	Exosomes	(Peinado et al., 2012)
Tumor escape from immune system	Exosomes, Microvesicles	(Clayton et al., 2007), (Szajnik et al., 2010), (Andreola et al., 2002)
Metabolic disease		
Diabetes: activate marginal zone–like B cells in NOD mice, an effect associated with onset of diabetes	Extracellular vesicles	(Bashratyan et al., 2013)
Insulin resistance in treated adipocytes influenced by pro-inflammatory macrophages	Extracellular vesicles	(Zhang et al., 2015)
Inflammatory disease		
Rheumatoid arthritis: associated joint inflammation by inducing coagulation and contributing to fibrin deposition	Microvesicles	(Berckmans et al., 2002)

1.3 Circulating microRNAs and exosome-associated miRNAs: regulators of gene expression

MicroRNAs constitute a class of small non-coding RNAs ranging from 18-25 nucleotides in length, produced by RNase III proteins, namely Dicer and Drosha (Ha and Kim, 2014). The regulatory role of microRNAs (miRNAs) in different cellular processes and disease

pathogenesis has drawn much attention to the potential of miRNAs as biomarkers. Whereas some miRNAs regulate specific genes, some miRNAs have master regulatory functions and regulate hundreds of targets (He and Hannon, 2004). MicroRNA biogenesis is initiated in the nucleus of a cell and finalized in the cytoplasm, where they are loaded onto the so-called RNA induced silencing complex (RISC complex). RISC then targets mRNAs usually located at their 3' untranslated region (UTR), resulting in either target mRNA degradation or translational repression (Bartel, 2009) (Figure 1.1). Other roles such as the regulation of epigenetic changes and target regulation at the 5′ UTR are also attributed to miRNAs (Fabbri et al., 2013) and it is estimated that miRNAs regulate the translation of more than 60% of protein-coding genes (Esteller, 2011). Extracellularly, biologically active miRNAs can be found in two distinct forms: exosome-associated miRNAs and free floating miRNAs, with the majority of miRNAs in biofluids associated with exosomes (Gallo et al., 2012). These reports have introduced new opportunities in causal biomarker discovery in exosome-associated miRNAs.
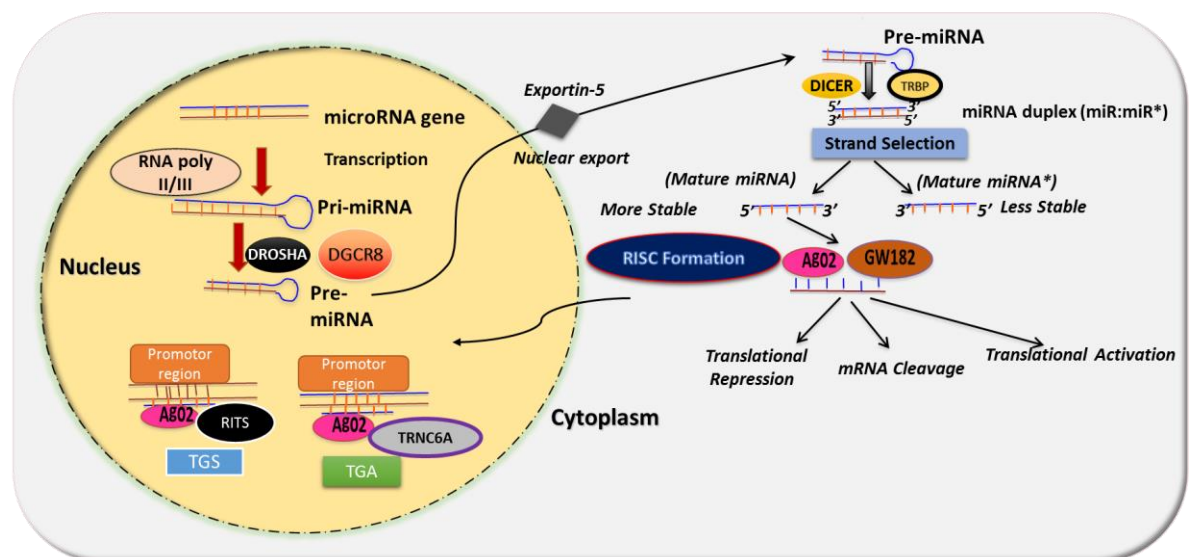
Figure 1.1: MicoRNA biogenesis and function. MicroRNA can originate from apparently dedicated non-coding RNA transcripts, coding transcripts and other non-coding sequences, including from regions that may normally be subject to translation or alternative splicing. Primary miRNAs (pri) are transcribed from the genome by RNA polymerase II/III in the nucleus. Pri-miRNAs are cleaved by the Drosha/DGCR8 complex to form precursor (pre) miRNAs. Pre-miRNAs are next transported to the cytoplasm via exportin-5. Dicer along with TRBP cleaves pre-miRNAs to mature miRNAs, with strand selection taking place at this stage. The functional strands form a complex with Ago2 and GW182 and thus constitute the RNA-inducing silencing (RISC) complex. Binding onto targets with complete or partial complementary induces mRNA cleavage, translational activation or suppression (Roberts, 2014; Matsui et al., 2013; Moschos, 2013).

It is now very well established that a large number of miRNAs play active roles in the pathogenesis of disease and are frequently dysregulated in many distinct indications. These characteristics enable researchers to use them for diagnostic purposes or as therapeutic targets (Heneghan et al., 2010). Interestingly, deep sequencing data showed that miRNAs are the most abundant type of RNA in plasma-derived exosomes, corresponding to 76% of all mappable reads (Huang et al., 2013). Target gene enrichment analysis and functional experimental results suggest that highly abundant exosome-associated miRNAs may have important functions in protein phosphorylation, RNA splicing, and the modulation of immune functions (Momen-Heravi et al., 2015a; Momen-Heravi et al., 2015b; Huang et al., 2013). Given these and other effector roles have been attributed to exosomal miRNAs, miRNAs constitute the most well studied group of the exosome-associated transcriptome.

1.4 Function of exosomes in liver physiology and pathology

Exosomes derived from cholangiocytes and hepatocytes have been suggested to play a role in intercellular communication between hepatocytes, cholangiocytes, and sinusoidal endothelial cells (Witek et al., 2009; Masyuk et al., 2010). Thus, biliary exosomes were reported to induce a decrease of the phosphorylated-to-total extracellular signal-regulated kinase (ERK)1/2 ratio, an increase in miRNA-15A expression levels and a decrease in the proliferation of cholangiocytes (Masyuk et al., 2010). Exosomes isolated from hepatitis c virus (HCV)-infected human hepatoma Huh 7.5.1 cells were reported to contain a complete sequence of viral RNA, functional viral proteins and, importantly, the ability to transmit HCV infection to other naïve human hepatoma cells (Ramakrishnaiah et al., 2013; Bukong et al., 2014). Exosomes were also reported to contribute to the antiviral response of interferon alpha (IFN-α) to the mouse hepatitis virus strain A59 and adenovirus in an *in vivo* mouse model (Li et al., 2013). Elsewhere, in a hepatocellular carcinoma (HCC) model, co-culture experiments demonstrated that exosomes derived from HCC cells could induce HCC cell growth, migration, and metastasis and deliver miRNAs to the recipient cells (Wei et al., 2015).

Exosomes isolated from a colorectal cancer cell line (HT-29), which has a substantial potential for metastasis, were also shown to significantly promote metastatic tumor formation by Caco-2 colorectal cancer cells; thus, whilst Caco-2's ordinarily exhibit poor liver metastatic potential (Wang et al., 2015). Interestingly, the recipient mice also presented high levels of C-X-C chemokine receptor type 4 (CXCR4) in the metastatic

microenvironment. Thus, these findings were proposed to imply that exosomes may play a role in promoting colorectal cancer metastasis, by employing CXCR4-expressing stromal cells to develop a susceptible metastatic microenvironment (Wang et al., 2015). This thesis is corroborated from evidence derived by other groups on the role of stromal CXCR4 in promoting the formation of metastatic niches, angiogenesis, and tumor growth (Guo et al., 2016; Yang et al., 2015). Similarly, exosomes released from CD90+ cancer cells were reported to be enriched in long non-coding RNA (LncRNA) H19, promoted angiogenic phenotype and cell-to-cell adhesion in endothelial cells (Conigliaro et al., 2015). Additionally, it has been reported that in pancreatic ductal adenocarcinoma (PDAC), PDAC-derived exosomes promote liver pre-metastatic niche formation in naive mice (Costa-Silva et al., 2015). Thus, macrophage migration inhibitory factor (MIF) was highly expressed in PDAC-derived exosomes and resulted in recruitment of bone marrow-derived macrophages. Moreover, PDAC-derived exosomes were taken up by Kupffer cells (KCs), causing the secretion of transforming growth factor β and upregulation of fibronectin production by hepatic stellate cells. The resulting inflammatory and fibrotic microenvironment thus was interpreted to prime the liver for metastasis (Costa-Silva et al., 2015). Elsewhere, exosomes secreted from motile HCC cell lines enhanced the migratory and invasive abilities of MIHA cells (an immortalized, non-tumorigenic, normal human hepatocyte cell line), activating the phosphoinositide 3-kinase (PI3K)/AKT and mitogen-activated protein kinase (MAPK) signaling pathways (He et al., 2015). HCC tumor-derived exosomes were also shown to contain a special miRNA signature, which appears to modulate identified transforming growth factor β activated kinase-1 (TAK1) pathways and enhance transformed cell growth in recipient cells, further promoting hepatocarcinogenesis (Kogure et al., 2011). Hepatocyte-derived exosomes were also shown to possess a regenerative capacity by delivering the synthetic machinery to form sphingosine 1 phosphate (S1P) in target primary hepatocytes, leading to an increase in cell proliferation and liver regeneration after ischemia/reperfusion injury or partial hepatectomy (Nojima et al., 2016). Interestingly, the function of liver cell derived exosomes appears to extend into metabolism. Thus, repeated injections of exosomes isolated from the peripheral blood of mice fed a high-fat diet to mice on a regular diet, resulted in aggregation of activated immature myeloid, $CD11b^+Ly6C^{hi}Ly6G^-$ cells in the liver. This was accompanied by chronic inflammation characterized by an increase in serum interleukin 6 (IL-6), alanine aminotransferase (ALT), and aspartate aminotransferase (AST)) and the promotion of fatty liver disease (Deng et al., 2009). From a clinical perspective, circulating exosomes in patients with primary biliary cirrhosis, an autoimmune liver disease, were also shown to significantly change co-stimulatory molecule expression on antigen-

presenting populations in an *ex vivo* disease model (Tomiyama et al., 2015). Figure 1.2 summarizes exosome biogenesis and the role of exosomes in liver physiology and pathology.
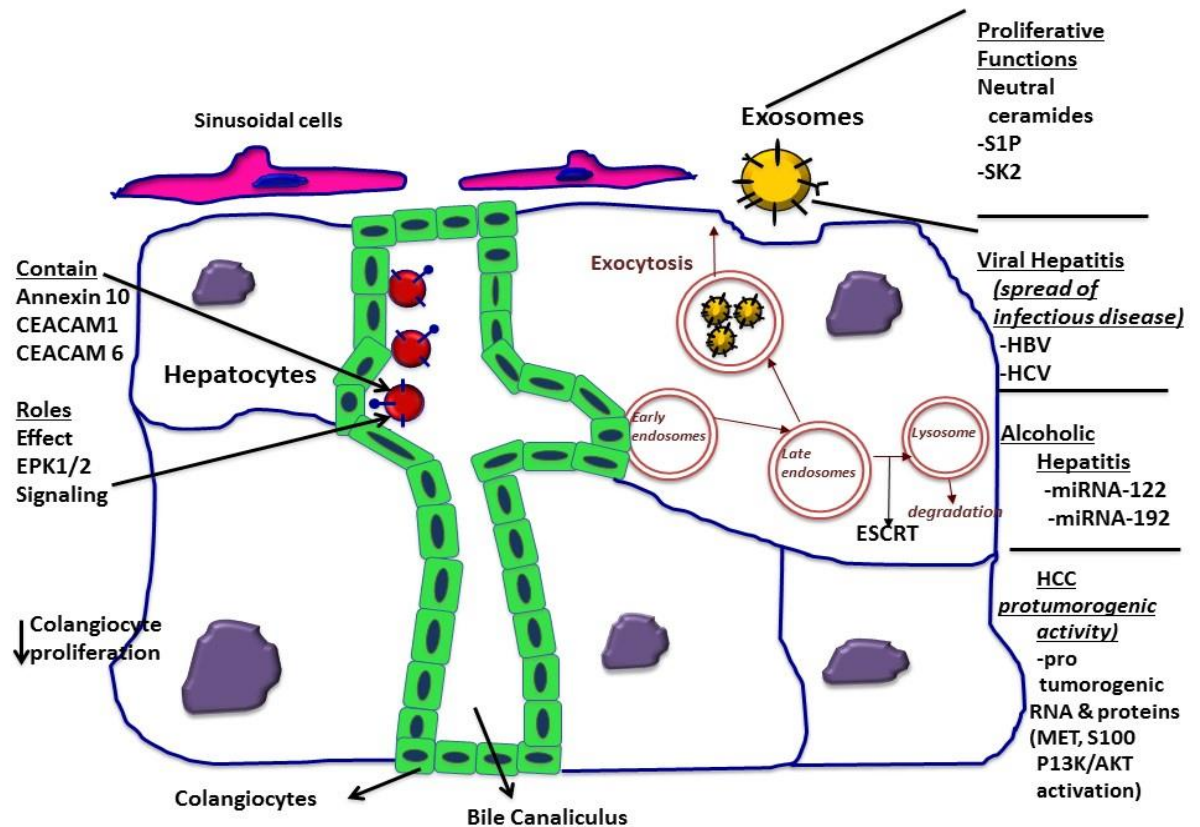
Figure 1.2: Exosome biogenesis and role of EVs in different liver pathologies

1.5   Exosomes/EVs as biomarkers of disease

The National Institutes of Health define biomarkers as "A characteristic that is objectively measured and evaluated as an indicator of normal biologic processes, pathogenic processes, or pharmacologic responses to a therapeutic intervention"(Biomarkers Definitions Working, 2001). "Liquid biopsy" represents an emerging novel approach in biomarker discovery for diagnostics, monitoring and evaluation of prognosis, as well as treatment outcomes in various diseases (Jia et al., 2014; Crowley et al., 2013), and refers to the collection of biofluid samples that contain biomarkers of disease, typically neoplastic. Comprehensive profiling of cells and biofluids using proteomic, genomic, and transcriptomic analysis has resulted in a paradigm shift on the understanding of disease pathogenesis mechanisms, the possibility of early diagnosis and the monitoring of prognosis. Accordingly, EVs can be purified from readily available biofluids, both invasive and non-invasive, such as serum, plasma, urine, CSF and saliva. The fact that exosomes are natural carriers of biomolecules that improve their biological stability, as well as the emerging understanding of their pivotal, often causal roles in the development and progression of disease, positioned them as promising substrates

for the discovery of clinically relevant diagnostic and prognostic biomarkers. Thus, the gamut of relevance has thus been shown to include multiple cancers, autoimmune disease, metabolic disorders, infectious disease, and other systemic pathologies (Kalani et al., 2014; San Lucas et al., 2015; Sadovska et al., 2015), opening up new perspectives in the field of liquid biopsy diagnostics.

Beyond the general increase in EV concentrations under pathological conditions the encapsulated proteins, lipids and nucleic acids have been reported by multiple groups to inform disease status (Akers et al., 2013; Turchinovich et al., 2011; Galindo-Hernandez et al., 2013), even with mechanistic roles in pathogenesis (Candelario and Steindler, 2014; Bergsmedh et al., 2001; Buzas et al., 2014). Crucially, these roles can establish discovery of causal biomarkers instead of simply correlational biomarkers. Secondly, by focusing analytics onto the exosome fraction, the complexity of biofluids can be reduced, thereby diminishing data noise and increasing signal levels, i.e. facilitating the detection of less abundant biomarkers (Boukouris and Mathivanan, 2015; Willis and Lord, 2015; Momen-Heravi et al., 2015b) - a phenomenon described as "less being more". Thus, subsets of low abundance biomarkers in biofluids can be highly enriched in the exosomal sorting process (Properzi et al., 2013). For example, aquaporin protein families, which are key players and indicators of renal ischemia/reperfusion injury, have been recovered from exosomes isolated from urine; in stark contrast, they are poorly detectable in complete urine (Takata et al., 2008; Properzi et al., 2013; Sonoda et al., 2009). Thirdly, the lipid bilayer of the exosome protects nucleic acids and proteins from RNases, proteinases, DNases, and other enzymatic activity present in the biofluids, thereby extending analyte stability (Willis and Lord, 2015; Momen-Heravi et al., 2014a; Racicot et al., 2012). Fourthly, exosomes themselves are very stable and can perfectly survive different storage conditions (e.g. -20 °C, -80 °C) over periods of at least 3 months (Kalra et al., 2013). Thus, in a multiplex study on ovarian cancer patients which identified eight miRNAs for discrimination of ovarian cancer from benign ovarian disease, miRNA levels were not affected by pre-analytical variables such as storage time and collection (Taylor and Gercel-Taylor, 2008). Similar miRNA profiles were reported in serum samples stored for a short time at 4 °C (up to 96 h) and when the serum samples were kept at -70°C for 28 days (Taylor and Gercel-Taylor, 2008). Fifthly, different studies have reported increased sensitivity for exosome-based biomarkers compared to whole serum and urine biomarkers (Ogata-Kawata et al., 2014; Logozzi et al., 2009; Madhavan et al., 2015). For instance, miRNAs found in exosomes isolated from sera of patients with colorectal cancers, showed higher sensitivity (90.0 %) compared to serum carcinoembryonic Antigen (CEA) and cancer antigen 19-9 (CA19-9) (30.7 and 16.0%

respectively) (Ogata-Kawata et al., 2014). Similarly, higher levels of disease-specific biomarkers were reported by others in the exosome fraction of biofluids compared to the exosome-depleted fraction (Madhavan et al., 2015; Bala et al., 2012). For example, levels of miRNA-4644, miRNA-3976, miRNA-1246, and miRNA-4306 were significantly elevated in pancreatic cancer exosomes compared to controls, while these miRNAs were only slightly elevated in exosome-depleted serum of patients with pancreatic cancer (Madhavan et al., 2015). In line with these reports, in alcoholic hepatitis and inflammatory liver injury, miRNA-122 and miRNA-155 were predominantly found in the exosome fractions of plasma/serum, as opposed to the exosome-depleted fractions (Bala et al., 2012).

1.6 Exosomes as biomarkers of liver diseases: challenges and opportunities

As sedentary lifestyles and dietary changes become more common, the health burden of liver diseases is increasing (Nseir et al., 2014). Unfortunately, the silent nature of liver disease progression and the absence of symptoms until late phases pose challenges to timely diagnosis. Given the invasiveness and risk associated of liver biopsy, exploration of minimally invasive liver diagnostic methods has attracted considerable attention (Aithal et al., 2012). Importantly, the outcomes of a diverse set of liver diseases including alcoholic hepatitis, steatosis, viral and bacterial hepatitis, liver autoimmune disease and fibrosis are understood to potentially benefit from early diagnosis (Aithal et al., 2012). Traditionally, liver biopsy has been considered the gold standard for assessing accurately liver injury across various liver pathologies. In lieu of this approach, the extent of liver injury has been correlated to the levels of hepatic enzymes in blood, usually alanine aminotransferase (ALT), aspartate aminotransferase (AST), and alkaline phosphatase (ALP)/gamma-glutamyl transpeptidase (GGT). Nevertheless, serum hepatic enzyme activities lack both sensitivity and specificity (Gallo et al., 2012). Moreover, the levels of these biomarkers do not always properly reflect the stage of liver disease and extent of hepatocellular injury and can poorly discriminate between transient (e.g. dietary) vs established insults (Kim et al., 2008). However, recent findings have presented various novel liquid biopsy biomarkers as suitable, minimally invasive alternatives (Mohankumar and Patel, 2015). Thus, with the introduction of systems-wide analytical methodologies, commonly referred to as "Omic technologies", the proteome, transcriptome, lipidome, and metabolome have been explored for their biomarker potential.

Increased levels of various subpopulations of circulating exosomes have been reported in patients with hepatitis C and acute liver failure, compared to healthy subjects (Brodsky et

al., 2008; Agarwal et al., 2012). Full-length soluble protein tyrosine phosphatase γ (sPTPRG) isoforms associated with exosomes have been reported to be well-correlated with different stages of liver injury (Moratti et al., 2015). Soluble CD81 was identified to be increased in exosomes isolated from sera in patients with chronic hepatitis C compared to patients with cured hepatitis and healthy individuals (Welker et al., 2012). Elsewhere, using affinity immune isolation, circulating exosomes enriched in liver-origin protein Hepatocyte paraffin 1 (Hep par 1) isolated from plasma of hepatocellular carcinoma patients (Brodsky et al., 2008) were positively correlated with liver tumor size (Brodsky et al., 2008). In addition to CD81, a panel of exosomes isolated from urine of acute liver injury animal models contained differentially expressed proteins including CD26, solute carrier family 3 member 1 (Slc3A1), and CD10 and were suggested as biomarkers of liver disease in acute liver injury animal models (Conde-Vancells et al., 2010).

High-throughput plasma exosome-associated miRNA profiling showed that nine miRNAs (miRNA-1225-5p, miRNA-1275, miRNA-638, miRNA-762, miRNA-320c, miRNA-451, miRNA-1974, miRNA-1207-5p, and miRNA-1246) were differentially expressed in patients with chronic hepatitis C and controls which allowed categorizing subjects as chronic hepatitis C patients or healthy controls with 96.59% accuracy (Murakami et al., 2012). Similarly, exosome-associated miRNA-18a, miRNA-221, miRNA-222 and miRNA-224 recovered from serum exosomes were significantly elevated in patients with HCC compared to patients with chronic hepatitis B or liver cirrhosis. Importantly, the whole serum levels of circulating miRNAs showed less sensitivity and specificity for detection of HCC compared to the exosome-associated miRNA fraction (Sohn et al., 2015), justifying the diagnostic value of exosome-specific analysis. Similarly, miRNA-21 was significantly higher in exosomes isolated from sera of patients with HCC; the improved discriminatory power and diagnostic accuracy compared to miRNA-21 measurement in the exosome-depleted serum fraction highlighted the exosomal origin of this biomarker. Interestingly, levels of exosome-associated miRNA-21 were higher in patients with liver cirrhosis which is the primary risk factor for developing HCC, and high grade tumor stage (Wang et al., 2014). On the other hand, decreased levels of miRNA-718 were associated with HCC re-occurrence after liver transplant and tumor aggressiveness in different cohorts of patients (Sugimachi et al., 2015). Importantly, although exosome-associated miRNAs showed interesting results for biomarker studies, this area of research is still in the descriptive phase and the results are not validated in large independent cohort studies.

INTRODUCTION

Although EVs have been successfully isolated from multiple biofluids, including plasma (Caby et al., 2005), serum (Chen et al., 2013), urine (Raj et al., 2012), saliva (Sivadasan et al., 2015), amniotic fluid (Asea et al., 2008), and breast milk (Lasser et al., 2011), there are considerable inconsistencies in the isolation methods employed. Several established methods were introduced and utilized for the isolation and purification of exosomes, including ultracentrifugation, antibody-coated magnetic beads, microfluidic devices, polymeric precipitation technologies, size exclusion methods, sieving, porous nano-structures, as well as emerging technologies. Although each method features advantages and disadvantages, it is important to note that none have shown superiority for all purposes and comparative efficacy studies are limited to only a handful of diagnostic scenarios. In fact, the method of isolation has been demonstrated to directly affect the reproducibility and reliability of all downstream analyses: any uncertainty and errors in the isolation procedure may also irreversibly change outcomes, conclusions and ultimately the validity of any obtained results (Witwer et al., 2013). Thus, presently none of the reported methods has dominant superiority for all diagnostic purposes and method selection can be based on the type of biofluid, EV target sub-population, clinical setting, or a combination of methods. In spite of the fact that most approaches rely upon a high level of purity, the selection of one method over another in the clinical setting is greatly dependent on the goal in mind. As with other biological products, purity, concentration, yield, and selective isolation in a rapid and cost effective manner remain the principal goals. However, preferential aim tradeoffs should be made depending on the circumstances, in order to maximize overall effectiveness.

In spite of the emerging understanding of the mechanistic role and diagnostic value of EVs, important limitations continue to exist in conducting exosome-based biomarker discovery. The most important challenges are pre-analytical, problems in reproducibility, and obstacles in characterization and isolation methods (Momen-Heravi et al., 2013; Witwer et al., 2013). Currently, the lack of a standardized protocol for isolation hinders translation into the clinical setting. Validation studies supporting transition from discovery to diagnostic use require the development of standardized, reproducible and quantifiable isolation and characterization methods (Momen-Heravi et al., 2013; Witwer et al., 2013; Jia et al., 2014; Momen-Heravi et al., 2012a) as well as the establishment of appropriate normative controls (Witwer et al., 2013).

1.7 MicroRNA-targeted gene therapy and conventional gene delivery vehicles

Notwithstanding the diagnostic and potentially causal value of EV microRNAs, these biomolecules are established regulators of physiology, pathogenesis and disease. Therefore, correcting miRNA deregulation by miRNA mimics and inhibitors seems as an attractive method to control aberrant cell functions. Therapeutic oligonucleotides in their so-called naked (i.e. unformulated) forms are very difficult to deliver due to chemical instability, susceptibility to RNases and lack of controlled distribution to relevant tissues and cells (Takakura et al., 2001; Soutschek et al., 2004; Min et al., 2010). Gene delivery vehicles (GDVs) including viral vectors and cationic liposomes were introduced to overcome these limitations (Gehrig et al., 2014; Awada et al., 2014). Suitable viral vectors can be found amongst adeno-associated viruses (AAV), adenoviruses, herpes viruses and lentiviral vectors (Serguera and Bemelmans, 2014). However, all of these can induce moderate to severe immune response against both vehicles and transgenes. Although among viral vectors AAVs induce milder immune reactions and limited cellular response, AAVs can induce humoral responses and the formation of AAV neutralizing antibodies, which can obstruct efficacy (Xiao et al., 1996; Masat et al., 2013). Moreover, capsid-specific T cell responses directed toward transduced cells can result in short-lived transgene expression due to clearance of transduced cells (Masat et al., 2013). Additional risks include genomic integration, immune-related diminished efficacy over repeated administration, high rate of insertional mutagenesis, and lack of ability to transfer large RNA-based cargos. Amongst non-viral, synthetic systems, cationic liposomes are mostly cytotoxic and immunogenic (Zhang et al., 2005), have low transfection efficacy and can be quickly cleared from the circulation (Seow and Wood, 2009; Awada et al., 2014). Use of immune 'stealth' and renal clearance control approaches (e.g. poly-ethylene glycol) further diminishes transfection efficiency, unless the system is upgraded with appropriate receptor targeting ligands- at significant cost-of-goods, chemistry and manufacturing controls (CMC) expense (Nicolaides et al., 2010).

In some cases, the simultaneous use of immunosuppressive agents is also recommended to prevent adverse immune response and increase cellular uptake (Jiang et al., 2006; Wang et al., 2007). For example, in rhesus macaques, a regimen consisting of Mycophenolate mofetil (MMF) and tacrolimus administered before and after adeno-associated virus serotype 8 (AAV8) vector expressing human factor IX hFIX (AAV8-hFIX) was safe and lead to higher transduction efficacy (Jiang et al., 2006). Similarly, Bortezomib decreased anti-AAV titers up to 10 fold in mice after vector administration (Karman et al., 2012). Administration of a

non-depleting anti-CD4 antibody targeting CD4+ T helper at the time of vector delivery was also reported to attenuate the antibody responses to AAV vectors (McIntosh et al., 2012). Liposomal small interfering RNA (siRNA) delivery vehicle induced inflammatory response was inhibited by the glucocorticoid receptor agonist dexamethasone, without reducing siRNA efficacy (Abrams et al., 2010). Thus, it would appear that the immune-activation properties of both viral vectors and synthetic delivery systems necessitate the use of concomitant immunosuppressive strategies to enhance uptake and reduce the adverse immune responses, which complicates drug formulation and reduces administration opportunities (Masat et al., 2013).

Bacteriophages are another class of GDVs which have exhibited good safety and stability (Jepson and March, 2004). However, their clinical use in gene therapy applications is limited due to the robust antibody responses and rapid elimination by the reticuloendothelial system (RES) (Molenaar et al., 2002; Bakhshinejad and Sadeghizadeh, 2014). The substantial hazards of traditional GDVs has limited their applications to cases which benefits highly outperform hazards. Presently, there are only two gene therapy products whose clinical use has been approved by European regulators, Alipogene tiparvovec (Glybera®; uniQure biopharma B.V, Amsterdam, NL) and Strimvelis (GSK2696273; GlaxoSmithKline, Brentford, UK). Alipogene tiparvovec is a gene therapy product for the treatment of lipoprotein lipase deficiency (LPLD), a rare autosomal recessive disorder is caused by mutation in the genes codes lipoprotein lipase (LPL) (Gaudet et al., 2016). Glybera consists of a LPL gain-of-function allele delivered by an AAV vector. Clinical data showed efficacy of the drug in expression of LPL-protein in injected muscles and a diminished incidence and severity of pancreatitis attacks up to 6 years post-treatment (Gaudet et al., 2016). As a result, the European Medicines Authority approved Glybera for adult familial LPLD patients. However, the incidence is very low (1 in 1,000,000) and the price for treatment is presently over 1 million US dollars. Strimvelis has been recently approved for the treatment of severe combined immunodeficiency due to adenosine deaminase deficiency (ADA-SCID) in patients who cannot undergo a bone-marrow transplant due to the lack of a suitable, matched donor. The incidence of ADA-SCID is <9 out of every 1,000,000 live births. The drug consists of an autologous CD34+ enriched cell fraction that contains CD34+ cells transduced with retroviral vector (LXSN vector), encoding the human adenosine deaminase (ADA) complementary DNA (cDNA) sequence, thereby replacing defective ADA in immune cells; long term follow up (median 4 years) showed 100 % survival rate (Hoggatt, 2016; Cicalese et al., 2016). The price for a treatment is over 600,000 US dollars, with the manufacturer offering a full treatment cost refund in case of lack of efficacy. Altogether, high prices,

limited markets, public perceptions over gene therapy, lack of long term human safety studies, regulatory issues, and possible immunogenicity are limiting factors in the extension of gene therapy (Narayanan et al., 2014) and its application beyond orphan disease. In this context, exosomes have attracted attention as alternative drug delivery vehicles. Key among the reasons for evaluating EVs are their long circulating half-life, lower manufacturing cost, intrinsic ability to target tissues, biocompatibility, minimal or no immunogenicity even with repeated administration, and no inherent toxicity reported thus far (Ha et al., 2016; Turturici et al., 2014; Marcus and Leonard, 2013).

1.8 MicroRNA-targeted therapy using exosomes as delivery vehicles

Given miRNA are naturally found in exosomes, this EV subset has attracted considerable attention in the scientific community as a putative solution for RNA interference (RNAi) delivery. Indeed, the natural ability of exosomes to deliver different endogenous nucleic acids is well documented (Valadi et al., 2007; Deregibus et al., 2007). For instance, it has been shown that EVs derived from endothelial progenitor cells can deliver miRNA to human microvascular and macrovascular endothelial cells and activate the PI3K-AKT signaling pathway (Deregibus et al., 2007). Valadi et al., 2007, showed that human mast cell derived exosomes can deliver mRNA to murine mast cells and those mRNAs were translated (Valadi et al., 2007). Notably, it has been found that EVs contain several key proteins and ribonucleic acids involved in RNA processing and RNA transport including GW182, Argonate 2 (AGO 2), double-stranded RNA-binding protein Staufen homolog 1(STAU1), and Staufen homolog 1 (STAU2), suggesting that RNA delivery is dynamically controlled and evolutionary evolved in exosome biology (Collino et al., 2010; Gibbings et al., 2009; Zhang et al., 2010). All these findings help to position exosomes as highly suitable candidates for drug delivery, particularly nucleic-acid based delivery.

Although exosomes are generally nanoparticulate structures with monodisperse size distribution sometimes similar to phage, viruses and synthetic GDVs, they exhibit key advantages in terms of stability, distribution, targeting, efficacy, metabolism and elimination. Unlike the limited compositions of synthetic GDV, exosomal lipid bilayers contain cholesterol, sphingomyelins, glycerophospholipids with long and saturated fatty acyl chains and desaturated molecular species such as phosphatidylethanolamines. This rigid lipid composition decreases the uptake of exosomes by macrophages *in vitro* and may also underpin RES cellular uptake (Laulagnier et al., 2004; Allen et al., 1991). In contrast, bacteriophages exhibit a rapid clearance by the RES (Drulis-Kawa et al., 2012).

Notably, one of the great benefits of exosomes as biological GDVs appears to be their high efficacy in delivering nucleic acids without inducing adverse immune reactions (Banizs et al., 2014), the biggest challenge of viral systems. Thus, early studies in mice indicated that repeated intra-venous administration of autologous exosomes isolated from dendritic cells did not result in any immune activation or maturation of splenic dendritic cells (Wahlgren et al., 2012; Morelli et al., 2004).

Importantly, there are also some reports regarding the immune tolerance of EVs even between species. For example, exosomes derived from human mesenchymal stem cells were reported both as well-tolerated and functional in immune-competent mice (Arslan et al., 2013). In another report, EVs derived from human embryonic kidney 293 (HEK293) cells were also well-tolerated and functional in T cell deficient (RAG2$^{-/-}$) mice, successfully delivering let-7a miRNA to epidermal growth factor receptor (EGFR)-expressing breast cancer xenografts (Ohno et al., 2013).

Crucially, the capacity of EVs to deliver nucleic acids is not restricted to biologically generated compounds. Thus, exogenous nucleic acids (e.g. synthetic, fluorescently tagged miRNA-150 oligonucleotide mimic) were transfected into human monocytic THP-1cells, and recovered from EVs isolated from the transfected THP-1 cell culture medium. Moreover, these EVs were able to transfer miRNA-150 to dermal microvascular endothelium (HMEC-1) cells, which had very low level of miRNA-150 initially, and reduce the levels of the miRNA-150 target, c-Myb to strongly increase HMEC-1 cell migration across transwell filters up to 2.5 fold (Zhang et al., 2010). In a murine Alzheimer's disease model, synthetic siRNA was delivered via exosomes to the brain, outperforming conventional siRNA-transfection reagent complexes (Altogen Biosystems, Las Vegas, NV, USA) in crossing blood brain barrier (Alvarez-Erviti et al., 2011). Whilst injection of siRNA transfection reagent complexes failed to decrease β-secratase1 protein mRNA levels and associated protein expression, intravenously injected, targeted exosomes derived from autogenous dendritic cells efficiently delivered siRNA, specifically to cortical section of brain and led to a 62% knockdown of β-secratase1 protein, a therapeutic target in Alzheimer's disease (Alvarez-Erviti et al., 2011). Wahlgren *et al*., 2012 showed that siRNAs can be loaded into human plasma exosomes via electroporation and those exosomes can be internalized by human monocytes (Wahlgren et al., 2012). Crucially, the electroporetically encapsulated siRNA also appeared effective within the transduced monocytes and induced knockdown of the targeted proteins.

Although recent studies have opened new horizons in the use of exosome-based delivery methods for targeting different pathways, there are several challenges that have to be addressed before clinical use of exosomes can be pursued. Firstly, to produce clinical grade exosome preparations, isolation techniques should be standardized and reproducible with sterility assurance (Witwer et al., 2013) as a minimum, in line with the CMCs applied to other biologics and in context with manufacturing standards for non-viral nano/microparticulate drug delivery systems. Thus, exosome products should be characterized in terms of size, surface markers, aggregation risk/potential, and cargo profile as well as presence of isolation-related impurities such as polymer or beads and cell culture media components. Secondly, given exosome contents are different based on the parental cell type and status (Jia et al., 2014), the choice of exosome type for delivery is expected to be crucial and should be based on the content of the exosomes, target macromolecules, and the type of donor and recipient cells. Thirdly, although clinical and animal studies have revealed that autologous exosomes are well-tolerated even after repeated administration (Escudier et al., 2005), the long-term clinical safety, particularly in heterologous transfer and in the context of latent infection, given the transmissibility of HCV via exosomes, should be determined.

1.9   Aim and scope of this thesis

Understanding the function of EVs and miRNAs and their role in pathogenesis is a very active line of research. A search in the PubMed database for the terms exosomes OR microvesicles OR extracellular vesicles yielded more than 12200 indexed articles in July 2016. However, the work conducted thus far is still in the descriptive phase and hampered by challenges in isolation and analytical methods, as well as our precise understanding of the role of exosomes/EVs in disease biogenesis. Using miRNA-based targeted therapy and utilizing exosomes for nucleic-acid based drug delivery is another attractive approach for disease treatment. However, the potential for success is balanced by a substantial need for development, standardization, and tailoring based on the disease in question, if not the molecular pathways dysregulated in specific patient cohorts. This research aimed to establish and compare methods for isolation and characterization of exosomes and explore the functional role of exosomes and exosomal miRNAs in the pathogenesis of different diseases including alcoholic hepatitis, hepatitis C, and head and neck cancer. The resulting outputs have broadened the scope and methods for using EVs and miRNAs for diagnostic purposes in these indications. My research has led to a clearer understanding of the bio-distribution of exosomes and their encapsulated miRNAs *in vivo* and *in vitro*, as well as the establishment

of a workflow for harnessing the delivery potential of exosomes to pursue miRNA/RNA targeted therapies in both *in vitro* and *in vivo* models.

Chapter 2
Materials and Methods

2.1 General methods

2.1.1 RNA isolation

Total RNA was extracted using a Direct-zol™ RNA MiniPrep isolation kit (Zymo Research Corp, Irvine, CA) or RNeasy mini kit (Qiagen, Germantown, MD). Isolated exosomes from blood (150 µl) or culture supernatant (500 µl) were lysed in 500-1,000 µl of QIAzol Lysis reagent, based on the pellet size and number of exosomes measured by Nanoparticle Tracking Analysis (Nanosight, Malvern, Worcestershire, UK) as described in section 2.1.6.1. The standard manufacturers' protocols were followed, and extracted RNA was eluted in 25 µl of RNase-free water (Thermo Fisher Scientific, Waltham, MA) for downstream analysis. The RNA was quantified using NanoDrop 1000 (Thermo Fisher Scientific). Isolated RNA was profiled using an Agilent Bioanalyzer 2100 (Agilent technologies, Santa Clara, CA) with a Small RNA Chip for exosomal RNA. For saliva samples, total RNA was extracted by RNeasy kit (Qiagen) from 440 µl of saliva, according to the manufacturer's protocol. A NanoDrop spectrophotometer (Thermo Fisher Scientific) and a 2100 Bioanalyzer (Agilent Technologies) were used for assessment of RNA quantity and quality.

2.1.2 MicroRNA analysis

TaqMan® miRNA Assays (Applied Biosystems, Foster City, CA) were used for the detection and relative expression quantification of different miRNAs, according to manufacturer's protocol, as described elsewhere in detail (Momen-Heravi et al., 2014a). Reverse transcription (30 min, 16 °C; 30 min, 42 °C; 5 min 85 °C) was performed using a TaqMan stem loop primer, 10 ng RNA, TaqMan primers and a miRNA reverse transcription kit (Applied Biosystems) in an Eppendorf Realplex Mastercycler (Eppendorf, Westbury, NY). 5µl cDNA was mixed with 5µl TaqMan Universal PCR Master mix (Applied Biosystems) and quantitative real-time PCR performed using a Bio-Rad CFX96 iCycler. In primary human hepatocytes, and hepatoma cells, RNU-48 was used as internal normalizer

as recommended by the manufacturer, after systematic assessment of RNA stability in different human tissues and cell lines and amenability to the miRNA assay design. The small RNA marker small nucleolar RNA MBII-202 (snoRNA202) was used to normalize the Ct value in RAW 264.7 macrophages, mouse hepatocytes, liver mononuclear cells, and KCs as recommended by manufacturer for murine samples. In experiments involving miRNA analysis of exosomes, synthetic *C. elegans* (cel)-miRNA-39 (5 µl of a 5 fmol/µL stock tube) was spiked during the total RNA isolation process and used to normalize the qPCR data as an endogenous control. Where indicated, NormFinder was used to identify the suitable endogenous normalizer (Andersen et al., 2004). TaqMan® Pri-miRNA Assays were done using FAM dye- labeled TaqMan with glyceraldehyde 3-phosphate dehydrogenase (GAPDH) as an internal control (Barber et al., 2005). For each sample, two independent reverse transcription reactions were generated, and each experiment was done in triplicate. miRNA Ct values were normalized, and the relative expression levels of specific miRNA were presented in accordance with the $2^{-\Delta\Delta Ct}$ method (Livak and Schmittgen, 2001). The amplification efficiency of qPCR was verified previously at 99.9 % (Ruijter et al., 2009).

2.1.3 Quantitative real-time polymerase chain reaction (qPCR) for coding RNA targets

For mRNA analyses, 1 µg of total RNA was used to transcribe cDNA using an iScript™ cDNA synthesis kit (Bio-Rad Laboratories). 5x iScript reaction mix (4 µl) and iScript reverse transcriptase (1 µl) were used with a final volume per reaction of 20 µl. Complete reaction mix was incubated for 5 min at 25 ℃, 30 min at 42 ℃, 5 min at 85 ℃ and held at 4 ℃. Final PCR mixture contained 2.5 µl each of forward and reverse primers, 7.5 µl of 2× SYBR PCR mix (Applied Biosystems), and 4 µl of sample. PCR was performed in a Bio-Rad CFX96 Real-time PCR Detection system (Bio-Rad Laboratories) applying universal cycling conditions (2 min at 50 °C, 10 min at 95 °C, 40 cycles of 15 s at 95 °C, and 1 min at 60 °C). Cycle threshold (CT) values were determined by automated threshold analysis with CFX manager software (Bio-Rad Laboratories). The primer sequences are provided in Supplementary table 1. mRNA levels were normalized based on 18S RNA levels (Suzuki et al., 2000), and relative expressions were calculated using the $2^{-\Delta\Delta Ct}$ method.

2.1.4 Statistical analysis

Based on the data distribution, one-way analysis of variance (ANOVA) or a Kruskal-Wallis nonparametric test was used to assess differential gene expression levels. Student's *t* tests or Mann-Whitney *U* tests were performed for pair-wise comparisons in accordance with the

underlying distribution. Data were presented as mean ± standard error of mean (SEM) or mean ± standard deviation as indicated. In experiments aimed at biomarker discovery, the ability of a specific biomarker to discriminate between patients and control groups was evaluated by constructing the receiver operating characteristic curve: the measure of test accuracy combining sensitivity and specificity, the area under the curve (AUC), was calculated (Metz, 1978; Hajian-Tilaki, 2013). For establishing correlations, a Pearson correlation test was used. For statistical analyses, GraphPad Prism v.4.03 (GraphPad Software Inc.), SPSS 14.0 (SPSS Inc., Chicago, IL), and nSolver™ Analysis Software were used. P values ≤ 0.05 were considered statistically significant, with false discovery rates controlled at 5% by Benjamini–Hochberg (Benjamini and Hochberg, 1995) where relevant.

2.1.5 Western blot

An established laboratory protocol was used for western blotting. Briefly, proteins were extracted using RIPA buffer (Thermo Fisher Scientific) and run on 10 % w/v SDS-PAGE gels. Proteins were transferred onto the nitrocellulose membrane (0.2 µm pore–size) (Bio-Rad Laboratories). Prior to transfer, the gel was placed in transfer buffer for 15 min and transfer sandwich assembled and placed in the cassette (Bio-Rad Laboratories). Transfer was performed overnight at 4 °C at a constant current of 10mA. Following transfer, membrane was blocked for 1 h in Tris-buffered saline (TBS) buffer (Sigma-Aldrich) supplemented with 5 % w/v non-fat dry milk and 0.1 % v/v Tween-20 (TBST) (Abcam, Cambridge, MA). The blot was incubated overnight with the primary antibody of interest (at a final concentration of 1 µg/ml) at 4 ℃ and then washed with TBST 3 times and incubated for 1 h with horseradish peroxidase-conjugated secondary Immunoglobulin G (IgG) based on the primary antibody source and protein target (dilution 1: 10,000). A Clarity™ Western ECL substrate kit (BioRad) was used to visualize the blot according to the manufacturer's instructions. Briefly, substrate kit components were mixed in a 1:1 ratio. A volume of 8 ml of this solution was incubated with the membrane for 5 min. The blot was analyzed using a Fujifilm LAS-4000 luminescent image analyzer.

2.1.6 Characterization of EVs

2.1.6.1　　　Nanoparticle tracking analysis (NanoSight)

Nanoparticle tracking analysis (NTA) is a technique that allows the determination of concentration and size of EVs suspended in biofluids or tissue culture samples. The system uses a laser light scattering technique to determine the size (measured in nanometers) and the concentration of EVs (particles per ml) based on Brownian motion (Dragovic et al., 2011;

Momen-Heravi et al., 2012a). The velocity of each vesicle is captured with a highly sensitive CCD camera and calculated with image processing software. The concentration range of 10^8 to 10^9 particles per ml is reported to be in the linear range of the device. Using a NanoSight NS300 system (Malvern, Malvern, UK), size and concentration of EVs were determined in different biofluids and tissue culture supernatants. Before running each set of measurement experiments, the NanoSight was calibrated with 100 nm polystyrene beads (Thermo Scientific) and the samples recorded for 60 s at room temperature. The exact temperature was recorded, and kept constant during the measurements, using the instrument's temperature controller. The NTA software processed the video captures and determined the size distribution of particles in nanometers and the concentration of the particles in particles/ml. Each sample was measured three times.

2.1.6.2   Transmission electron microscopy (TEM)

TEM sample preparation, exosomes were re-suspended in phosphate-buffered saline (PBS) (Thermo Fisher) and transferred to a formvar-coated copper grid (Polysciences, Warrington, PA). The samples were allowed to settle for 30 min and washed sequentially with PBS, using absorbing paper in between the washing steps. Fixation was done by dropwise addition of 2 % v/v paraformaldehyde (Sigma-Aldrich) onto parafilm (Cole-Parmer, Chicago, IL) and placing the grid on top of the paraformaldehyde drop for 10 min at room temperature. The preparation was followed by five 10 µl washes with deionized water (5 megaohm) and specimens were contrasted by adding 2 % v/v uranyl acetate (Sigma-Aldrich) for 15-20 min at room temperature. Finally, drops of 0.13 % v/v methyl cellulose (Sigma-Aldrich) and 0.4 % v/v uranyl acetate were added to the samples (Bukong et al., 2014). The samples were visualized by a Philips CM10 Electron Microscope (Philips, Amsterdam, The Netherlands) located at University of Massachusetts Medical School operating at 60 to 100 Kv.

2.1.6.3   Scanning Electron Microscopy (SEM)

Huh 7.5 cells were cultured in 12-well plates (Falcon™ Polystyrene Microplates, Thermo Fisher) at density of 10^5. Cells were fixed with 2.5 % glutaraldehyde for 2 h in a Sorensen Phosphate buffer (0.1 M, pH 7.4). After fixation, cells were washed with 1 ml of PBS (pH 7.4) three times for 5 min, and fixed with 1 % w/v Osmium tetroxide in 0.1 M PBS (pH 7.4) for 1 h. The samples were next dehydrated by serial washing with 500 µl of increasingly concentrated alcohol diluted in water (30 %, 50 %, 75 %, 85 %, 95 %, 100 % v/v). The samples were mounted on a specimen stub (TED PELLA, Redding, CA) and sputter coated

with gold/palladium (Sigma-Aldrich). The samples were visualized using a MKII FEI Quanta 200 FEG MKII scanning electron microscope (FEI Company, The Netherlands).

2.2 Investigating the role of exosomes & miRNA in alcoholic liver disease

2.2.1 *In vivo* binge alcohol human study

The study subjects consisted of 11 healthy male individuals with no history of alcoholism or alcohol use habits, who were not consuming more than 12 alcoholic drinks per week. In the United States a standard alcoholic drink contains approximately 14 g of pure alcohol as defined by National Institute on alcohol abuse and alcoholism (Dawson, 2011). The study was approved by the Institutional Review Board for the Protection of Human Subjects in research at the University of Massachusetts Medical School (Study approval #2381). The study was carried out in accordance with the approved institutional guidelines. Written informed consent was obtained and samples were de-identified. Alcohol was given to the subjects as 2 ml of 40 % v/v vodka per kg body weight in a final total volume of 300 ml orange/strawberry juice. The control group took the same volume of orange/strawberry juice at the same time points. Blood was collected at baseline and at 0.5 h, 1 h, 2 h, 3 h, 4 h, and 24 h post-alcohol consumption in serum separating tubes (BD Biosciences, San Jose, CA).

2.2.2 Animal studies

All animal studies were approved by the Institutional Animal Care and Use Committee of the University of Massachusetts Medical School. Six to eight week old female C57BL6/J animals were used for chronic alcohol feeding and binge alcohol drinking studies (n = 6 per group). For the chronic alcohol consumption model, the animals received 5 % (v/v) ethanol (36 % ethanol-derived calories) containing the Lieber-DeCarli diet (EtOH) for 5 weeks and control animals received a pair-fed (PF) diet with an identical amount of calories where the alcohol-derived calories were replaced with dextran-maltose (Bio-Serv, NJ, USA). The mice in the binge alcohol consumption group received 5 g/kg of 50 % (v/v) ethanol diluted in water via oral gavage. After 6 h and 12 h binge alcohol consumption, animals were euthanized by pentobarbital overdose and cervical dislocation. Blood was collected from the animals via cardiac venipuncture and serum was separated from the whole blood by allowing the blood to clot in an upright position for 30 min followed by centrifugation for 15 min at 1500 x g within one hour of collection. The serum was then aspired and stored at -80 °C.

2.2.3 Cell culture

Huh 7.5 cells (passage 11), primary human hepatocytes (maximum number of divisions 69-80), and RAW 264.7 cells (passage 9) were cultured in Dulbecco's modified medium (DMEM) (Gibco) supplemented with 10 % v/v exosome-depleted fetal bovine serum (FBS) (Exo-FBS™, Thermo fisher), and 1 % v/v of 10,000 U/mL penicillin/streptomycin (Thermo Fisher). Huh 7.5 cells and RAW 265.7 cells were cultured in 12 well plates at a seeding density of $2x10^5$ and $1x10^5$ cells/well respectively. For experiments involving ethanol treatment, 25 mM (mmol/L), 50 mM (mmol/L), and 100 mM (mmol/L) of ethanol were added to the cells for different durations (24 h, 48 h, and 72 h). THP1 monocytes (passage 11) were cultured in RPMI media (Gibco) supplemented with 10 % v/v exosome-depleted FBS, in a 5 % v/v CO_2 atmosphere at 37 °C. For co-culture experiments, exosomes purified from Huh 7.5 cells were added to the THP1 cells for 8 h at 50–100 µg/ml concentrations of exosomal total protein. This concentration was comparable to the exosomal total protein concentration quantified in human samples by Pierce BCA Protein Assay Kit (Thermo Fisher).

2.2.4 Exosome isolation

For exosome isolation from cell culture, cells were cultured in T75 flasks (Sigma-Aldrich) at seeding densities of $2.2x10^6$ cells and a total volume of 10 ml culture media. After two days, supernatants were centrifuged at 1500 g for 10-15 min to remove cells. This step was followed by centrifugation at 10,000 g for 20 min to deplete residual cellular debris. After serial filtration (0.8 µm, 0.44 µm and 0.2 µm) of supernatants, the ExoQuick-TC™ (System Biosciences) kit was used to precipitate the supernatant following the manufacturer's guidelines. Isolated exosomes were re-suspended in 500 µl PBS. The isolation and resuspension volume ratio was 20:1.

In order to isolate exosomes from sera of human subjects and mice, exosomes were isolated from 150 µl of sera with ExoQuick reagent (System Biosciences, USA) according to the manufacturer's recommended protocol. The cell culture suspension was transferred to micro/ultracentrifuge tubes and THP1 cells pelleted by centrifugation at 500 x g at 4 °C; based on the density of exosomes, such particles are unlikely to co-precipitate with the THP1 monocytes in these separation conditions (Thery et al., 2006). Exosomes would remain in the supernatant and would be discarded. In experimental groups which involved lipopolysaccharide (LPS) Escherichia coli 0111:B4) (Sigma-Aldrich), 10 nM LPS was added to the THP1 cells 6 h before the readouts. LPS, derived from Gram-negative bacteria

in the intestinal microflora, has been identified as a major factor in the pathogenesis of alcoholic hepatitis, affecting various cell types on account of in gut permeability disturbance which facilitates systemic access of LPS via portal circulation (Szabo and Bala, 2010).

2.2.5 Confocal microscopy

Cell culture supernatant exosomes were labeled using a PKH67 green fluorescent cell linker kit (Sigma-Aldrich, St Louis, MI). Briefly, a 250 µl PBS suspension containing 10^8 exosomes (counted with NTA as described in section 2.1.6.1) was added to 250 µl Diluent C. Dye solution was prepared according to the manufacturer's recommendation by adding 2 µl of PKH67 dye solution to 500 mL of diluent C. The 500 µl exosome suspension and dye solution were mixed by pipetting. Recipient THP1 cells were co-cultured with the labeled exosomes in ratio of 1:1 for 6 h and then washed off three times by three times centrifugation of cells (500 x g for 15 minutes) in PBS and discarding the supernatant. Cells were fixed with 1 mL of 2 % v/v formaldehyde (Sigma-Aldrich) in PBS. Uptake was visualized in fixed cells after 8 h using a Leica TCS SP5 II laser scanning confocal microscope (Leica Microsystems, Wetzlar, Germany) equipped with Diode 405 nm and Ar lasers for excitations at 405 nm and 496 nm respectively. Nuclei were stained with DAPI (blue) (Thermo Fisher). Samples were equilibrated with PBS and approximately 250µl of diluted DAPI (300 nM) was added to the coverslip covering the cells. The samples were incubated for 5 min and then rinsed three times with 500 µl PBS. The samples were mounted with ProLong® Gold antifade reagent (Thermo Fisher). Plasma membrane was contrasted and visualized with a Nomarski interference mode. Confocal Z stacked images (0.2 µm stack step, 1 µm range) were obtained. The Imaris software (Bitplane Scientific Software, Concord, MA) was used to construct 3D projections of image stacks.

2.2.6 MicroRNA-targeted therapy via electroporation and transfection

MicroRNA-122 mimics (Ambion, Foster City, CA), heme oxygenase 1 (HO-1)-targeting siRNA (Life Technologies, USA) and relevant controls, including siRNA scrambled control and miRNA control mimic were introduced to THP1 cells via electroporation using the following protocol: 2×10^5 cells were re-suspended in 150 µl complete RPMI media. A volume of 150 µl Gene Pulser® electroporation buffer was added and the mixture was kept on ice for 5 min. Electroporation was performed immediately after using the previously optimized conditions of 300 kV and 1500 µF (Momen-Heravi et al., 2014a). The cells were transferred to wet ice for 10 min and then cultured in media for 24 h in 12-well plates

(Thermo Fisher). Equimolar amounts of scrambled control oligonucleotide sequences (control miRNA mimic; Ambion) were introduced to cells via electroporation using the same approach.

MicroRNA mimics and relevant controls were forward transfected into RAW264.7 macrophages by Lipofectamine RNAiMAX (Life Technologies, USA) based on the manufacturer's protocol for cell transfection. Briefly, cells were transfected at 60 % confluency in 6-well plates. Lipofectamine RNAiMAX Reagent (9 µl) was diluted in 150 µl Opti-Mem medium (Invitrogen, Waltham, MA). Micro-RNA-122 mimic (3 µl) was added to Opti-Mem medium (150 µl). Diluted miRNA-155 mimic was then added to diluted Lipofectamine RNAiMAx Reagent (1:1 ratio) and incubated for 5 min. The miRNA-lipid complex was added to the cells in a dropwise fashion. The final amounts of miRNA-122 mimic and Lipofectamine RNAiMAx used per well were 25 pmol miRNA-122 mimic mass and 7.5 µl Lipofectamine, respectively.

2.2.7 LPS challenge protocol

After 48 h the cells were washed and treated with 10 nM LPS (*Escherichia coli* 0111:B4) (Sigma-Aldrich) for 6 h. Relative expression levels of HO-1 were quantified by qPCR and tumour necrosis factor alpha (TNFα) protein levels were measured in the supernatants by ELISA as described in detail in section 2.2.10.

2.2.8 Kuppfer cell (KC) and liver mononuclear cell (MNC) isolation

KC were isolated using an established protocol from pair-fed or alcohol-fed animals (n = 8) as described previously (Bala et al., 2011). Briefly, the liver was perfused under terminal anesthesia with 0.9 % w/v NaCl saline (Sigma-Aldrich) for 10 min, *in vivo* digestion was performed using Liberase enzyme (F. Hoffmann-la Roche, Basel, Switzerland) (40 µg/ml) for 5 min at room temperature, followed by an *in vitro* digestion for 30 min. The non-hepatocyte fraction of the liver was separated by Percoll density gradient (GE Healthcare, Pittsburg, PA) centrifugation. Briefly, the cell pellet was re-suspended in 10 ml of Hanks buffer (Thermo Fisher) mixed with 5 ml Percoll and centrifuged at 800 g for 60 min (4 ℃).

The inter-cushion fraction was washed 2 times with DMEM medium (centrifuged at 50 x g for 2 min) and adhered to cell culture 150 mm plastic plates (Thermo Fisher) in DMEM supplemented with 5% v/v fetal bovine serum. The non-adherent fraction was separated and washed, and the adherent KC population was used for downstream analysis or cell culture.

Liver mononuclear cells (MNCs) were isolated from another group of mice (n = 8) and separated by Percoll gradient using a literature protocol (Hritz et al., 2008).

2.2.9 Pretreatment of THP1 monocytes with miRNA-122 inhibitor via exosomes

The workflow of the series of these experiment included the following: First, exosomes were isolated from THP-1 cells and loaded with miRNA-122 inhibitor. miRNA-122 inhibitor loaded exosomes were added to the recipient naïve THP1 cells and co-cultured for 12 h with exosomes derived from ethanol-treated Huh7.5 cells. Afterwards THP-1 exosomes were washed off and ethanol-treated exosomes were added to the recipient THP-1 cells. Briefly, exosomes harvested by Exoquick-TC (System Biosciences) as described in section 2.2.4. Exosomes were re-suspended to a final concentration of 50 µl/ml in PBS buffer and added to Gene Pulser electroporation buffer (Bio-Rad Laboratories) at a 1:1 ratio. Oligonucleotides such as microRNA-122 inhibitor (Ambion) or negative control for miRNA inhibitor (Ambion) at final amount of 300 pmol were added to the exosome sample containing 1 µg/µl exosomal protein. The samples were transferred to a 0.2 ml electroporation cuvettes and electroporation was undetaken at 150 kV and 100 µF in a Gene pulser II System (Bio-Rad Laboratories). The loaded exosomes were treated with one unit of ribonuclease H (RNase H) (1 U/µl) (Thermo Fisher) for 1 h at room temperature to degrade free-floating or surface-adsorbed oligonucleotides and were re-isolated using ExoQuick-TC™ to a final concentration of 50 µg/ml of exosomal protein. Loaded exosomes were quantified by NTA and co-cultured with THP1 monocytes at 1 particle per cell ratio. After 12 h of co-culture, the exosomes were washed off by centrifugation of cell suspension at 500 x g for 10 min at 4 ºC. Afterward, the cell pellet was washed for 2 times in 10 ml PBS by centrifugation at 500 x g for 10 min at 4 °C. After the last wash with PBS, complete 1 ml RPMI media was added to the cell pellet and 6 h later exosomes derived from ethanol-treated Huh7.5 cells (ethanol exosomes) were added to THP-1 cells in a 1:1 ratio.

2.2.10   Enzyme-linked immunosorbent assay (ELISA)

Levels of TNFα (BD Biosciences, San Diego, CA), MCP1 (Biolegend, San Diego, CA) and Interleukin 1 beta (IL-1β) (R&D Systems, Minneapolis, MN) were measured in cell-free supernatants by enzyme-linked immunosorbent assay ELISA based on the manufacturer's recommendations. Briefly, for quantification of human TNFα and monocyte chemoattractant protein-1 (MCP1), anti-TNFα (150µl diluted capture antibody) and anti-MCP1 (100µl diluted capture antibody) were added to each well of 96-well Nunc-Immuno™ polystyrene

Maxisorp ELISA flat bottom plates (Thermo Fisher) and incubated overnight at 4 °C. TNFα and MCP1 plates were washed after 16 h 3 times with 300 µl of wash buffer provided by the supplier. For IL-1β microplates were coated with 200 µl (5 µg/ml) of a monoclonal antibody specific for human IL-1β. 300 µl of samples and standards (with concentration ranging from 3.9 –2000 pg/ml) were added to the plates and incubated for 2 h at 37 °C. The plates were washed 3 times with PBS. IL-1β, TNFα, or MCP-1 conjugate (polyclonal antibody against proteins conjugated to horseradish peroxidase) (200 µl) was added and incubated for 1 h at room temperature. After 3 more washes, 200 µl of substrate solution (1:1 of hydrogen peroxide and tetramethylbenzidine (R&D Systems) was added to the wells and incubated for 15 min at room temperature. The reaction was halted by adding 50 µl of stopping reagent. Optical densities were measured at 450 nm using a Synergy HTX Multi-Mode Reader (Winooski, VT) plate reader and data was processed with Gen5 v. 3.0 Software (Winooski).

2.3 The role of exosomes and miRNA-122 in HCV pathogenesis

2.3.1 Cell lines, primary human hepatocytes (PHH) and HCV J6/JFH-1 virus

Huh7.5 (passage 12), Huh7.0 (passage 11), primary human hepatocytes, and CD81-deficient Huh7.25 cells (passage 9) were grown and cultured according to the previously described method (Akazawa et al., 2007; Blight et al., 2002). Huh7.5, Huh7.0, and CD81-deficient Huh7.25 cells were cultured in T75 flasks in DMEM (Gibco) supplemented with 10 % v/v exosome-depleted fetal bovine serum (FBS) (Thermo fisher), and 1 % v/v of 10,000 U/mL penicillin/streptomycin (Thermo Fisher). After cells reached 70-80 % confluency, they were split 1:2. For splitting, culture medium was removed and cells were washed 3 times with 5ml PBS. Five ml Trypsin Ethylenediaminetetraacetic acid (EDTA) (Gibco) was added to cover the cells at the bottom of the flask. After cell detachment, conditioned media containing 10 % v/v FBS was added and cells were seeded at densities of $0.3x10^6$ in 12-well plates. In the exosome experiments, exosome depleted FBS (System Bioscience) was used.

The pFL-J6/JFH1 plasmid which encodes the entire viral genome of a chimeric strain of HCV-2a, was obtained from Charles M. Rice laboratory. Xbal (10 U/µL) (Thermo fisher) digestion was done to linearize plasmid. The plasmid was transcribed by a T7 RiboMAX (Promega, Madison, WI) in order to generate the full length viral genomic RNA. RQ1 RNase-free DNAse was added in concentration of 1 unit per microgram of template DNA and incubated for 15 min at 37 °C. One volume of phenol (pH 4–5):chloroform:isoamyl alcohol (125:24:1) (Sigma-Aldrich) was added and vortexed for 1 minute and centrifuged at

12000 x g in a microcentrifuge for 2 min. The upper aqueous phase was transferred to a fresh tube and 1 volume of chloroform:isoamyl alcohol (24:1) was added and then centrifuged at 12000 x g for 2 min. The upper aqueous phase was transferred to a fresh tube. A 0.1x volume of 3M Sodium Acetate (pH 5.2) and 1 volume of isopropanol or 2.5 volumes of 95 % v/v ethanol was added and mixed on ice for 5 min and centrifuged at the top speed in a microcentrifuge (~21,000 × g) for 10 min. The supernatant was aspirated and pellet was washed with 1 ml of 70 % v/v ethanol. The pellet was dried under vacuum and the RNA sample was re suspended in 100 µl nuclease-free water.

The RNA (10 µg) was transfected into Huh7.5 cells by electroporation (280V, 1000µF) using a Gene Pulser (Bio-Rad). The Huh 7.5 cells were cultured in complete condition medium to produce replication-competent HCV virus (J6/JFH1; genotype 2a) (Lindenbach et al., 2005; Mohd-Ismail et al., 2009).

HCV J6/JFH-1 virus and exosome concentrations in culture supernatants were measured using a NanoSight LM10 (Malvern). The multiplicity of infection (MOI) of infectious viral particles or infectious exosomes was determined by the number of particles and by quantitative real-time PCR as described previously (Bukong et al., 2013).

2.3.2 Exosome isolation and purification from patients' sera and cell lines

Cell culture supernatants (10 ml) or patient sera (500 µl) were collected and centrifuged at 2500 revolutions per minute (rpm) for 10 min (4 °C) to remove cell debris. The resulting supernatants were serially filtered through 0.8 µm, 0.4 µm, and 0.2 µm filters and were subsequently loaded into a Amicon Ultra-15 Centrifugal Filter Unit with an Ultracel-100 membrane (EMD Millipore, Billerica, MA) to be centrifuged using a Beckman GH 3.8 Swing Bucket Rotor (Beckman Coulter, Brea, CA) for 30 min at 4 °C to concentrate samples to 1ml. These were mixed with the appropriate volume of Exoquick-TC reagent (ratio of 5:1) (System Bioscience) or Exoquick (System Bioscience) (ratio of 4:1) respectively as indicated by the manufacturer for exosome isolation.

HCV infected patients and healthy controls were recruited from the Hepatology clinical unit at the University of Massachusetts Medical School (Worcester, MA, USA). This research protocol was approved by the institutional review board (#2284). Blood samples were collected and serum was analyzed for HCV RNA using RT-PCR.

Concentrated culture supernatants (500 µL) or filtered patient sera (150 µL) were mixed with 1500 µL of Exoquick-TC reagent (System Biosciences, USA) or 50 µL of Exoquick (System Biosciences), respectively. The samples were incubated for 1 h at 4 °C. Exosomes were precipitated by centrifugation at 1400 rpm for 10 min at 4 °C and re-suspended in 100 µl PBS. In the experiments involving the isolation of exosomes from virus suspensions, positive selection of exosomes was performed using anti-CD63 immuno-magnetic capturing method. Primary anti-CD63 antibody (25 µl) (Abcam, USA) was added to the concentrated supernatant (500 µl) and incubated for 4 h at 4 °C. Secondary antibody coupled to magnetic beads (50 µl) (Miltenyi Biotec, Auburn, MA) was added to the concentrated supernatant (500 µl). LD columns (Miltenyi Biotec) were prewashed with 5 ml of 1x PBS for 3 times and columns were attached to the Miltenyi Biotec MidiMACS separator attached to a Miltenyi Biotec MultiStand. The column was placed with the column wings to the front into the magnetic field of the MidiMACS Separator and exosome suspension was added to the column. The column was washed with 5 ml PBS to eliminate other particles not expressing CD63. The column was detached and washed with 400 µl of PBS to re-suspend CD63$^+$ exosomes. Quantification of the number of virus particles or exosomes was performed using a NanoSight LM10 system (NanoSight). HCV RNA copy numbers were quantified by RT-PCR previously (Bukong et al., 2013). Briefly, 10 µL of viral RNA was reverse transcribed to cDNA (Applied Biosystems, USA). The final reaction volume was 20 µL. Viral cDNA (5 µl) in addition to pFL-J6/JFH1 plasmid standard (5 µl) were used for qPCR to contain 10, 100, 1000, 10,000, 100,000, 1000,000, 10,000,000 copies per 5 µL. This standard curve was used for quantification of the amount of viruses in exosomes, supernatant, and cells.

2.3.3 Co-immunoprecipitation, RNA Chromatin immuno-precipitation (ChIP) and analysis of exosomes

Exosomes purified from cell culture supernatants or patient sera were fixed at room temperature with 4 % v/v formaldehyde buffered saline (Sigma-Aldrich). After fixation, exosomes were lysed in 100 µl sodium dodecyl sulfate (SDS) ChIP lysis buffer (Millipore), supplemented with protease inhibitor (Sigma Aldrich) at a 1:10 ratio and RNase inhibitor (Ambion) (1 U/µl) to a final inhibitor concentration of 1 U/µl. Primary anti-Ago2 antibody (Anti-Ago2, 10 µg/ml; Abcam, Cambridge, MA) was added to 50 µg of exosomal total protein and incubated for 90 min at 4 °C. 20 µg of re- volume of A/G PLUS Agarose beads from the stock concentration of 0.5 ml agarose/2.0 ml (Santa Cruz, Dallas, Texas) was added to the sample and the tube was incubated on a rocker platform for an additional 60 min at 4°C. Immunoprecipitates were collected by centrifugation at 1100 g for 5 min at 4 °C. Pellets were washed for three times with SDS ChIP lysis buffer (500 µl) and by repeating

1100 g for 5 min at 4 °C centrifugations and pellet re-suspended in 35 µl of 1x electrophoresis sample buffer. The immunoprecipitated protein-RNA complexes were used for downstream western blot analysis or RNA isolation.

2.3.4 Use of targeted siRNA and miRNA inhibitor therapy and cell transfections

The following siRNA and miRNA inhibitors were used: human heat shock protein 90 (HSP90) siRNA (Santa Cruz, USA), scrambled control siRNA (Santa Cruz), hsa-miRNA-122 anti-miRNA miRNA Inhibitor (Ambion, USA) and anti-miRNA Negative Control (Ambion, USA). miRNA inhibitors were introduced into Huh 7.5 cells using the liver *in vivo* altogen transfection reagent (Altogen Biosystems, USA).

Evaluation of miRNA inhibitors in Huh7.5 cells was performed using a forward transfection protocol at final oligonucleotide concentrations of 30 nM. Briefly, 8×10^4 cells were plated in 12 well plates for 24 h in 1 ml growth media to ensure adherence. Ahead of transfection, 4 µl of liver in vivo altogen transfection reagent was vortex-mixed with 45 pmol oligonucleotide dissolved in RNAse free water (Thermo Fisher) at 100 µl final volume. During a 20 min room temperature incubation of the transfection mix, the cells were washed 3x with 0.5 ml of 1x PBS and fresh media was added (900 µl), supplemented with 100 µl of transfection mix at the end of the mix incubation period. Cells and supernatants were harvested at the indicated time points.

2.3.5 Use of protease inhibitor and vacuolar-type H⁺-ATPase inhibitor (bafilomycin A1) for the inhibition of HCV infectious exosomes and virus

Using 10^5 Huh7.5 cells in 12-well plates, Telaprevir (VX-950; Selleckchem, Houston, Texas) was added at 10 ng/ml and 20 ng/ml concentrations, 24 h after infection with 1 MOI of virus suspension or exosomes derived from HCV-infected hepatocytes. Alternatively, Bafilomycin A1 (Sigma-Aldrich) was dissolved in dimethyl sulfoxide (DMSO) and administered to cells at different concentrations (12.5 nM, 25 nM, 50 nM and 100 nM) with the final DMSO concentration of DMSO being 0.01% v/v. After 1 h, HCV virus suspension and exosomes derived from HCV-infected cells were added to the Bafilomycin A1-treated Huh7.5 cells at an MOI of 1. After 24 h, the media were removed and cells washed 3 times with 1 ml PBS. Viral RNA entry was assessed by performing qRT-PCR (Forward Primer: 5′-TCTGCGGAACCGGTGAGTAC-3′; HCV Reverse primer: 5′-

TCAGGCAGTACCACAAGGCC-3') for detection of positive sense HCV 5′ UTR on 500 ng RNA extract samples obtained as described in section 2.1.1.

2.4 Salivary miRNA as biomarkers of oral cancer

2.4.1 Saliva collection and RNA extraction

This protocol was approved by the Institutional Review Board (Texas A&M University/Baylor College of Dentistry; # 0361). The saliva samples were collected from 34 subjects: 9 oral squamous cell carcinoma (OSCC) patients before surgical resection of tumor, 8 patients with oral squamous cell carcinoma in remission (OSCC-R), 8 patients with oral lichen planus (OLP), and 9 healthy controls (HCs). Unstimulated saliva was collected from the participants between 6 and 11 am, following a previously published protocol (Cheng et al., 2011). Briefly, participants were asked to refrain from drinking, eating, or applying oral hygiene procedures on the day of saliva collection. Individuals rinsed their mouth with water before saliva collection to minimize contamination of the samples. After 5 min, the participant sat upright and spat into a 50 mL Falcon tube, which was kept on ice. A maximum of 8 mL of saliva was collected from each individual in 30 min.

Saliva samples were centrifuged at 2,600 g for 15 min at 4 °C to remove the cellular debris. The RNase inhibitor (SUPERase-In, Ambion, USA) was added to the supernatant (5 µL of SUPERase-In per mL of supernatant), as previously described (Hu et al., 2008). RNA isolation was done as described in section 2.1.1.

2.4.2 NanoString nCounter miRNA assay for miRNA profiling

The whole genome multiplexed NanoString nCounter miRNA expression assay (NanoString Technologies, Seattle, WA) was used for miRNA profiling according to the manufacturer's protocol. Briefly, 100 ng of total RNA in 3 µl was used as input material. A unique DNA tag was ligated onto the 3′ end of each mature miRNA in the samples, providing specific identification for each miRNA species present. The tagging was done in a multiplexed ligation reaction using reverse complementary bridge oligonucleotides, which disposed the ligation of each miRNA to its designated tag. Hybridization reactions were done at 64 °C for 18 h with a final concentration of 10 µL Reporter CodeSet, 10 µL hybridization buffer, 5 µL aliquot from the miRNA sample preparation protocol and 5 µL Capture ProbeSet per reaction. Afterwards, excess tags were washed away using a two-step magnetic bead-based purification on the nCounter™ Prep Station and the resulting materials were hybridized with a panel of fluorescently barcoded reporter probes which were specific to the miRNAs. Levels

of miRNAs were quantified with the nCounter Prep Station and Digital Analyzer by enumerating individual miRNA- specific fluorescent barcodes. A high-density scan (600 fields of view) was performed and samples were normalized to the geometric mean of the top 100 most highly abundant miRNAs (Leichter et al., 2015).

2.4.3 Real-time quantitative polymerase chain reaction for salivary miRNA

Real-time quantitative polymerase chain reaction (qPCR) was done to validate significant candidates obtained by the NanoString nCounter miRNA assay as described in section 2.1.2. Significant candidates were determined using Welch's t-test, which assess the likelihood that a set of gene counts is significantly different than the set of background counts. Samples were first screened for identifying a stable endogenous normalizer in miRNA profiling data. We systematically screened for stability of different miRNAs by testing 10 pooling samples and 32 individual saliva samples of different study groups, using the NormFinder algorithm version 0.953 (Andersen et al., 2004). NormFinder determines the intragroup and intergroup variations using a model-based approach. It combines these two types of variation into a stability value, effectively adding the two sources of variation to obtain a practical measure of the systematic error of an investigated gene measurement, enabling gene rank ordering and grouping. Since miRNA-191 expression levels showed the lowest intragroup and intergroup variability, it was used as a reference internal normalizer. All reactions were run in triplicate. The qPCR reactions were carried out in an MJ Research PTC-200 Thermal Cycler and miRNA expression was compared using the $2^{-\Delta\Delta Ct}$ method as explained in section 2.1.3. One-way analysis of variance (ANOVA) was used to assess differential expression between groups followed by Tukey's HSD test for pairwise comparison.

2.5 Methods for exosome-based targeted therapy

2.5.1 Cell culture and exosome isolation

Murine B cells (M12.4) were used as the source of vehicle exosomes in miRNA inhibitor and miRNA mimic studies. M12.4 cells were cultured in an RPMI medium, in addition to 10 % v/v exosome-depleted FBS (Exo-FBS™, Mountain View, CA, USA), and 1 % w/v penicillin / streptomycin (Gibco®). After 12 h, the cells were stimulated by CD40 (5 μg/ml) (PeproTech, USA) and Interleukin 4 (IL-4) (50 ng/ml) (PeproTech, USA). Three days later, the culture media were collected and exosomes were isolated by Exoquick as described in section 2.2.4. RAW 264.7 macrophages were cultured in Dulbecco's modified medium (Invitrogen) plus 10 % v/v FBS at seeding density of 8 x 10^4 /well/2 ml medium (passage

number of 14) in 12-well plates for co-culture experiments. RAW 264.7 macrophages were used for exosome production at seeding density of 3 x 10^6 /12 ml medium in T-75flasks (passage number of 14).

2.5.2 Optimizing loading conditions of exosomes with miRNA-155 mimic

A PBS suspension of freshly isolated exosomes was diluted in Gene Pulser® (Bio-Rad Laboratories, USA) electroporation buffer at a 1:1 ratio. miRNA-155 mimic or negative miRNA control 1 (Ambion) at a final mass of 150 pmol was added to 0.25 μg/μl, 0.5 μg/μl, 1 μg/μl, and 1.5 μg/μl of exosome sample. Cold (4 ℃) electroporation cuvettes (gap width: 0.2 cm) were used and the exosomes were electroporated at various voltages (0.130 kV to 0.200 kV) at a constant capacitance of 100 μF. After optimization of the voltage, the effect of variation in capacitance was assessed. Electroporation was performed using a Gene pulser II System (Bio-Rad Laboratories). One unit of RNase H was administered per exosome suspension for 1 h to eliminate free floating or surface-adsorbed oligonucleotides. Exosomes were next re-isolated using Exoquick-TC™. Synthetic *C. elegans* (cel)-miRNA-39 (5 µl of a 5 fmol/μL stock tube) was spiked during the total RNA isolation process and used to normalize the qPCR data as an endogenous control The relative amount of encapsulated miRNA-155 was determined using TaqMan® miRNA Assays as described in section 2.1.2.

Next, to determine the most efficient isolation method to re-isolate exosomes after the electroporation procedure, we compared the three methods of ultracentrifugation, CD63 immunomagnetic isolation, and Exoquick-TC™. In the first step, exosomes were isolated using CD63 immunomagnetic beads as delineated in section 2.3.2. 150 pmol of miRNA-155 mimic was electroporated into 50 μg of exosomes. The RNase H was added to the exosome suspension for a total duration of 1 h to eliminate free floating, unloaded miRNA-155 mimic. Exosomes were re-isolated with different isolation methods including ultracentrifugation, immunomagnetic isolation, and Exoquick-TC™. Ultracentrifugation was performed at 100,000 g for 90 min using fixed angle 75 Ti rotor (Beckman Coulter), at 4°C. Exoquick-TC™ and immunomagnetic isolation methods were performed as outlined in section 2.2.4. Cel-miR-39 (150 pmol) was added to the samples before RNA isolation and RNA isolation was done as described in section 2.1.1. The experiments were performed in triplicate and the amount of recovered miRNA-155 was quantified by TaqMan® miRNA Assays as described in section 2.1.2. The cycle number at which the reaction reached an arbitrarily-placed threshold (CT) was determined for each sample and the relative amount of miRNA-155 to

cel-miR-39 was described using the equation $2^{-\Delta CT}$ where $\Delta Ct = (Ct_{miRNA-155} - Ct_{cel-miR-39})$ (Schmittgen et al., 2008).

In order to quantify the efficacy of loading, B cell derived exosomes were purified and loaded with miRNA-155 using the optimal conditions (e.g. voltage and concentrations). After loading, exosomes were re-isolated using the Exoquick-TC™ reagent according to the manufacturer's instructions. To remove aggregates of miRNA-155 mimic outside the exosomes, the exosome pellet was treated with one unit of RNase H. Exogenous cel-miRNA-39 was spiked to the samples before RNA isolation and used an exogenous control to calculate loading efficiency. Subsequently, the total RNA was extracted. The proportion of miRNA-155 mimic that was loaded into the exosomes was calculated using the following formula:

$$f_{miRNA-LE} = \left(\frac{V_c C_c MW_c}{V_s C_s MW_s}\right)\left(\frac{RE_s}{RE_c}\right)$$

Where $f_{miRNA-LE}$ (miRNA-LE is the miRNA loading efficiency) is the fraction of miRNA which was successfully loaded into the exosomes; V_c is the volume of added exogenous spiked control; C_c is concentration of exogenous control; MW_c is molecular weight of the exogenous control; V_s is the volume of electroporated miRNA sample; C_s is the concentration of the sample; MW_s is the molecular weight of the loaded miRNA-155 mimic; RE_s is the relative expression of miRNA-155 mimic and RE_c is relative expression of the control (spiked cel- miRNA-39). Using this formula, our "optimal" loading protocols led to efficient loading of miRNA-155 mimic into the exosomes (55.06%).

2.5.3 Enzyme-linked immunosorbent assay (ELISA)

TNFα protein levels were measured using a Mouse TNFα ELISA kit (BD Biosciences, USA) as described in section 2.2.10. Supernatants (400 µl) were collected from the cells and centrifuged at 2000 g for 10 min to remove cellular debris and then frozen at −80 °C until use. Protein levels of IL-1β, TNFα, and MCP1 were quantified in the supernatant by ELISA. The quantification of TNFα (BioLegends, USA), MCP1 (BioLegend Inc., USA) and IL-1β (R&D Systems, USA) were carried out based on the manufacturers' recommendations using a Synergy HTX Multi-Mode ELISA reader.

2.5.4 Lactate Dehydrogenase (LDH) cytotoxicity assay

The lactate dehydrogenase (LDH) level was measured in the supernatant of RAW264.7 macrophages based on the manufacturer's recommendation (Abcam). Released LDH in culture supernatants of RAW macrophages was quantified 36 h after delivery of miRNA-155 inhibitor via different methods with relevant controls. The percentage of cytotoxicity was calculated by subtracting the LDH content in the supernatant of remaining viable cells from the total LDH in the supernatant of untreated controls. Staurosporine (20 nM) (Abcam) served as a positive control for cell death. The final absorbance was measured at 490 nm with a Synergy™ HTX Multi-Mode Microplate Reader. Results were expressed as the mean of three independent experiments.

2.6 Biodistribution of miRNA-155 and exosomes

2.6.1 Animal studies

Mice deficient in miRNA-155 (miRNA-155 knockouts; KO) and C57/Bl6J wild type (WT) (eight- to ten-week old) male or female mice were purchased from Jackson Laboratory (Farmington, CT). All experimental protocols were approved by the Institutional Animal Use and Care Committee of the University of Massachusetts Medical School (Worcester, MA). Female WT mice were injected with saline or 2.5 mg/kg CpG (Sigma-Aldrich) by intraperitoneal injection (i.p.) at 24 h intervals for three days to increase miRNA-155 in the circulation (Petrasek et al., 2011). On day 4, the mice treated with CpG received 0.5 mg/kg LPS (i.p.) 3 h before sacrifice. At the end of treatment, mice were cheek bled and plasma was separated from the blood and stored at $-80\,°C$ for downstream analysis. The liver and other tissues were washed several times with PBS and immediately either snap frozen in liquid nitrogen (protein analyses) or diced and placed in RNA*later* (Qiagen, USA) for downstream experiments.

EDTA-containing microtainer tubes (BD Biosciences) were used for blood collection and plasma was isolated by centrifugation at 2000 g for 10 min at room temperature. The centrifugation step was performed twice to minimize platelet contamination. The separated plasma fraction was aliquoted and stored at $-80°C$ for further analysis.

2.6.2 Tissue collection, perfusion and cell isolation

At the desired time points of the experiments, various organs were removed, immediately washed in PBS, blotted on tissue and stored in RNA*later* at $-80\,°C$. Different liver cell

populations were isolated after perfusion based on a described protocol (Csak et al., 2011). Briefly, mice were anesthetized with ketamine (300 mg/kg, i.p.) and the liver was perfused with sterile saline solution for 10 min followed by *in vivo* digestion with 50 ml of Hanks balanced salt solution (HBSS) solution and 0.8 mg/mL of collagenase type 1 (Sigma Aldrich) for 5 min. The perfused liver was set on a petri dish containing 15 ml HBSS and 0.02 % collagenase (Sigma Aldrich) and cells separated. To separate hepatocytes, the cell suspension was centrifuged (200 g for 5 min) at room temperature (Csak et al., 2011). The pellet containing hepatocytes was washed with 5 ml PBS twice. The cell number was quantified with a Beckman Coulter Z1 cell counter (Beckman Coulter, Fullerton, CA) according to the manufacturer's instructions. Hepatocytes were cultured in DMEM Low Serum with 1 % w/v Penicillin-Streptomycin (Thermo Fisher) and 10 nM insulin (Thermo Fisher). Mononuclear cells and KCs were isolated using an established protocol as described in section 2.2.8 and in the literature (Hritz et al., 2008; Bala et al., 2011).

Chapter 3
Results

3.1 The role of exosomes in the pathogenesis of alcoholic liver disease

Different liver cells including hepatocytes, KCs, hepatic stellate cells, and sinusoidal endothelial cells are affected by the deleterious effects of alcohol and participate in the pathogenesis of alcoholic liver disease (Cohen and Nagy, 2011). Immune cells are also affected by alcohol and play pivotal roles in the process (Nagy, 2015; Gao and Bataller, 2011). Thus, alcohol-induced damage has been reported to lead to the release of pro-inflammatory cytokines, lipid messengers, chemokines, and reactive oxygen species that further potentiate cell damage (Brenner et al., 2013). It has been previously shown that circulating exosomes in relevant mouse disease models carry miRNA-122 (Bala et al., 2012), a liver specific miRNA, mainly found in hepatocytes but considerably less so in other tissues and other cell types including immune cells: it's function outside the liver is unknown (Lagos-Quintana et al., 2002). Tissue-specific miRNA profiling in different organs has previously shown that miRNA-122 represents 70–80 % of the total miRNA in hepatocytes (Lagos-Quintana et al., 2002). It has been previously reported that exosomes can be taken up by monocytes and modulate their function. For example, exosomes were taken up by human monocytic THP-1 cells and transferred their miRNA-223 to those cells. Functional activity of miRNA-223 was confirmed by 3′-UTR luciferase reporter vector to which miRNA-223 binds (Ismail et al., 2013). We hypothesized that exosomes derived from ethanol-exposed hepatocytes can convey messages to monocytes and modulate their immune function (Momen-Heravi et al., 2015a; Saha et al., 2015).

3.1.1 Binge alcohol consumption increases the number of circulating exosomes in sera of healthy human subjects and mice

It has been shown that binge alcohol drinking can induce deleterious health effects and rapid increase in serum endotoxin and 16S rDNA, a marker of bacterial translocation from the gut, as well as increase in circulating inflammatory cytokine profile such as TNF-α, IL-β, and MCP-1 (Bala et al., 2014). We thus first evaluated the change in the number of exosomes

after binge alcohol drinking. Measurement of exosome numbers in the sera of healthy individuals (n = 11) before and after binge alcohol drinking was done at various time points (30 min-24 h) by a Nanoparticle Tracking Analysis (NTA) system. These studies revealed that the number of exosomes in man increased significantly as early as 30 min after drinking and this increase remained statistically significant at other tested time points (1 h, 2 h, 3 h, 4 h, and 24 h) (Figure 3.1A). Profiling of these exosomes revealed significantly higher levels of the liver-specific miRNA-122 specifically, peaking after 4 h of alcohol consumption compared to baseline levels. There was no substantial difference in miRNA-122 expression level in control subjects at different corresponding time points. Thus, although other miRNAs were also elevated in response to binge alcohol consumption, the levels of e.g. miRNA-155 peaked at 30 min, suggesting differential exosomal miRNA release kinetics in response to alcohol consumption (Figure 3.1B). In stark contrast, control subjects receiving the same volume of juice did not exhibit any statistically significant exosome and exosome-contained miRNA changes across any of the timepoints surveyed.

In mice, binge alcohol consumption induced a significant increase in the total serum number of exosomes 6 h and 12 h post ethanol consumption ($p < 0.05$) (Figure 3.1C). In line with the human data, expression levels of exosomal miRNA-122 (12 h) were significantly increased compared to saline-fed animals ($p < 0.05$) (Figure 3.1D). Similarly, in the chronic alcohol feeding model, after 5 weeks, the number of circulating exosomes in serum was significantly increased compared to the pair-fed control mice (Figure 3.1E), as were the levels of exosomal miRNA-122 (Figure 3.1F).
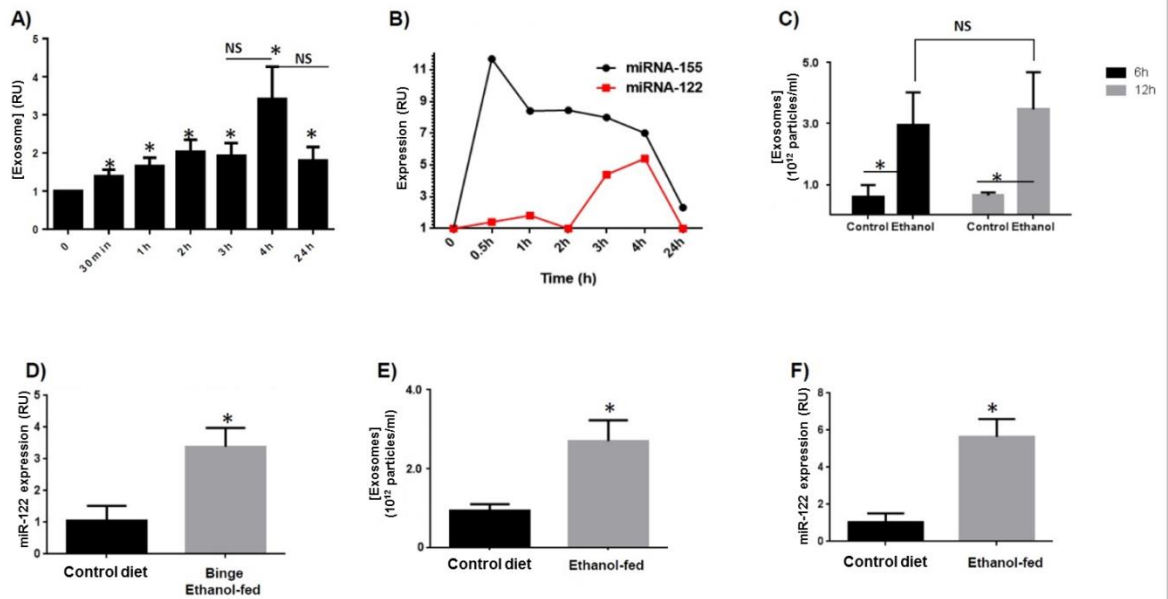
Figure 3.1: Effect of alcohol in exosome production in humans and mice. (A) Changes in total serum exosome concentration after alcohol binge drinking in healthy human subjects relative to pre-drinking levels, as determined by NTA (n=11). Units are given in RU (Relative Units) (B) Serum exosomal miRNA-155 and miRNA-122 levels in humans during a 24 h binge drinking alcoholic challenge study. (C) Exosome levels in mouse sera 6 h and 12 h after binge alcohol drinking as determined by NTA. (D) Exosomal miRNA levels in mouse sera after a binge-ethanol feeding challenge. (E) Effect of chronic alcohol feeding (n=6) for 5 weeks on serum exosomes as quantified by NTA. (F) miRNA-122 levels in mouse serum exosomes after a 5 week alcohol diet. The results were averaged from three independent experiments. (*indicates $p < 0.05$ versus control conditions)*This figure is adapted from Momen-Heravi et al., 2015, Scientific reports*

3.1.2 The number of exosomes correlates with ALT levels

Serum exosome concentration (particles/ml) showed a strong and statistically significant correlation with ALT levels (IU/L) (Spearman's Rho, $r = 0.8$; $p < 0.05$; Figure 3.2A). A significant fraction of total serum RNA was associated with the serum-exosomes compared to the exosome-depleted serum (Figure 3.2B).
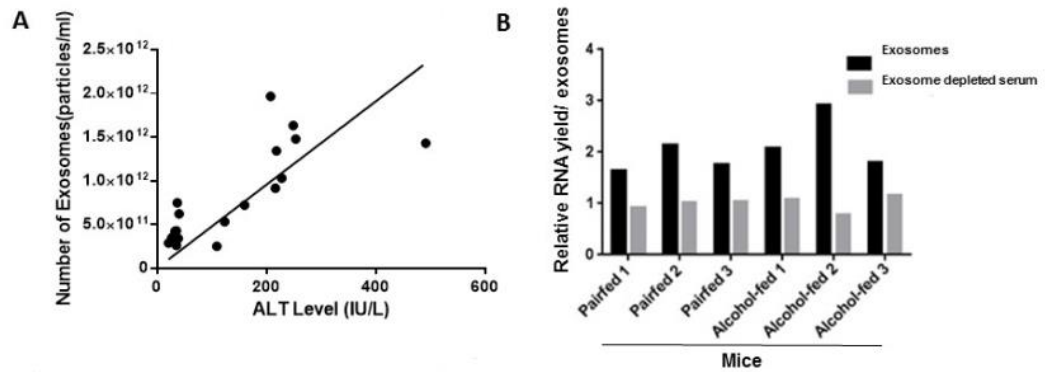
Figure 3.2: Correlation between the number of exosomes and ALT level and relative RNA yield of exosomes. (A) Correlation between serum ALT level and exosome number in the sera of chronically alcohol-fed mice. (B) Fraction of total RNA associated with exosomes in pair-fed and control mice, expressed relative to the geometric mean of total RNA yield from exosome depleted serum. Relative amount of total RNA associated with exosome fraction was calculated with regards to that geometric mean.

This figure is adapted from Momen-Heravi et al., 2015, Journal of Translational Medicine

3.1.3 Alcohol increases the exosome production in hepatocytes

Treatment of Huh 7.5 cells with various concentrations of ethanol as a model of human alcohol consumption (25 mM: moderate consumption; 50 mM: heavy consumption; 100 mM binge/chronic consumption) showed a significant increase in the number of exosomes at different time points post ethanol exposure (24 h, 48 h, and 72 h; $p < 0.05$; Figure 3.3 A, B, C) in both a dose- and time-dependent manner. Accordingly, the mRNA expression level of Rab 27b, the protein that plays a role in late endosomal formation (Ostrowski et al., 2010), was significantly increased after ethanol exposure ($p < 0.05$), suggesting activation of exosome biogenesis pathways by alcohol treatment (Figure 3.3D).
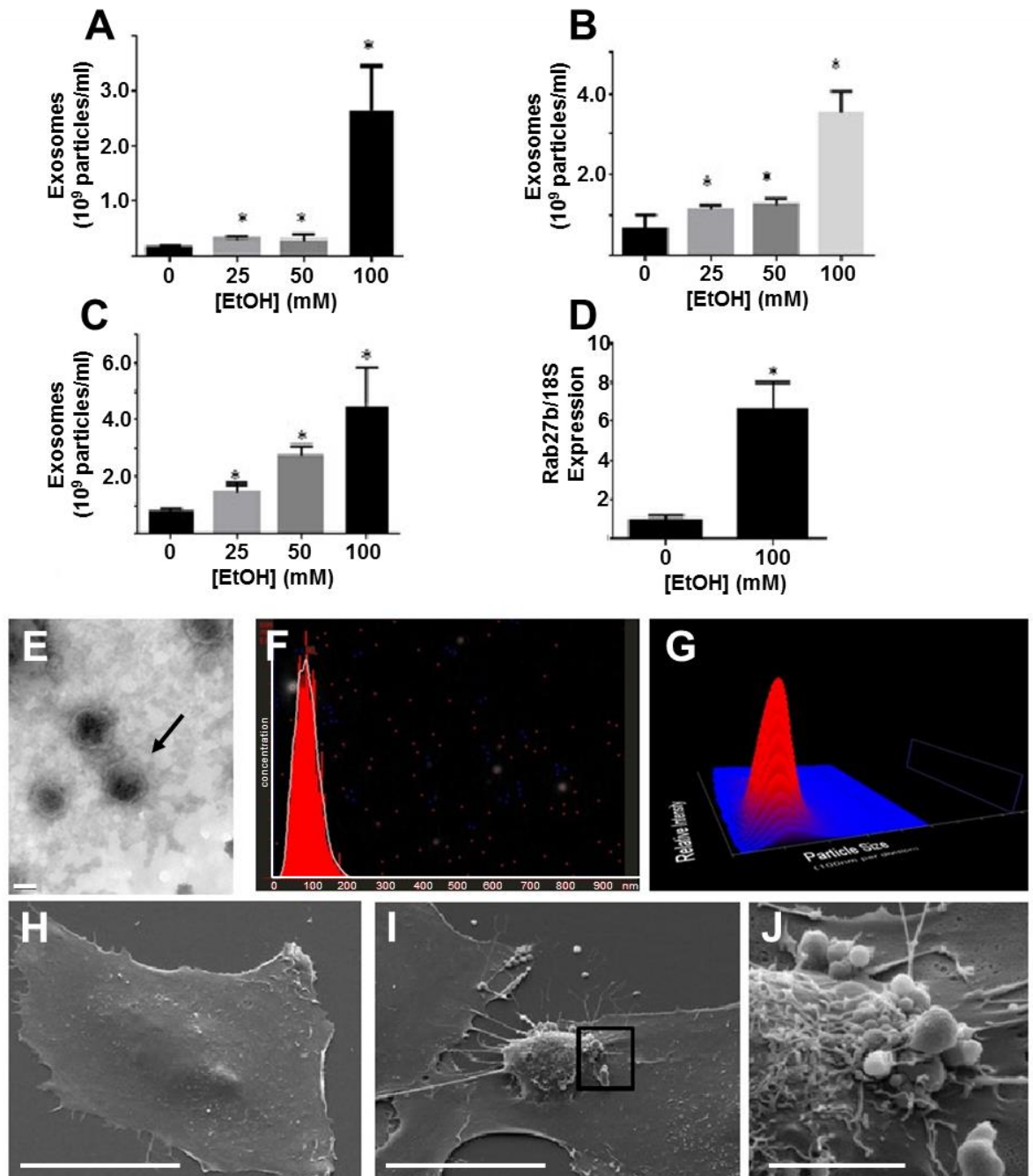
Figure 3.3: The effect of ethanol on the production of exosomes by Huh7.5 cells. Cells were exposed to increasing concentrations of ethanol ahead of collection and analysis of exosomes by NTA at 24 (A), 48 (B) and 72 hrs (C). (D) The level of Rab27b was quantified by qRT-PCR in Huh7.5 cells 48 h after 100 mM ethanol treatment. (E) TEM of exosomes isolated from Huh7.5 cells isolated after 48 h of 100 mM ethanol treatment (scale bar: 50 nm). The arrow indicates a single exosome. (F), (G) Exosome size distribution identified with NTA. (H),(I),(J) SEM of exosomes produced by Huh 7.5 cells treated with 100 mM ethanol for 48 h. SEM Scale bars: 30 µm (H,I), 5 µm (J). Statistically significant changes in exosome release or gene expression are indicated by '*' ($p < 0.05$ compared to the control conditions). *This figure is adapted from Momen-Heravi et al., 2015, Scientific reports.*

3.1.4 Characterization of exosomes derived from cultured and primary hepatocytes

Given dose and time dependent exosome release effects were most prominent under the binge/chronic consumption model conditions, further analysis was focused to this aspect of the disease. Exosomes derived from Huh7.5 cells had diameters in the range of 50–150 nm and showed the previously described liposome-like morphology on TEM (Momen-Heravi et al., 2012a) (Figure 3.3E). The mean vesicle size was 90 nm and they expressed the exosomal marker CD63 (Figure 3.3 F&G). Scanning electron microscopy (SEM) showed an increased number of exosomes after ethanol treatment in accordance with NTA measurements. (Figure 3.3H).

RNA size profiling showed an increase in exosomal small RNA cargo after ethanol treatment (100 mM) which was also observed with small RNAs (Figure 3.4 A-C). Given miRNA-122 is the principally expressed miRNA in Huh7.5 cells, we investigated miRNA-122 expression in this system. Thus, treatment of Huh 7.5 cells with ethanol resulted in a slight increase in cellular miRNA-122 levels, however, exosomes derived from ethanol-exposed Huh7.5 cells demonstrated significantly elevated levels of miRNA-122 ($p < 0.05$; Figure 3.4C and D). In contrast, the level of miRNA-29b was significantly decreased in the exosome fraction after ethanol exposure ($p < 0.05$; Figure 3.4E). MicroRNA 29b has been reported to play roles in the pathogenesis of liver diseases such as biliary atresia, liver fibrosis and cirrhosis (Szabo and Bala, 2013). This data indicated that miRNA sorting into the exosomes is a regulated and specific process.
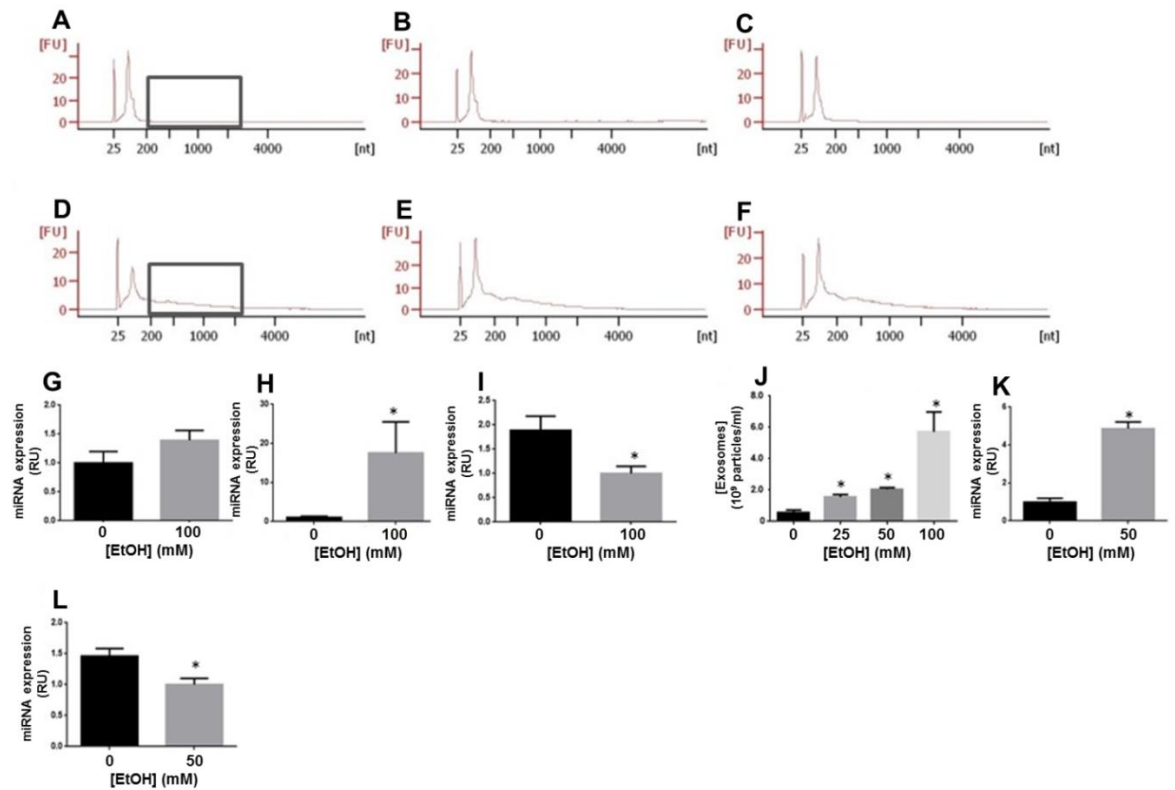
Figure 3.4: Characterization of exosomal small RNA and miRNA cargo in Huh 7.5 cells and primary human hepatocytes. (A-F) The graphs represent results obtained from an Agilent bioanalyzer small RNA kit, characterizing the distribution of the RNA cargo of exosomes. (A-C) Represents the small RNA profile in the control exosomes derived from Huh7.5 cells in three different specimens. (D-F) Represents the small RNA profile in the exosomes derived from ethanol-exposed Huh7.5 cells in three different samples. The difference in distribution of non-coding RNAs in exosomes derived from ethanol-exposed cells compared to exosomes derived from control cells is annotated by gray boxes in the graphs. (G) Levels of miRNA-122 were quantified in the Huh 7.5 cells treated with ethanol (100 mM) and control cells using a TaqMan® miRNA assay. (H) Levels of miRNA-122 were quantified in the exosomes derived from ethanol-treated (100 mM) Huh7.5 cells and control exosomes using a TaqMan® miRNA assay. (I) The levels of miRNA-29b were quantified in the exosomes derived from ethanol-exposed (100 mM) Huh7.5 cells and control exosomes by a TaqMan® miRNA assay. (J) The total number of released exosomes was quantified in primary human hepatocytes treated with different dosages of ethanol (25 mM, 50 mM, and 100 mM) for 48 h by an NTA system. The total number was shown as particles/ml. (K) The levels of miRNA-122 was quantified in the exosomes derived from primary human hepatocytes after administration of ethanol (50 mM for 48 h) by a TaqMan® miRNA assay. (L) The levels of miRNA-29b in the exosomes derived from primary human hepatocytes were quantified after administration of ethanol (50 mM for 48 h) by a TaqMan®

miRNA assay. The results are obtained from three independent experiments. (*indicates $p < 0.05$ compared to the control conditions)

This figure is adapted from Momen-Heravi et al., 2015, Scientific reports

To validate the cell culture findings, we next evaluated exosome production in primary human hepatocytes after ethanol exposure. Thus, repetition of the studies ranging 25-100 nM [EtOH] recapitulated both the increased exosome production and altered miRNA-122 and miRNA-29b gene expression changes ($p < 0.05$) (Figure 3.3 J-L).

3.1.5 Exosomes derived from ethanol-treated hepatocytes horizontally transfer mature miRNA-122 to monocytes

To investigate the function of these ethanol-induced, hepatocyte-derived exosomes with respect to the immune system, exosomes derived from ethanol-exposed Huh7.5 were co-cultured with a monocytic cell line. Thus, co-culture of PKH2 (green fluorescent cell linker) labeled hepatocyte-derived exosomes resulted in uptake of exosomes by THP-1 monocytes after 6 h, as shown by confocal microscopy (Figure 3.5).
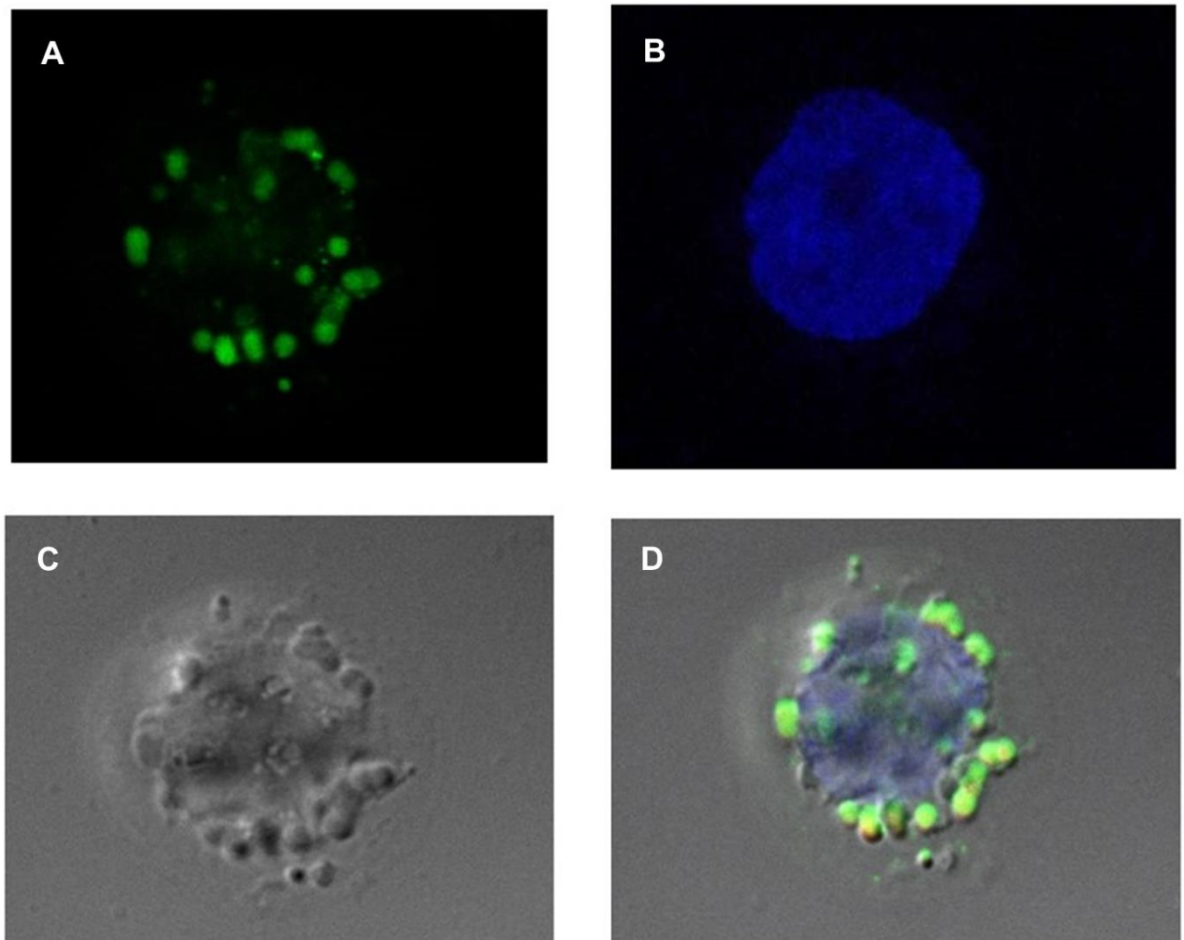
Figure 3.5: Confocal microscopy, fluorescent labeled exosomes were taken up by THP1 monocytes. Exosomes were fluorescently labeled with PKH67 (A, green) and co-cultured with THP1 monocytes for 6 h. DAPI was used for the staining of nuclei (B). Nomarski Interference Contrast (NIC) was used for visualizing the cytoplasm (C). THP1 monocytes had taken up exosomes, which was indicated by the presence of green fluorescently labeled exosomes in the cytoplasm of the THP1 cells after merging the images (D). (Magnification:40k)

This figure is adapted from Momen-Heravi et al., 2015, Scientific reports

Furthermore, the observed exosome uptake resulted in a 5–8 fold increase in the expression level of the mature form of miRNA-122 in THP1 monocytes, in an alcohol and TLR4 signaling-independent fashion as indicated through relevant controls (Figure 3.6A). To preclude the possibility this was on account of miRNA-122 transcription induction in the exosome-receiving THP1 cells we measured the expression levels of pri-miRNA-122. Thus, whilst Pri-miRNA-122 was exclusively detected in hepatocytes, transcript levels were below the assay detection limit in the THP-1 cells irrespective of stimulus used (Figure 3.6B). In line with these *in vitro* findings, KCs and liver mononuclear cells (MNCs) isolated from chronic alcohol-fed mice revealed increased levels of miRNA-122 compared to the control pair-fed mice (Figure 3.6C&D).
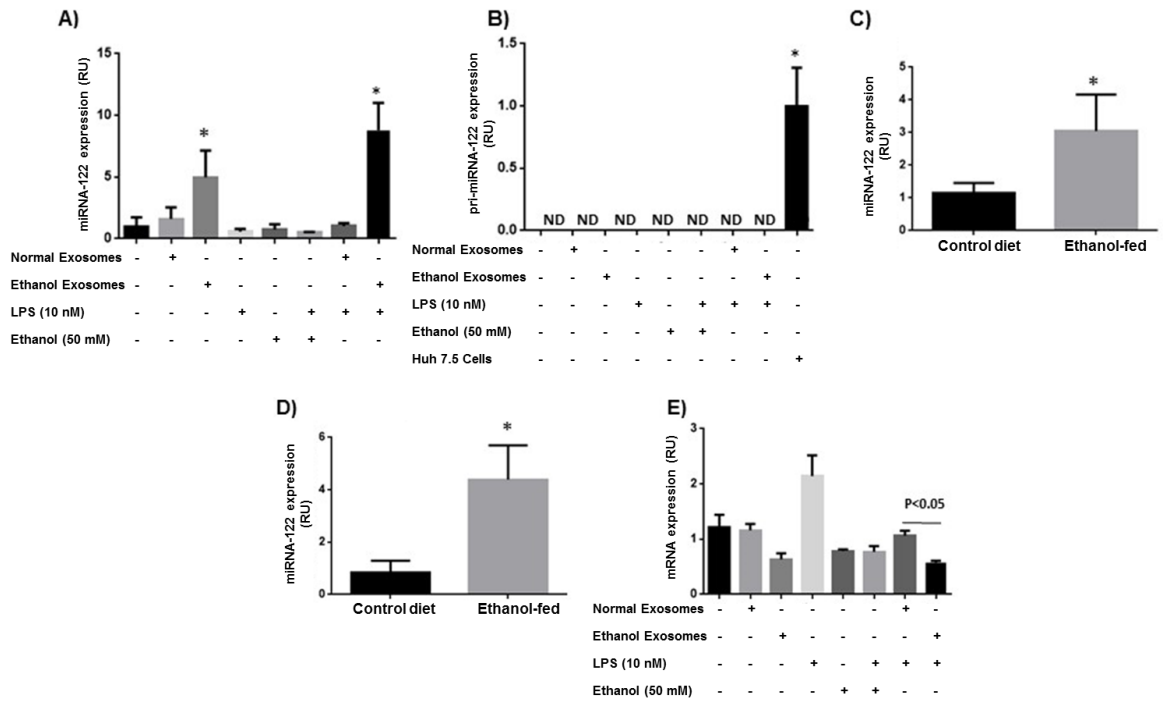
Figure 3.6: Horizontal transfer of mature form of miRNA-122 to the THP1 cells by ethanol-treated Huh7.5 cells. (A) Exosomes were added to the THP1 cells for 8 h and after that exosomes were washed off and the culture media was replaced. Levels of miRNA-122 were quantified in THP1 monocytes by a TaqMan® miRNA assay. RNU-48 was used as internal control to normalize the Ct values between the samples. (B) pri-miRNA-122 in THP1 monocytes was quantified by a TaqMan® Pri-miRNA Assay. The positive control was RNA extracted from Huh7.5 cells. GAPDH was used as an internal control normalizer for real-time qPCR. (C) Liver mononuclear cells (MNCs) were isolated and miRNA-122 levels were compared between ethanol-fed (5 weeks) mice and pair-fed (control) mice ($n = 8$). snoRNA202 was used as a normalizer of Ct values between the samples. (D) Levels of miRNA-122 were compared between ethanol-fed (5 weeks) mice and pair-fed (control) mice in isolated Kupffer cells ($n = 8$). Ct values between the samples were normalized based on snoRNA202. (E) Expression levels of Heme oxygenase 1 (HO-1) mRNA, reciprocal target of miRNA-122, were quantified in different experimental groups using qPCR. 18S was used as an internal normalizer. The results were obtained from three independent experiments. (*indicates $p < 0.05$ compared to control conditions)

This figure is adapted from Momen-Heravi et al., 2015, Scientific reports

3.1.6 Exosome-mediated transfer of miRNA-122 can modulate monocyte function

Although these results confirmed uptake of exosomal miRNA-122 by monocytes after hepatocyte injury with alcohol, the functional relevance of this phenomenon remained

unresolved. HO-1 has been previously described to be a target of miRNA-122 as evidenced through reciprocal expression of these two molecules (Shan et al., 2007; Yachie et al., 2003; Drechsler et al., 2006). Mechanistically, transfection of hepatocytes with antagomir of miRNA-122, 2'-O-methyl-antagomir miRNA-122, into Huh-7 cells, resulted in increased HO-1 levels in hepatocytes. Interestingly, inhibition of miRNA-122 also decreased Bach1which is a repressor of HO-1. HO-1 has been shown to have inhibitory effects on reactive oxygen species- and cytokine-mediated cell damage (Yachie et al., 2003; Li et al., 2012b). Accordingly, miRNA-122-containing, ethanol-induced hepatocyte exosomes resulted in the significant decrease of HO-1 levels in exosome-receiving THP-1 cells (Figure 3.6 E). To examine the relationship of hepatocyte alcohol injury with the inflammatory functions of monocytes, the impact of alcohol-induced exosomes was assessed in the cytokine response of THP-1 cells stimulated with LPS. Significantly, these studies revealed an amplification effect on both the mRNA and protein production of TNFα and IL-1β by THP-1 cells ($p < 0.05$). Crucially, these effects were dependent on alcohol stimulation of the exosome producing hepatocytes, as normal exosomes failed to amplify the LPS-induced THP-1 pro-inflammatory response (Figure 3.7 A, B, C, D).
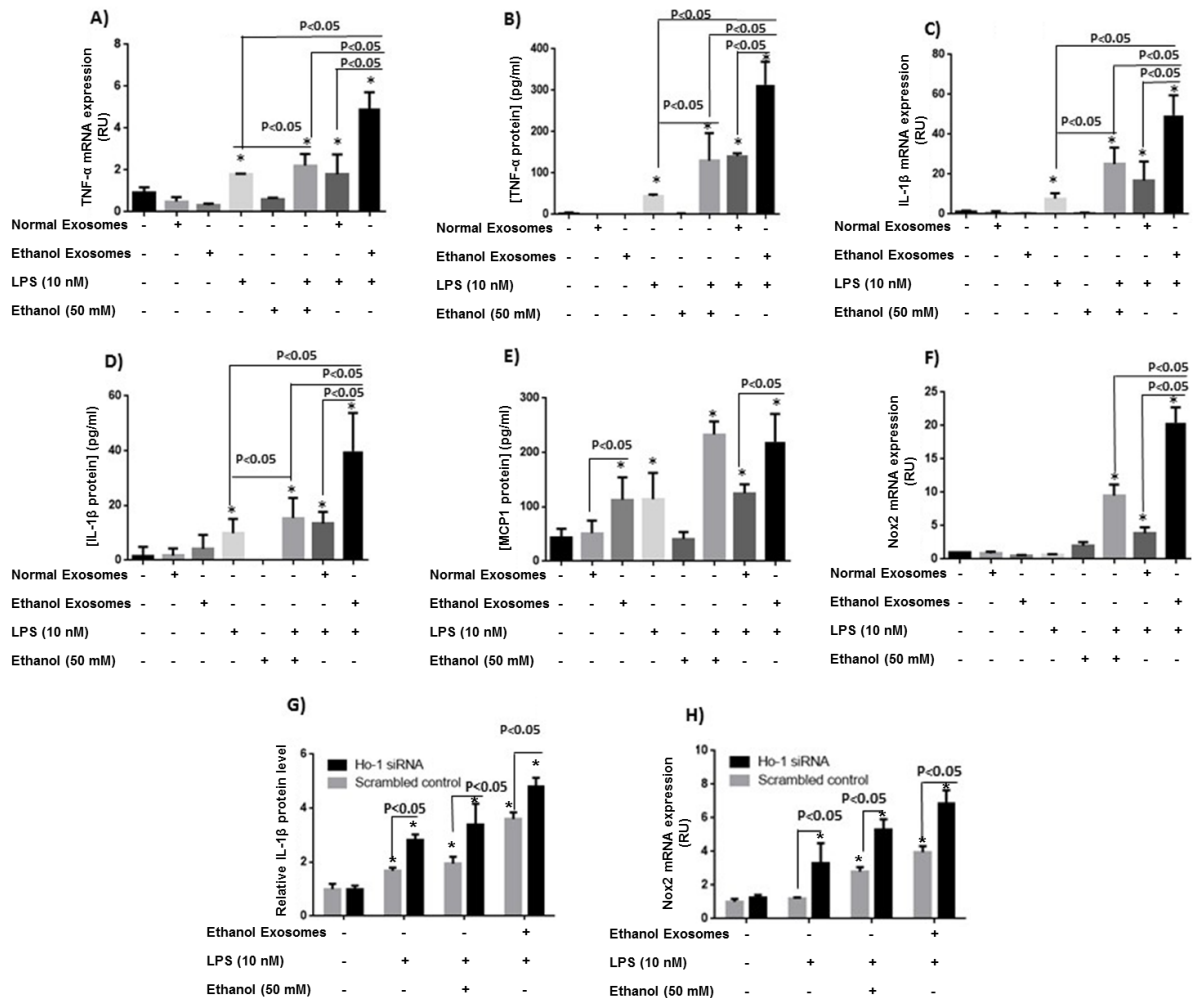
Figure 3.7: Immunomodulation effects of ethanol-treated hepatocytes on human THP1 monocytes. 100 mM ethanol was added to the Huh7.5 cells for 48 h. Exosomes were isolated by a combination of filtration and ExoQuick-TC™ as described in Chapter 2. Exosomes derived from ethanol treated cells and non-ethanol treated cells (normal exosomes) were administered to the THP1 human monocytes for 8 h. After 8 h, exosomes were washed out and the culture media was replaced. RNA and cell supernatant were harvested after 16 h and analyzed for downstream measurements. LPS (10 nM) was added to the THP1 monocytes 6 h before harvesting. (A) Levels of TNFα mRNA were quantified using a quantitative real-time PCR (qPCR). 18S was used as internal normalizer to normalize the Ct values between the samples. (B) TNFα protein levels in the supernatant were quantified by ELISA. (C) The levels of IL-1β mRNA expression in THP1 monocytes were quantified by a qPCR. 18S was used to normalize the Ct values between the samples. (D) The levels of IL-1β protein level in the supernatant were quantified by ELISA. (E) The levels of MCP1 protein in the supernatant were quantified by ELISA. (F) The expression level of NADPH oxidase 2 (Nox2) mRNA in the THP1 monocytes was quantified with a qPCR. The Ct values were normalized based on 18s. (G) HO-1 siRNA and scrambled siRNA control were introduced to the THP-1 cells by electroporation. Cells (2×10^5) were re-suspended in 150 µl complete RPMI media in addition to 150 µl Gene Pulser® Electroporation buffer. The mixture was

kept on ice for 5 min before electroporation. Electroporation was done at the optimal setting (300 kV and 1500 µF). After electroporation, cells were kept on ice for 10 min and were then seeded in the plate for 48 h. 10 nM LPS was administered to the THP1 cells 6 h before harvesting in the pertinent groups. Ethanol exosome was added 24 h before harvesting. After 48 h, levels of IL-1β protein were quantified by an ELISA. (H) After knockdown of HO-1 by introducing siRNA to the THP1 monocytes as delineated in the previous section, total RNA was extracted and levels of Nox2 mRNA expression were quantified using a qPCR. 18S was used to normalize the Ct values between the samples. The results were obtained from three independent experiments. (*indicates $p < 0.05$ compared to control condition)*This figure is adapted from Momen-Heravi et al., 2015, Scientific reports*

These findings suggested that exosomes derived from ethanol-exposed hepatocytes may increase sensitivity of THP1 monocytes toward an LPS challenge. Unlike TNF-α and IL-1β, MCP1 protein induction was directly induced by exposure of THP-1 cells to ethanol-induced hepatocyte exosomes, with no amplification of the LPS-induced MCP1 production effect; again, this response was dependent on ethanol stimulation of the exosome producing hepatocytes and not on account of direct ethanol exposure (Figure 3.7 E).

NADPH oxidase (Nox2) is a superoxide generating enzyme which is involved in the production of cellular machinery producing reactive oxygen species and plays an important role in the host defense (Bae et al., 2011). Nox2 is predominantly expressed in immune cells and its expression is controlled by HO-1, and induction of HO-1 suppresses activation of Nox2 (Datla et al., 2007; Soucy-Faulkner et al., 2010). HO-1 deficient mice showed increased expression of Nox2 and oxidative stress (Wenzel et al., 2015). In line with the observation of a sensitizing effect of exosomes derived from ethanol-exposed Huh7.5 cells, ethanol exosomes induced a statistically significant increase in the Nox2 levels in THP1 monocytes compared to the control groups, in the presence of LPS stimulation (Figure 3.7F). Collectively, these data indicated a chain of molecular events beginning with the uptake of bioactive miRNA-122 by THP-1 cells exposed to the ethanol-induced hepatocyte exosomes, which suppressed HO-1 expression, which in turn allowed overexpression of NOX2 (Figure 3.8).

To test this hypothesis, the effect of si-RNA mediated HO-1 suppression was examined on the LPS-driven THP-1 immune response. Accordingly, an increase in IL-1β protein levels in the presence of LPS was further enhanced through ethanol exosomes (Figure 3.7G). Effective knockdown of HO-1 resulted in a significant increase in Nox2 levels in the

presence of LPS and LPS + ethanol exosomes (Figure 3.7H). These data highlights suppressive role of HO-1 as regulator of inflammatory and ROS responses. Overall, these observations suggest the successful horizontal transfer of liver specific miRNA-122 from hepatocytes after ethanol treatment via exosomes. This miRNA-122 is functional and is able to modify THP1 responses to LPS through modulating the HO-1 pathway (Figure 3.8).
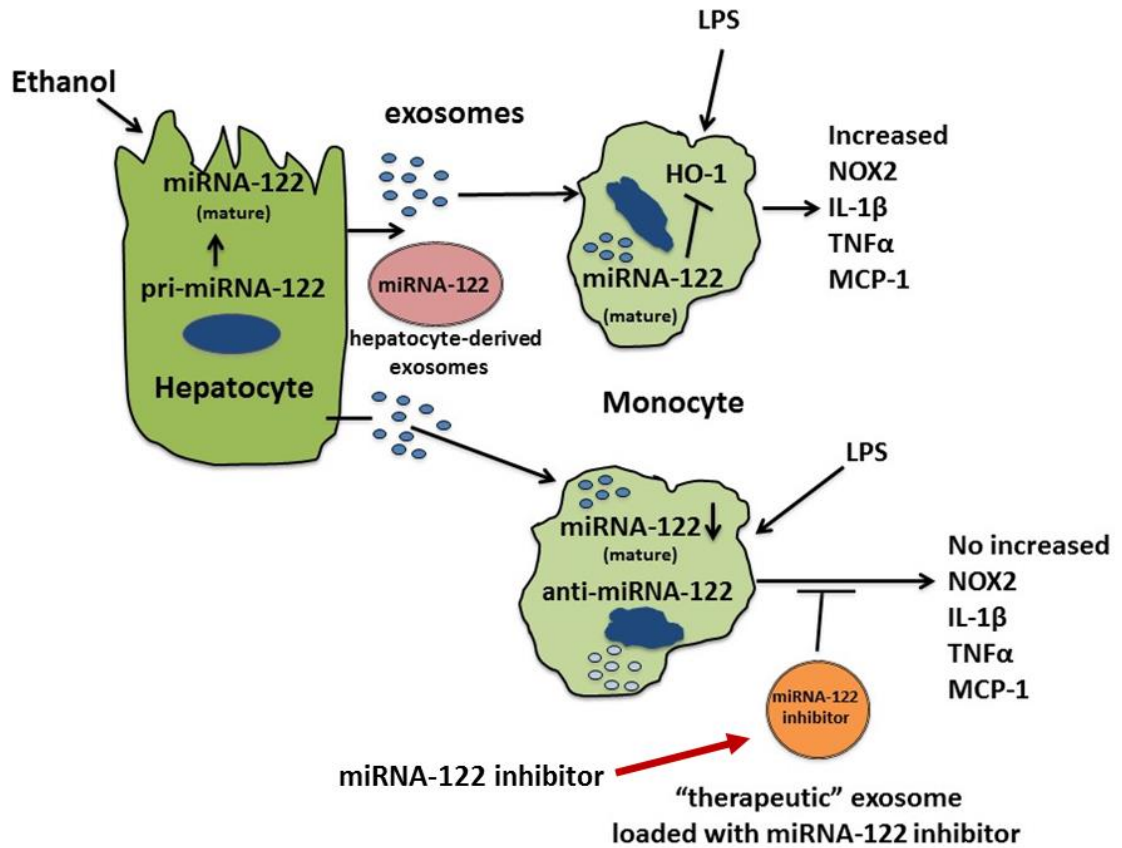
Figure 3.8: A schematic representation of the improved understanding of the functional role of exosomal miRNA-122 in the regulation of monocyte proinflammatory responses to alcoholic hepatocyte injury.

This figure is adapted from Momen-Heravi et al., 2015, Scientific reports.

To additionally confirm that the introduction of miRNA-122 to THP1 monocytes can modulate HO-1 and sensitize monocytes to LPS, a "simulation experiment" was designed. miRNA-122 was introduced to THP1 human monocytes and RAW264.7 macrophages by electroporation and transfection reagents, respectively (Figure 3.9A). Delivery of miRNA-122 mimic into the monocytes, resulted in significantly higher protein levels of pro-inflammatory cytokines TNFα and IL-1β in the presence of LPS stimulation in THP1 cells ($p < 0.05$) (Figure 3.9B&C). This imitated the sensitizing impact that we found in the presence of exosomes derived from ethanol-exposed hepatocytes, which are highly enriched in the mature form of miRNA-122.
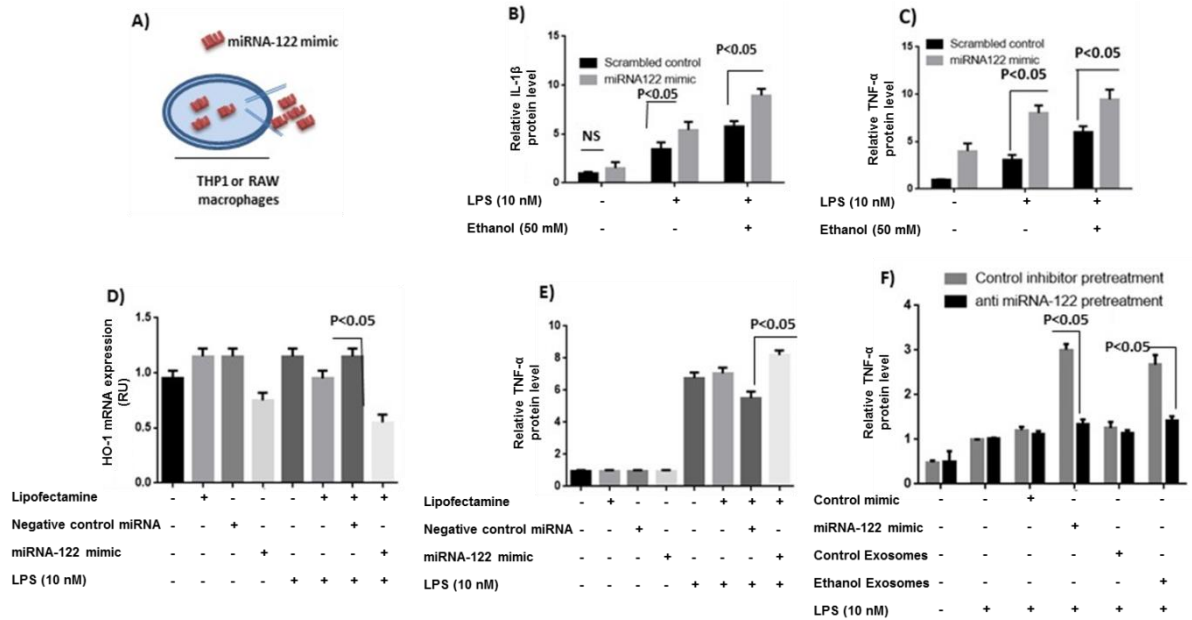
Figure 3.9: Simulation experiments to substantiate the induction of pro-inflammatory phenotype due to the miRNA-122 transfer and preventing pro-inflammatory effects of exosomes derived from ethanol exposed hepatocytes using exosome-mediated RNAi delivery. (A) A "simulation experiment" was designed to confirm that pro-inflammatory phenotype is due to the horizontal transfer of miRNA-122. miRNA-122 mimic was introduced to RAW264.7 macrophages and THP1 monocytes by transfection reagents and electroporation, respectively. (B) Electroporation (300 kV and 1500 µF) was used to introduce miRNA-122 mimic and control mimic to the THP1 cells. After 18 h, 10 nM LPS was added for 6 h and IL-1β ELISA analysis was performed on the supernatants. The results were obtained from three independent experiments and expressed as mean±SD of relative IL-1β protein levels. (C) Electroporation (300 kV and 1500 µF) was used to introduce miRNA-122 mimic and control mimic to the THP1 monocytes. After 18 h, LPS (10 nM) was added for 6 h and after that supernatants were collected for TNFα ELISA analysis. The results were obtained from three independent experiments and are expressed as TNFα protein level fold change. (D&E) miRNA-122 mimic and negative control mimic were introduced to the RAW264.7 murine macrophages with Lipofectamine® RNAiMAX transfection reagent. LPS (10 nM) was added 6 h before readings. After 48 h, mRNA expression levels of HO-1 were quantified by a quantitative real-time PCR. TNFα protein levels were measured by quantitative real-time PCR. Ct values between the samples were normalized based on 18S. (F) miRNA-122 inhibitor was electroporated into THP1-derived exosomes under optimal conditions, as described in Chapter 2. Loaded exosomes were added to the naïve THP1 cells for 12 h. After 12 h, exosomes were washed off and the media was replaced. Exosomes derived from ethanol-exposed Huh7.5 cells were added for 8 h. TNFα protein level was quantified in supernatants after 24 h. 6 h before readout 10 nM LPS was added. Positive control was directly electroporated miRNA-122 mimic into the THP1

monocytes. The results were obtained from three independent experiments. p<0.05 was considered statistically significant and is denoted in the figures.

This figure is adapted from Momen-Heravi et al., 2015, Scientific reports.

Transfection of RAW264.7 macrophages with a miRNA-122 mimic by Lipofectamine lead to a significantly decreased expression level of HO-1 mRNA ($p < 0.05$) and increased TNFα protein levels ($p < 0.05$), compared to the control group transfected with negative control miRNA (Figure 3.9D and E). These results mechanistically confirm the observations regarding horizontal transfer of miRNA-122 by exosomes derived from ethanol-treated hepatocytes to immune cells and observed pro-inflammatory cytokine production through modulation of the HO-1 pathway. In conclusion, given the fact that miRNA-122 exert function in monocytes by reducing HO-1 level, these data suggest that exosomal miRNA-122 derived from ethanol exposed hepatocytes is biologically active in monocytes, mediating an amplification of both the proinflammatory and ROS responses.

Based on our results, we hypothesized that the exosomal miRNA-122 function in THP-1 cells could be blocked by pretreatment of the THP-1 cells with antimiRNA-122. I previously developed a successful delivery of an exosome-mediated RNA targeted therapy, both *in vivo* and *in vitro*, which will be discussed in section 3.4 in detail. Using previously optimized methodology (Momen-Heravi et al., 2014a), THP1 derived exosomes were exploited as vehicles for the delivery of a miRNA-122 antisense inhibitor. Thus, the effect of anti-miRNA-122-loaded, THP-1-derived exosomes were assessed in this cell culture model of monocyte pro-inflammatory response to hepatocyte exosomes. In line with our hypothesis, use of these anti-miRNA-122-loaded exosomes significantly diminished the effects of ethanol-induced hepatocyte exosomes in terms of TNFα protein production ($p < 0.05$) (Figure 3.9 F).

3.2   The role of exosomes in HCV transmission

HCV infection is one of the most burdensome diseases in the world (Lavanchy, 2011). Hepatitis C virus infection can induce severe complications, such as liver cirrhosis and hepatocellular carcinoma (de Oliveria Andrade et al., 2009). It is estimated that 2–3 % of the world's population (nearly 170 million people) is infected with HCV, and more than 350,000 deaths occur annually due to HCV-related conditions, including hepatocellular carcinoma and liver cirrhosis (Averhoff et al., 2012; Lavanchy, 2011). Although HCV infection prevalence is reported to be <2% in United states and western Europe, HCV infection rates are higher (≥3%) in many countries in Latin America, eastern Europe and certain countries

in Africa. Egypt is reported to have the highest rate of hepatitis C in the world (estimated at >10%) (Averhoff et al., 2012). Although liver transplantation was introduced as a successful treatment, HCV re-infection of the newly transplanted liver is a common phenomenon (Vinaixa et al., 2013). Recent therapies with anti-HCV E1-E2, anti-CD81 and other neutralizing antibodies were not completely effective and suggested alternative means by which the virus could escape the immune system in the circulation and mediate infection (Timpe et al., 2008; Morin et al., 2012). Based on our observations and observations made by others of controlled RNA shuttling between cells via exosomal communication pathways (Momen-Heravi et al., 2015a) and role of exosomes in transmission of HIV (human immunodeficiency virus) (Wiley and Gummuluru, 2006), we postulated that exosomes derived from HCV-infected hepatocytes or infected patient sera might carry viral RNA and have the ability to mediate HCV transmission (Bukong et al., 2014).

3.2.1 Separation of HCV infected exosomes from free HCV viruses and exosome characterization

HCV is an enveloped, positive-strand RNA virus which is member of the genus Hepacivirus within the family of Flaviviridae. Electron microscopy (EM) studies have indicated that HCV virions are 40–80 nm in diameter (Lindenbach and Rice, 2013). One of the challenges in this study was the limitations in methodology regarding the isolation of pure exosomes vs viral particles. Importantly, HCV virions and exosomes have very similar densities and diameters (Bartenschlager et al., 2011; Catanese et al., 2013). Thus, the traditional ultracentrifugation and sucrose gradient isolation methodology was inadequate for segregating the two vesicle sub-populations. To address this, I developed a new method based on the combination and optimization of the precipitation method with the CD63 immuno-magnetic isolation to purify exosomes devoid of free virus from both cell culture supernatants (HCV J6/JFH-1 infected Huh7.5 cells) and HCV infected patient sera. Briefly, serial filtration (0.8 µm, 0.44 µm and 0.22 µm) was followed by exosome pelleting using the Exoquick-TC method (section 2.2.4) followed by immuno-magnetic selection for CD63^{+} to exclude virus carry-over. Isolated exosomes were analyzed by transmission electron microscopy, and NTA, demonstrating a vesicular shape and size range between 50 and 100 nm, in line with the previously described morphology of exosomes (Figure 3.10).
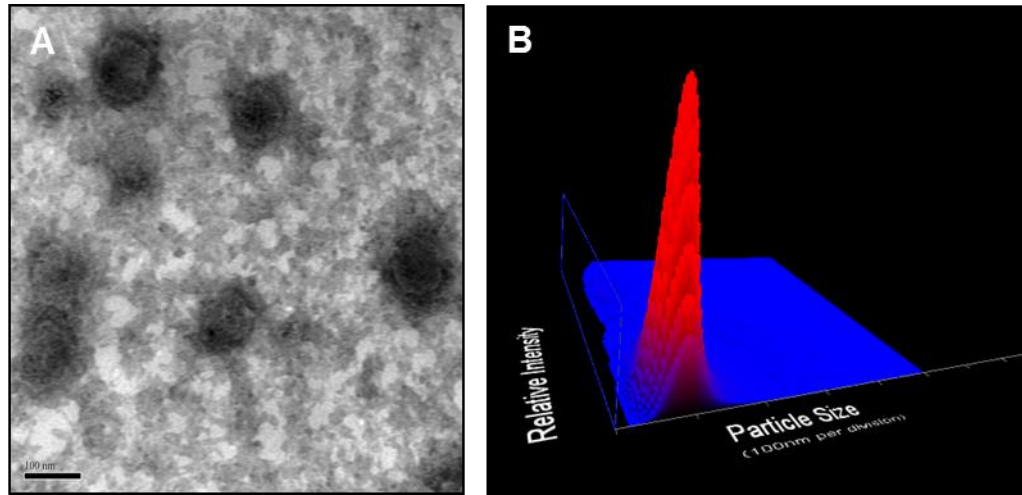
Figure 3.10: Characterization of exosomes derived from Huh7.5 cells. TEM(A) and NTA analysis(B) of exosomes derived from Huh7.5 cells confirm the morphology and size range of 50-100 nm; TEM scale bar:100 nm

Apolipoprotein E (APOE) is required for HCV virion infectivity and production. It has been reported that HCV virions are assembled as APOE-enriched lipoprotein particles (Chang et al., 2007). Apolipoprotein B is considered an exosome surface marker (Carayon et al., 2011). Consistently, HCV exosomes were enriched in Apolipoprotein B (APOB) which was absent from cell-free HCV virus preparations (Figure 3.11A). In contrast, Apolipoprotein E (APOE) was strongly associated with the HCV virus fraction and was significantly lower in the exosome fraction (Figure 3.11B). These observations suggested adequate separation of viral particles from the exosome fraction.
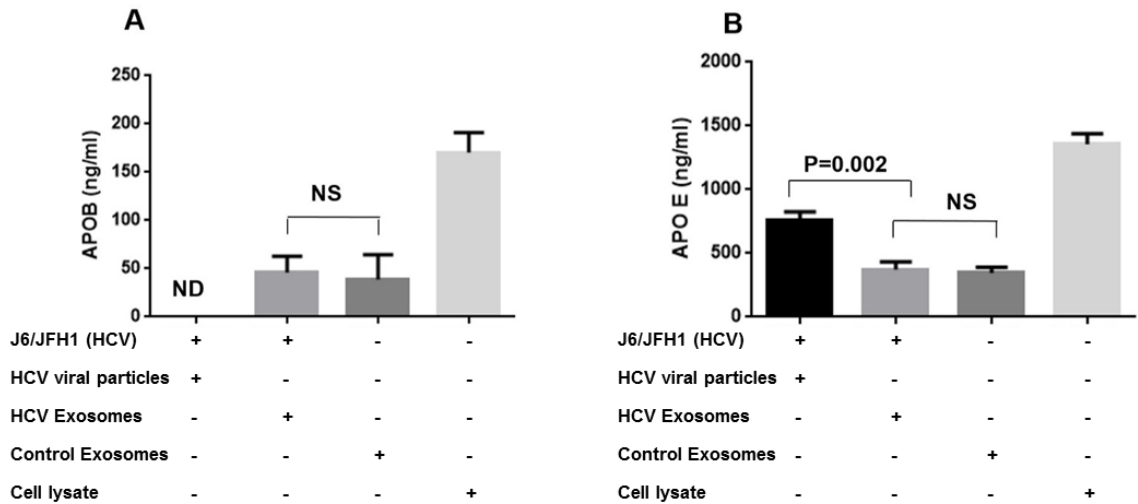
Figure 3.11: Comparative analysis of exosome and virus for APOE and APOB proteins. Exosomes and cell free virus were purified as described in Chapter 2. Equal numbers of exosomes and cell free virus were lysed in RIPA buffer and proteins were extracted. (A&B) ELISA for APOE and APOB was done according to the manufacturer's protocol. APOB was detectable in exosomes. There was not a significant difference in APOB contact between HCV exosomes versus control exosomes. HCV viral particles showed significantly higher levels of APOE compared to exosomes derived from HCV infected cells and control exosomes. Results are presented as mean ± SD and are the result of 3 independent experiments. (ND: Not detectable; NS: Not significant; p<0.05 was considered statistically significant)*This figure is adapted from Bukong and Momen-Heravi et al., 2015, PLoS Pathog.*

3.2.2 Exosomes containing HCV are enriched in Ago2 and miRNA-122 and can induce active infection

In line with recent studies reporting that Ago2, HSP90, and miRNA-122 contribute to the HCV life cycle (Wilson et al., 2011; Henke et al., 2008; Jopling et al., 2005), exosomes derived from HCV-infected Huh 7.5 cells contained higher levels of miRNA-122 (Figure 3.12A) and Ago2 protein (Figure 3.12B) compared to exosomes from non-infected cells. HSP90 levels were also elevated compared to the control exosome population, albeit at overall lower levels compared to Ago2 (Figure 3.12B). Similarly, serum exosomes purified from HCV infected, treatment-naïve and treatment non-responder subjects were rich in Ago2 and HSP90 in comparison with control healthy subjects (Figure 3.12C). In contrast, this was not observed in HCV treatment responders. Follow on CHIP analysis showed HSP90 and Ago2 formed complexes within HCV-containing exosomes, in line with the reports these proteins might stabilize the HCV genome replication complex (Figure 3.13).
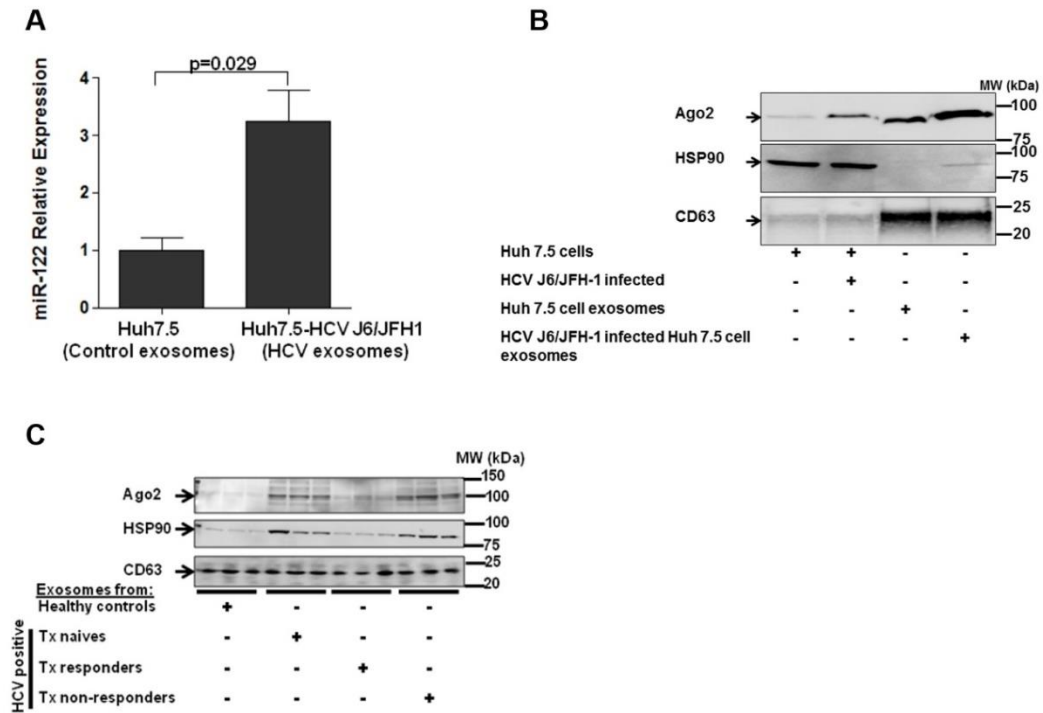
Figure 3.12: Exosomes isolated from HCV infected Huh7.5 cells and sera of HCV infected patients harbor HCV RNA, miRNA-122, HSP90 and Ago2. (A) miRNA-122 was significantly higher in exosomes derived from HCV J6/JFH1 infected Huh 7.5 cells compared to the exosomes derived from control Huh7.5 cells (B) Exosomes derived from HCV infected cells showed higher level of Ago2 compared to exosomes from non-infected cells. HSP90 levels were also elevated compared to the control exosome population, albeit at overall lower levels compared to Ago2 (C) Similarly, serum exosomes purified from HCV infected, treatment-naïve (Tx naïve) and treatment non-responder (Tx non-responders) subjects were rich in Ago2 and HSP90 in comparison with control healthy subjects. Patients were either treatment naïve (Tx naïves), responding (Tx responders), or non-responding (Tx non-responders). ($p < 0.05$ was considered statistically significant). The data was obtained from three independent experiments.

This figure is adapted from Bukong and Momen-Heravi et al., 2015, PLoS Pathog.

To determine whether HCV RNA was indeed shuttled to exosomes from infected hepatocytes, we next attempted to detect this by qRT-PCR in both cell culture derived and patient exosomes. Although qRT-PCR detection of HCV RNA implies transfer of the HCV genome to exosomes, this does not confirm whether the genome is physically intact and/or capable of replication and virion production. We thus resorted to testing the ability of these exosomes to mediate active HCV infection to uninfected Huh 7.5 cells and primary human hepatocytes. At first instance we established HCV exosome infectivity in cultured cells by serially passaging HCV exosome fractions across 2 uninfected Huh 7.5 cultures. Thus, exosomes from HCV-infected Huh7.5 cells were co-cultured with naïve Huh 7.5 cells for 12

h, and after another 24 h exosomes produced from the receiving cells were harvested and sub-cultured into a new, naïve Huh 7.5 culture (Figure 3.14A). Up to 10^7 genome equivalents of HCV were detected in the final recipient Huh 7.5 cells. In stark contrast, no HCV genome was detected in cells receiving exosomes from naïve cells. Similarly, comparable levels of infectivity were observed when HCV exosomes were tested against HCV virions at comparable mass ratios (Figure 3.14B). Significantly, replication was inhibited by a known HCV protease inhibitor, indicating either HCV protease protein inclusion, or translation-compatible HCV RNA inclusion in the exosomal fraction.
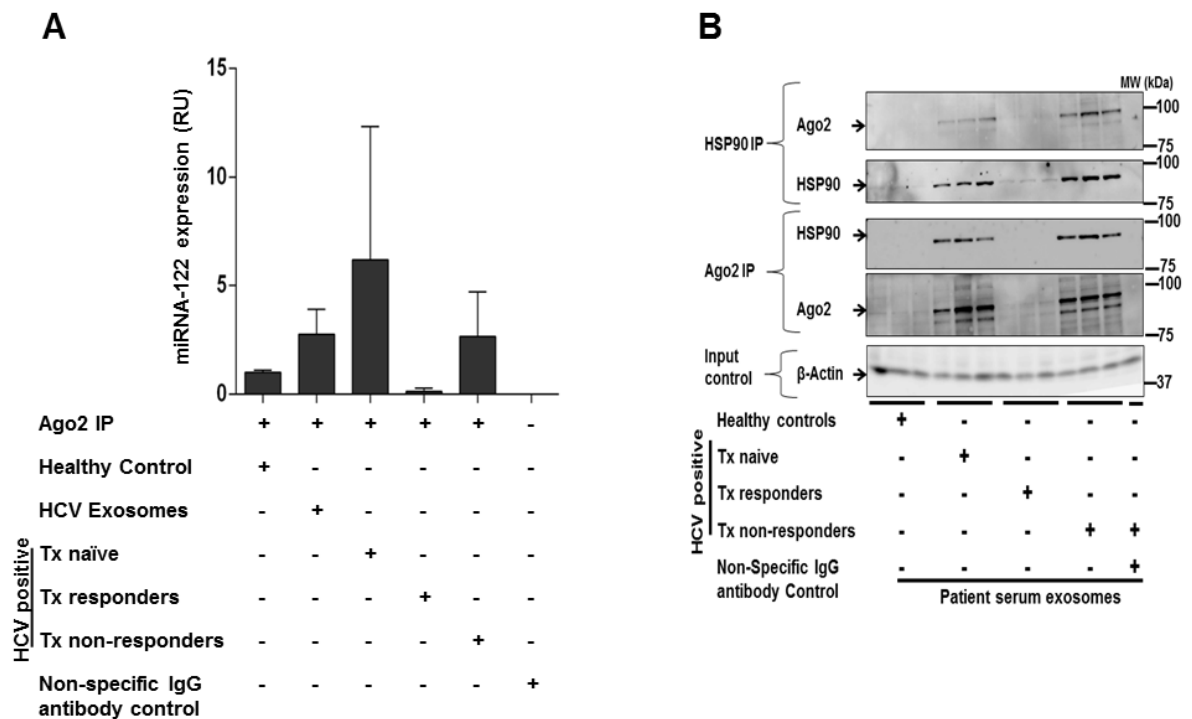
Figure 3.13: Exosomes from HCV infected Huh7.5 cells and sera of HCV infected patients contain replication competent HCV RNA, miRNA-122 and RISC complexes that enhance HCV infection. RNA ChIP analyses of Ago2 in exosomes isolated either from culture supernatants of HCV J6/JFH-1 infected Huh7.5 cells or from patient sera were subjected to Ago2 pull down followed by total RNA isolation which was analyzed for (A) miRNA-122 expression (B) Co-Immunoprecipitation of Ago2 and HSP90 complexes from exosomal protein lysate isolated from patient sera or culture supernatants of HCV J6/JFH-1 infected Huh7.5 cells. Rabbit IgG non-specific antibody served as IP control antibody. Experiments are representative of 3 independent experiments for cell culture supernatants and patient samples.

This figure is adapted from Bukong and Momen-Heravi et al., 2015, PLoS Pathog.

Next, we validated these findings in a similar study with primary hepatocytes by harvesting serum exosomes from HCV patients (+/- treatment and response) and evaluating their

infectivity in naïve primary human hepatocytes. Thus, 48 h post patient serum exosome exposure, substantial and comparable quantities of viral RNA were detected in cells treated with treatment-naïve and treatment non-responder patient serum exosomes (Figure 3.14C). Similarly, HCV RNA copy number at, or above the sample size limit of detection for patient serum exosomes resulted in log-scale increases in recipient primary hepatocyte HCV RNA levels (Figure 3.14D). Furthermore, the patient sera equivalent experiment comparing the infectious potential of HCV exosomes versus HCV virus in the presence or absence of HCV protease inhibitor (Figure 3.14E) resulted in comparable data to that obtained with culture-derived HCV and Huh 7.5 cells (Figure 3.14B).
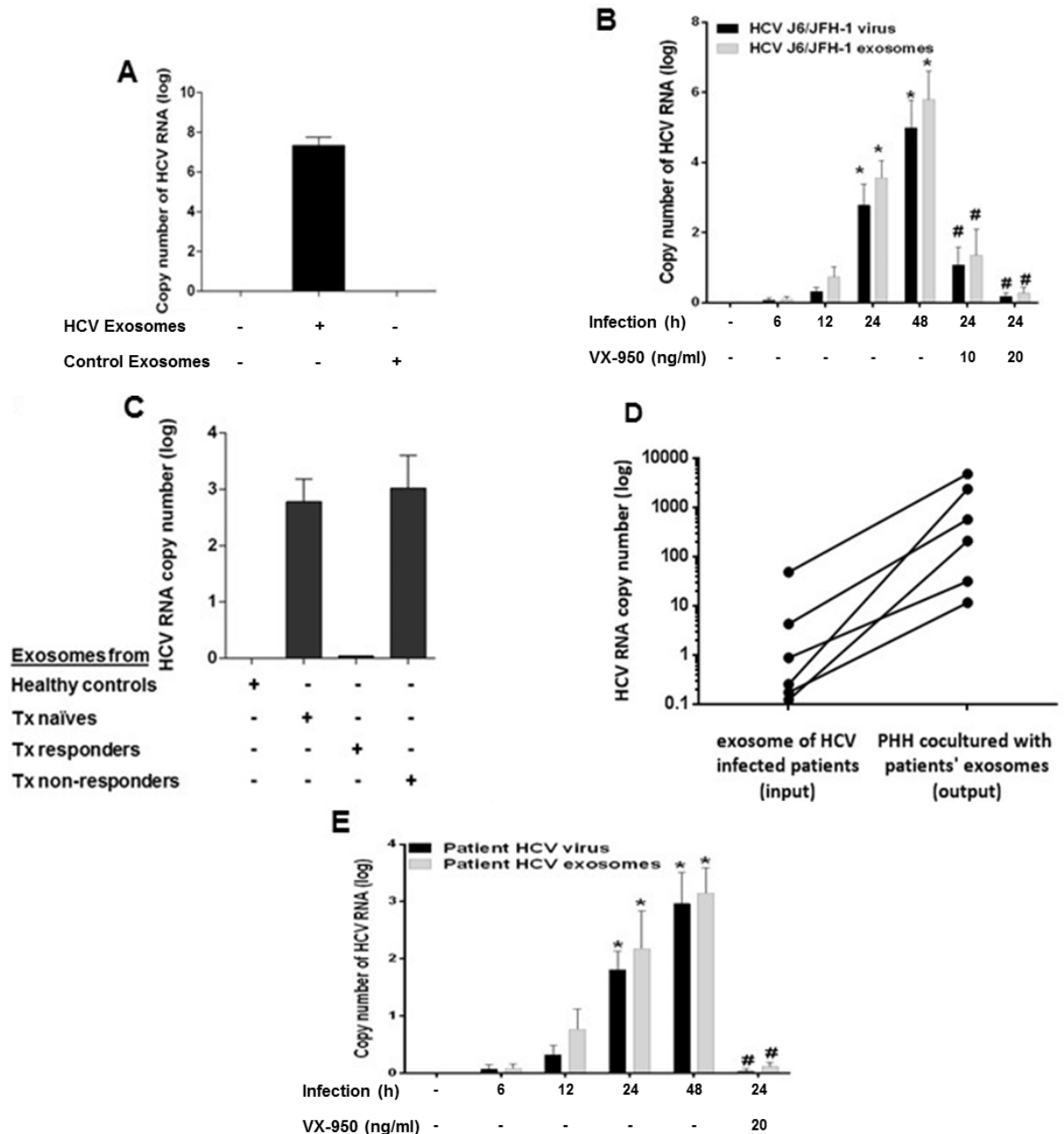
Figure 3.14: Exosomes derived from HCV J6/JFH-1 infected Huh7.5 cells transmit HCV infection to the human hepatoma cell line (Huh7.5 cells) and exosomes from sera of HCV infected patients transmit HCV infection to primary human hepatocytes. (A) Exosomes derived from HCV J6/JFH-1 infected Huh7.5 cells were added to Huh7.5 cells for 12 h, as well as different controls. After 12 h, exosomes were washed off and the culture media was replaced and cells were cultured for another 24 h. Afterwards, culture supernatants from these exosome-infected Huh7.5 cells were transferred to Huh7.5 cells and cultured for 24 h. Huh7.5 Cells were harvested and total RNA was extracted and HCV RNA was just detectable in exosomes derived from infected cells, determined by a qPCR. (B) The same starting amount of HCV virus or HCV exosomes was added to Huh 7.5 cells for 6 h. The media were replaced after 6 h and cells were cultured for the indicated time, with or without treatment with Telaprevir (VX-950) at the indicated concentration. The cells were lysed. Total RNA was extracted and analyzed by qPCR for HCV RNA. Viral replication was

inhibited by a known HCV protease inhibitor. (C) Exosomes were isolated from sera of three different patient groups (treatment non-responders, treatment naive, and treatment responders) and co-cultured with primary human hepatocytes (PHH). After 8 h, exosomes were washed off and the medium was replaced. 48 h post patient serum exosome exposure, substantial and comparable quantities of viral RNA were detected in supernatant of cells treated with treatment-naïve and treatment non-responder patient serum exosomes. (D) Exosomes were isolated from sera of HCV infected treatment naive patients by the anti-CD63 immunomagnetic isolation method and co-cultured with PHH. HCV RNA copy number at, or above the sample size limit of detection for patient serum exosomes resulted in log-scale increases in recipient primary hepatocyte HCV RNA levels (E) HCV viral particles and CD63 selected HCV exosomes were purified from sera of HCV infected patients. The isolated exosomes and free virus (MOI = 1) were used to infect primary human hepatocytes over the indicated time course. The results represent exosomes isolated from the sera of 4 different HCV infected treatment naive patients. The data is presented as mean ± SEM (p<0.05 was considered statistically significant).

This figure is adapted from Bukong and Momen-Heravi et al., 2015, PLoS Pathog.

3.2.3 Exosomes mediate CD81, SR-BI and APOE receptor-independent transmission of HCV

Given the HCV-loaded exosomes selectively purified by CD63 immunomagnetic methods resulted in comparable infectivity to HCV virions, we sought to explore how known surface markers of transmission are involved with the infectious potential of each fraction. Different molecules such as CD81, Scavenger receptor class B member 1 also known as SR-BI, APOE and HCV glycoproteins E1 and E2 (HCV E1/E2) have been identified as important host and viral molecules for the mediation of HCV infection (Rice, 2011). It has been shown that anti-CD81 and anti-HCV E1/E2 antibodies failed to completely block HCV infection, indicating alternative mechanisms of HCV transmission might exist (Morin et al., 2012; Meuleman et al., 2008). These findings lent support to our evidence that exosomes might provide the alternative route of virus transmission. Thus, we assessed whether the presence of anti-CD81 antibodies would prevent exosome-mediated or cell-free virus transmission of HCV.

Here, the capacity of culture-derived HCV virions to infect Huh 7.5 cells was reduced by up to 6 logs in the presence of an anti-CD81 Ab, as determined by resulting HCV RNA levels in recipient cells; in contrast, the effect on HCV-infected Huh 7.5 cell exosomes was only ~ 1 log and not statistically significant (Figure 3.15A). The effect was mirrored in terms of viral protein production levels (Figure 3.15B), where the 6 log difference in RNA levels

translated in undetectable virus protein levels by Western blotting. These results were reproduced in primary human hepatocytes with either patient-derived exosomes and virus or culture-derived infectious particles (Figure 3.15C&D). Furthermore, SR-BI and APOE antibody pre-treatment prevented culture-derived virus from transmitting into naïve Huh 7.5 cells, but had no impact on the infectivity of culture-derived HCV exosomes (Figure 3.15E&F). Taken together, these studies defined the functional differences in infectious potential between exosomes and virions obtained from HCV-infected cells (whether patient- or culture-derived), and validated the efficacy of the purification methodology in positively purifying virus-free exosomes by CD-63 immunomagnetic methodologies.
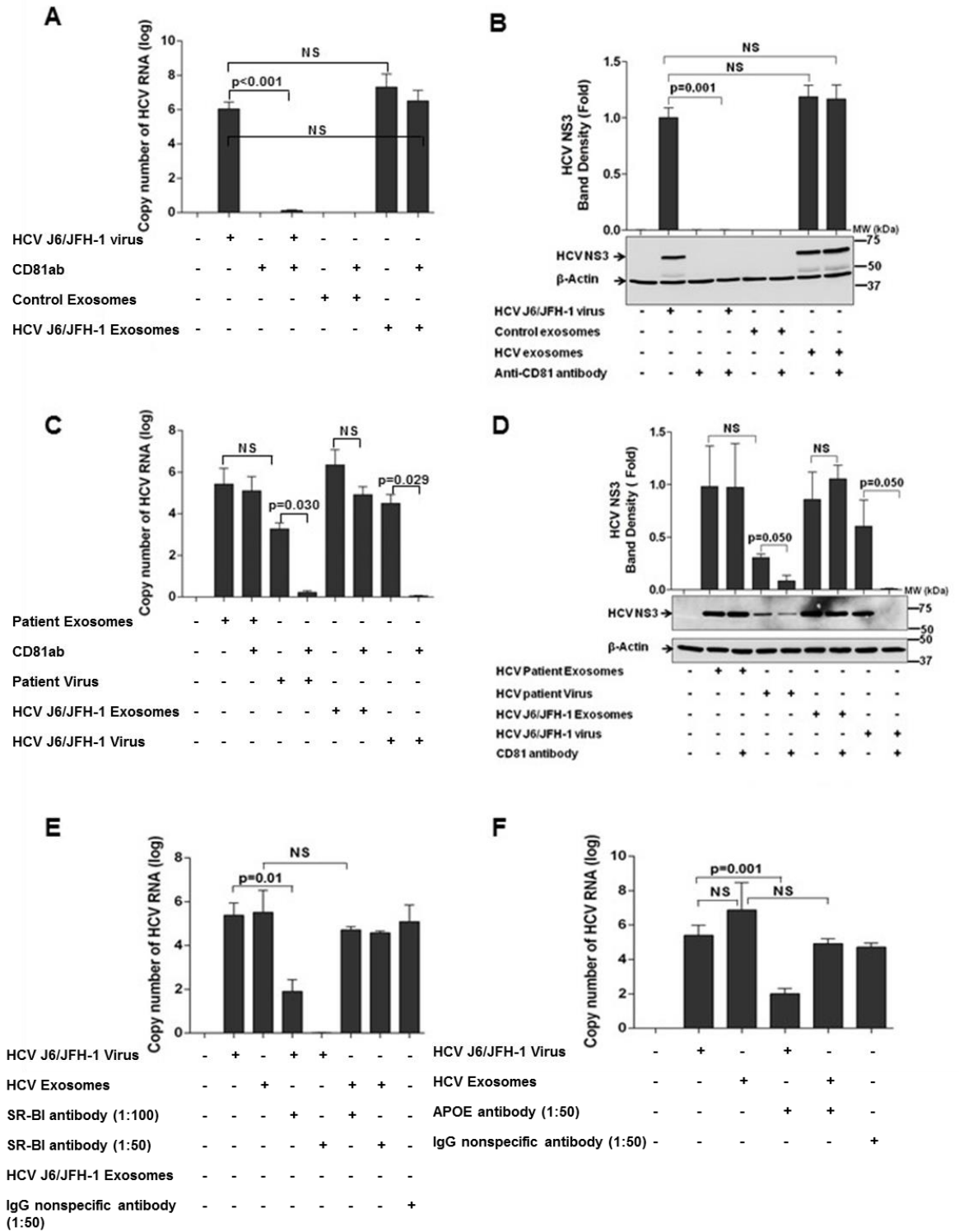
Figure 3.15: Exosomes from HCV infected Huh7.5 cells and HCV patients transmit HCV and induce active infection in the presence of anti-SR-BI, anti-CD81, and anti-APOE antibody. (A, B) Huh 7.5 cells were pretreated with CD81 antibody (1:50 dilution) or not pretreated, as indicated. Huh7.5 cells were infected with HCV J6/JFH-1 virus or with exosomes purified from culture supernatants of HCV J6/JFH-1 infected Huh7.5 hepatoma cells. After 8 h of co-culture, viruses and exosomes were washed off and fresh culture medium was added to the cells, followed by 40 h further incubation at 37 °C. Total protein and RNA were extracted from the cells and analyzed by (A) qPCR for HCV RNA showed

transmission of HCV RNA via HCV exosomes in the presence of CD81 antibody (B) western blotting (WB) for HCV non-structural protein 3 (NS3) showed presence of viral NS3 protein in the recipient cells after co-culture with HCV exosomes in the presence of CD81. (C & D) Exosomes isolated from sera or free HCV virus from treatment naïve patients were co-cultured with primary human hepatocytes, along with anti-CD81 antibody pre-treatment. Cells were lysed after 48 h and total RNA and proteins were harvested for HCV RNA quantification by a quantitative RT-PCR and by western blot for virus NS3 protein. An identical amount of infectious cell-free virus and HCV exosomes (MOI of 1) were used for all infections. HCV exosomes from isolated from treatment naïve patients transmitted infected to primary human hepatocytes in the presence of CD81 antibody. (E&F) Huh 7.5 cells were pretreated with anti-SR-BI antibody (1:50 or 1:100 dilution) or anti-APOE antibody (1:50 dilution) at different concentrations 1 h before infection. Huh7.5 cells were co-cultured with HCV J6/JFH-1 derived exosomes or free HCV J6/JFH-1 viruses for 48 h. Total RNA and protein was then extracted from the cells and analyzed for HCV RNA by qPCR. Protein extracts were analyzed by western blot for HCV NS3 protein. Infectious HCV virus and infectious HCV-exosomes (both MOI of 1) were used for all experiments. HCV J6/JFH-1 derived exosomes transmitted HCV RNA in the presence of APOE and SR-BI antibodies. Results are average of three independent experiments and are presented as mean ± SEM. p<0.05 was considered statistically significant.

This figure is adapted from Bukong and Momen-Heravi et al., 2015, PLoS Pathog.

3.2.4 MicroRNA-122 inhibitor can reduce HCV virus transmission

Given the established role of miRNA-122 in HCV biology, the enrichment of miRNA-122 in exosomes derived from HCV-infected cells in the presence of HCV genome (Figure 3.12), it was reasoned that miRNA-122 inhibitors might reduce HCV transmission via HCV-bearing exosomes. To investigate this hypothesis, HCV-exosomes were transfected with a miRNA-122 inhibitor or control, washed and re-purified with CD63 magnetic beads and used for the infection of naïve Huh7.5 cells. This protocol resulted in a statistically significant 50 % reduction in miRNA-122 levels in the recipient Huh7.5 cells. In contrast to control inhibitor loaded exosomes, administration of miRNA-122 inhibitor loaded HCV exosomes resulted in a significant reduction in intracellular miRNA-122 levels in Huh7.5 cells (Figure 3.16A). Specifically, reduced virus transmission, identified by decreased HCV NS3 protein, was found after infection of Huh 7.5 cells by HCV-exosomes loaded with the miRNA-122 inhibitor (Figure 3.16 B).
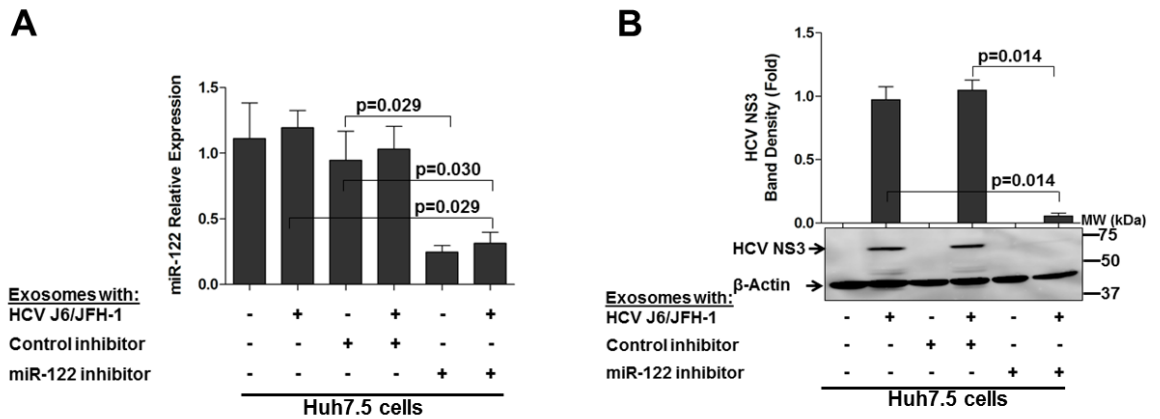
Figure 3.16: Inhibition of miRNA-122 within exosomes can reduce HCV transmission. (A) miRNA-122 inhibitor or control inhibitor complexed with Altogen liver specific in-vivo delivery reagent and were co-cultured with HCV exosomes for 20 min and exosomes re-purified. HCV exosomes loaded with miRNA-122 inhibitor or not as indicated were then transferred unto Huh7.5 cells and co-cultured for 24 h. This protocol resulted in a statistically significant 50 % reduction in miRNA-122 levels in the recipient Huh7.5 cells. (B) Western blot analyses of HCV NS3 protein indicated reduced virus transmission. Results are obtained from at least three independent experiments.

3.2.5 Inhibition of exosome-mediated HCV transmission via blockage of vacuolar-type H+-ATPase inhibitor

Bafilomycin A1, a vacuolar-type H+-ATPase inhibitor, an inhibitor of endosomal acidification that prevents the final fusion step between the virus envelope and the endosomal membrane was reported to completely block the virus entry (Tscherne et al., 2006). Previous work on HCV cell entry did not distinguish between exosomes and viral particles (Tscherne et al., 2006). In these studies, it was reported that vacuolar-type H+-ATPase inhibitor could block both virion entry and subsequent infection. Interestingly, endocytic exosome uptake was shown to be a pH-dependent procedure in an experiment evaluating exosome trafficking by tumor cells (Parolini et al., 2009). On this basis, an experimental model was setup utilizing bafilomycin A1 to evaluate the effect of low pH in preventing HCV exosome uptake by Huh 7.5 cells. Indeed, bafilomycin A1 successfully inhibited both virion and HCV exosome in a dose-dependent fashion (Figure 3.17).
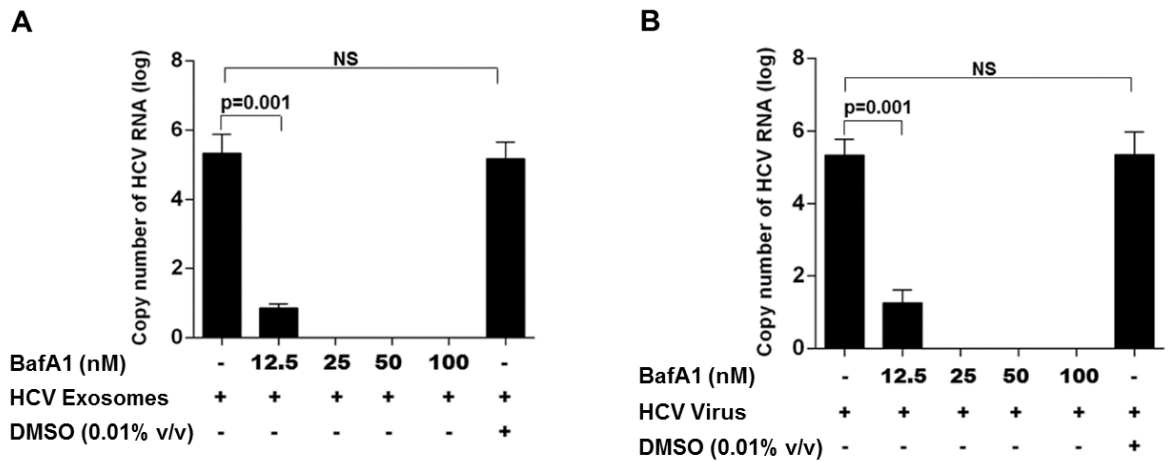
Figure 3.17: HCV transmission by exosomes and free virus can be blocked by vacuolar-type H+-ATPase inhibitor (bafilomycin A1). (A, B)Dose-dependent inhibition of infectious HCV (J6/JFH-1) virion and exosome uptake by Huh 7.5 cells by a vacuolar-type H+-ATPase inhibitor. Bafilomycin A1 (BafA1) was incubated at different concentrations for 1 h and the equal number of HCV J6/JFH-1 exosomes or cell free HCV virus (1:1) as determined by NTA was subsequently used to attempt infection of Huh7.5 cells. 24 h later total RNA was extracted from the cells and analysed by qRT-PCR for HCV RNA. The data was averaged from three independent experiments. Bafilomycin A1 (25 nM to 100 nM) effectively prevent HCV infection by HCV J6/JFH-1 exosomes or cell free HCV virus.
This figure is adapted from Bukong and Momen-Heravi et al., 2015, PLoS Pathog.

Taken together, this research has shown that exosomes derived from HCV-infected Huh7.5 hepatocytes and HCV-infected patients harbor HCV RNA and can induce active infection in primary human hepatocytes independently of CD81, APOE, and SR-BI. These HCV exosomes appear enriched in replication-competent HCV-RNA in complex with miRNA-122, Ago2, and HSP90. Modulation of miRNA-122, or the modification of the intracellular micro-environment through inhibition of a vacuolar-type H+-ATPase (V-ATPase) significantly altered the capacity of cells to become infected by HCV exosomes.

3.3 Exosome cargoes and biofluid miRNAs as cancer biomarkers

The results indicating the role of exosomes/miRNA in the pathogenesis of different liver diseases were reviewed in section 3.1 and 3.2. Besides liver disease, the role of exosomes/miRNAs in cancer progression and diagnostics is a very active area of research. Here, the role of exosomes in a mouse tumor model and the utility of miRNA salivary biomarkers in oral squamous cell carcinoma diagnostics will be discussed (Momen-Heravi et al., 2014b; Balaj et al., 2014).

3.3.1 Circulating exosomes/EVs carry amplifications of c-Myc and EGFR in a mouse tumor model

It has been suggested that cancer genotype changes such as gene mutations, transcriptome changes, amplifications, and epigenetic changes can be monitored through exosome/EV nucleic acid testing (Redzic et al., 2014). Two human tumor cell lines of medulloblastoma and epidermoid carcinoma which had amplications for the c-Myc and EGFR, respectively, were chosen for injection in immunocompromised mice. One month after injection of tumor cells to immunocompromised mice, the increased levels of transcripts for the human EGFR and c-Myc were reflected in circulating EVs in mice that had developed tumors. The expression level of both human c-myc and human EGFR correlated well with the amplification status in the original tumors. This data confirms the utility of EVs for the diagnosis of cancers. This finding supports the notion that circulating EVs might provide an easily accessible, informative and possibly causally linked substrate for cancer biomarker discovery and future treatment development.

3.3.2 Salivary miRNA for the detection of oral Squamous cell carcinoma

Biofluid miRNAs, including those recovered from human saliva, have recently drawn considerable attention as potential diagnostic biomarkers (Lin et al., 2015; Machida et al., 2015; Xie et al., 2015). One of the challenges of salivary miRNA diagnostics is the lack of control groups and lack of suitable endogenous control (EC) for salivary miRNA normalization. My efforts thus focused on evidencing a suitable EC for salivary miRNA assays relevant to oral cancer patients (Momen-Heravi et al., 2014b). The differential expression patterns of miRNAs among 4 groups of patients with oral squamous cell carcinoma (OSCC), patients with OSCC in remission (OSCC-R), patients with oral lichen planus, and healthy individuals were examined by a genome-wide high-throughput miRNA microarray.

In these studies, miRNA-191 was identified as a suitable endogenous normalizer since it showed minimal intergroup and intragroup variability across subject groups and pooled samples. Of the more than 700 miRNAs present in saliva, 13 miRNAs consistently showed statistically significant differential expression in OSCC patients when compared to healthy individuals. This signature included 11 under-expressed miRNAs (miRNA-136, miRNA-147, miRNA-1250, miRNA-148a, miRNA-632, miRNA-646, miRNA668, miRNA-877,

miRNA-503, miRNA-220a, miRNA-323-5p) and 2 overexpressed miRNAs (miRNA-24, miRNA-27b). Interestingly, miRNA-136 was also under-expressed in OSCC vs. OSCC-R. However, miRNA-27b levels were also significantly higher in OSCC vs. OSCC-R and oral lichen planus. This pointed to miRNA-27b elevation as a suitable biomarker for the stratification of OSCC from OSCC-R and oral lichen planus. Since there is a lack of minimally invasive biomarkers for detection of oral cancer we assessed the discrimination ability of miRNA-27b to classify the patients with OSCC versus control healthy subjects. Indeed, the resulting receiver operating characteristic curve (ROC curve) indicated that at the optimal cutoff value for miRNA-27b in OSCC patients versus healthy individuals, the sensitivity and specificity were 85.7% and 100.0%, respectively, with an area under the curve of 0.96 (Figure 3.18).

A

B

C

D

miRNA-27b	AUC (Area under the curve)	Standard error	95% confidence interval
OSSC vs. HCs	0.9643	0.04452	0.8770 to 1.052
OSSC vs. OSSC-R	0.8810	0.09658	0.6916 to 1.070
OCC vs. OLP	0.9821	0.02813	0.9270 to 1.037
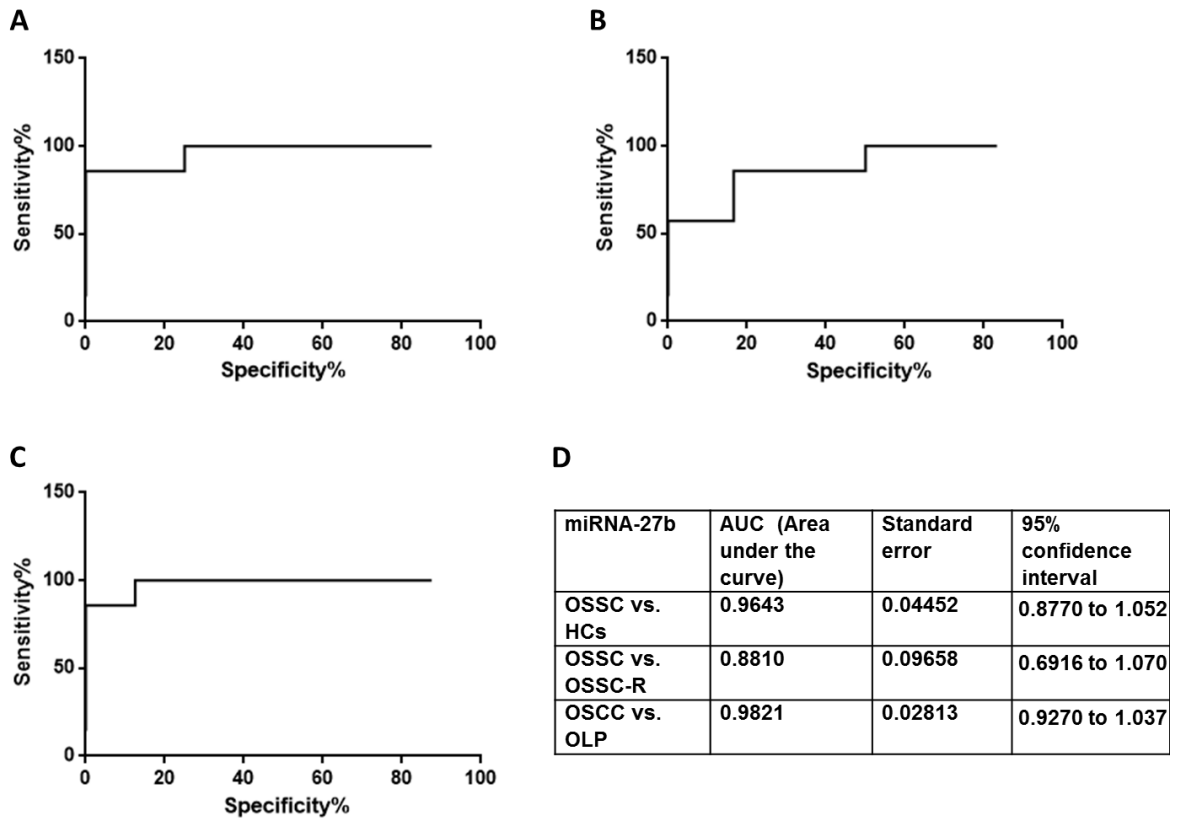
Figure 3.18: Curve of receiver operating characteristic and area under the curve for diagnostic accuracy of miRNA-27b. (A, B, C) Receiver operating characteristic curve analysis using differentially expressed miRNA 27b (miRNA-27b) for discriminating oral squamous cell carcinoma (OSCC) patients from OSCC patients in remission (OSCC-R), oral lichen planus (OLP) patients, and healthy controls (HCs). (D) Box presenting the area under the curve, sensitivity, specificity, and 95% confidence interval for every comparison between groups.

Although no study assessed the salivary biomarker utility of miRNA-27b in oral squamous carcinoma, miRNA-27b was reported to be correlated with other type of cancers which originate from epithelial cells. For example, miRNAs comprising the miR-23b/27b/24 cluster were found to correlate well with metastatic potential in mouse and human breast cancer cell lines and was elevated in metastatic lung lesions in human breast cancer patients (Ell et al., 2014). High expression levels of miRNA-27a/b correlated with poor response to chemotherapy in patients with esophageal cancer. In vitro mechanistic studies showed that esophageal cancer cells cultured in supernatant of miRNA-27a/b-transfected normal fibroblast showed diminished chemo sensitivity to cisplatin, compared with cancer cells cultured in supernatant of normal fibroblast. MicroRNA-27a/b-transfected normal fibroblast showed α-smooth muscle actin (α-SMA) expression, a marker of cancer-associated fibroblasts (CAF) as well as increased production of transforming growth factor-β (TGF-β) (Tanaka et al., 2015).

3.4 Exosome-based delivery of RNA interference and targeted miRNA therapy

Exosomes as natural nano-sized homogenous vesicles which can be used for drug delivery. Given their nanoscale size, and natural ability to deliver bio-macromolecules, we designed series of experiments to assess utility of exosomes in delivery of miRNA-155 mimic and inhibitor. MicroRNA inhibitors are synthetic, negatively charged miRNA target analogs, which are fully complementary, and have the ability to inhibit miRNAs function (Robertson et al., 2010). The negative charge of miRNA inhibitors necessitates the use of GDVs for delivery (Pecot et al., 2011). It has been shown that LPS induces miRNA-155 overexpression in RAW264.7 macrophages which results in the production of TNFα (Bala et al., 2011). Given the suggested role of miRNA-155 in LPS-induced TNFα production and the importance of macrophage inflammatory activation in different diseases we hypothesized that it might be useful to harness exosomes as vehicles to deliver a miRNA-155 inhibitor. B cells were chosen as source of exosome production since previous report documented excessive upon stimulation with CD40 and IL-4 (Saunderson et al., 2008). Moreover, our preliminary results suggested low endogenous level of miRNA-155 in stimulated B cells.

3.4.1 Purification and characterization of B cell derived exosomes for miRNA targeted therapy

B cell (M12.4) were stimulated with IL-4/CD40 and purified as described in Chapter 2. The mean diameters of the resulting exosomes were 98 nm (Figure 3.19A&B). The observed size and morphology were consistent with other reports in the literature (Atay et al., 2011). These exosomes expressed CD63 and CD81, but lacked GRP78 as identified by western blot (Figure 3.19C). The transmission electron microscopy (TEM) images showed the characteristic exosome morphology as observed in Figure 3.3 and size range of less than 150 nm (Figure 3.19D). Notably, NTA analysis indicated that upon stimulation of B cells with IL-4/CD40, exosome release increased drastically, up to 200-fold (Figure 3.19E).
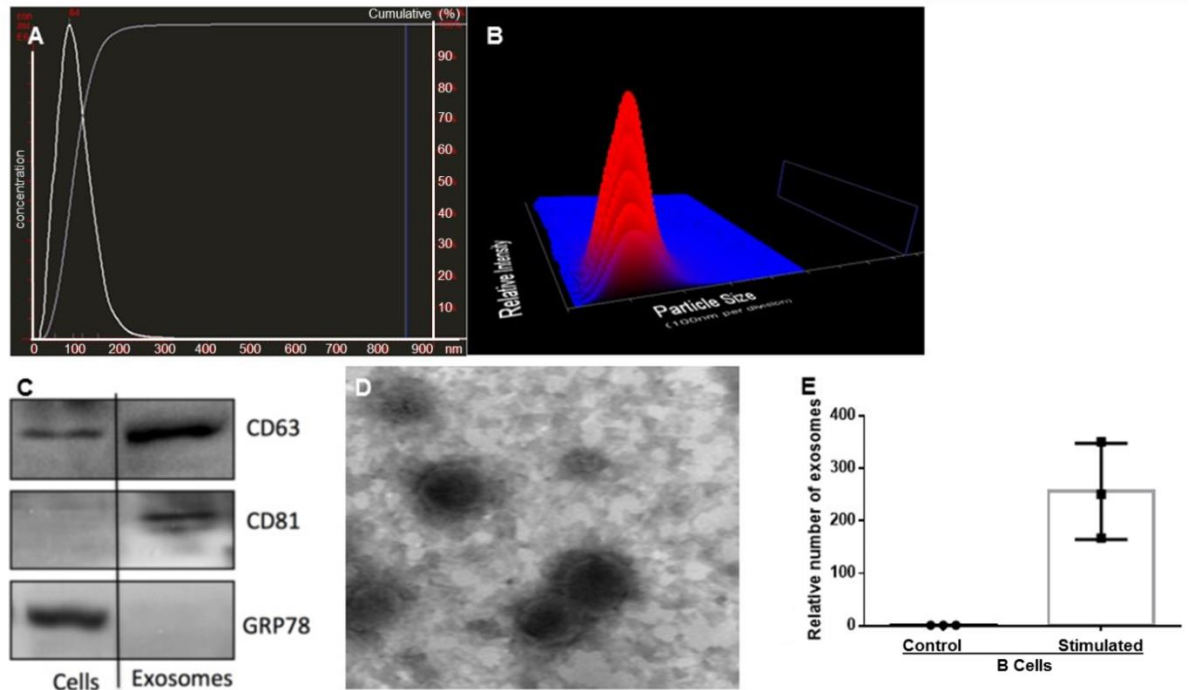
Figure 3.19: Characterization of B cell derived exosomes. (A) The diameter of stimulated B cell-derived exosomes was identified by NanoSight (mean diameter 98 nm). (B) The 3D graph represents particle size versus intensity versus concentration (particles/ml) of stimulated B cell-derived exosomes. (C) Isolated exosomes from murine B cells (M12.4 expressed exosomal markers, CD81 & CD63). (D) Transmission electron microscopy (TEM) image of B cell-derived exosomes showed the exosome morphology and a diameter of less than 150 nm. (E) The relative number of exosomes increased significantly after stimulation of B cells with IL-4&CD40 compared to the non-stimulated B cells (P<0.001). Results are obtained from three independent experiments.

This figure is adapted from Momen-Heravi et al., 2014, Nanomedicine

3.4.2 MicroRNA profile of B cell derived exosomes

To determine the suitability of B cell-derived exosomes as drug delivery vehicles for miRNA-155 modulating oligonucleotides, we first assessed miRNA-155 baseline expression in B cells and B cell-derived exosomes under both control and IL-4/CD-40 stimulation conditions. Interestingly, while intracellular levels of miRNA-155 were high in the stimulated B cells, the resulting exosomes had the lowest miRNA-155 level observed amongst these samples, at an exosome to stimulated parent B cell ratio of 1:54. (Figure 3.20). In contrast, the relative expression of miRNA-155 was comparable between RAW264.7 cells and their exosomes. Of note, the levels of cellular miRNA-155 were comparable between macrophages and B cells, even upon stimulation. These findings indicated selectivity of miRNA sorting into exosomes and confirmed that stimulated B cell-derived exosomes are almost devoid of miRNA-155. On this basis, IL4/CD40-stimulated B cell

exosomes appeared as potentially suitable delivery vehicles for miRNA-155-modulating therapy.
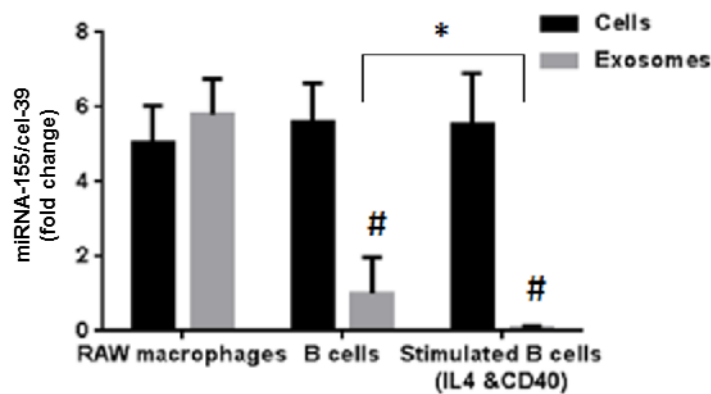
Figure 3.20: MicroRNA-155 expression in different exosomes and parental cells. Baseline expression levels of miRNA-155 in naive B cells, naïve RAW264.7 macrophages, and IL-4/CD 40-stimulated B cells and their exosomes was measured by qRT-PCR, normalized against spiked in Cel-39, signifying limited miRNA-155 sorting into stimulated B cell exosomes ($p<0.05$), further decreased compared to naïve B cell exosome miRNA-155 levels ($p<0.001$). The results are obtained from three independent experiments. (# indicates $p < 0.05$ versus parental cells).*This figure is adapted from Momen-Heravi et al., 2014, Nanomedicine*

3.4.3 Optimization of exosome loading by electroporation.

As described in Chapter 1, exosome-based delivery workflows should be tailored to the target disease, the cargo and the parental as well as targeted cells (Wahlgren et al., 2012). The workflow for efficiently loading murine B cell (M12.4) exosomes with miRNA-155 was defined and optimized ahead of delivering miRNA-155 mimics and inhibitors *in vitro* and *in vivo*. Electroporation-mediated loading of B cell-derived exosomes was optimized by comparison of different voltages, capacitance, and miRNA-155 mimic to exosome mass ratios, with loading quantified by TaqMan® qRT-PCR. Of the five voltages with a constant capacitance (100 µf) tested, 0.14 kV - 0.20 kV was significantly more efficient, with optimal loading achieved between 0.15-0.20 kV (Figure 3.21A). Under 150 kV, assessment of different exosome concentrations (0.25 to 3 µg/ml exosomal protein) indicated 0.5 µg/ml to 1 µg/ml exosomal protein to 150 pmol miRNA mimic achieved optimal encapsulation efficiency (Figure 3.21B).
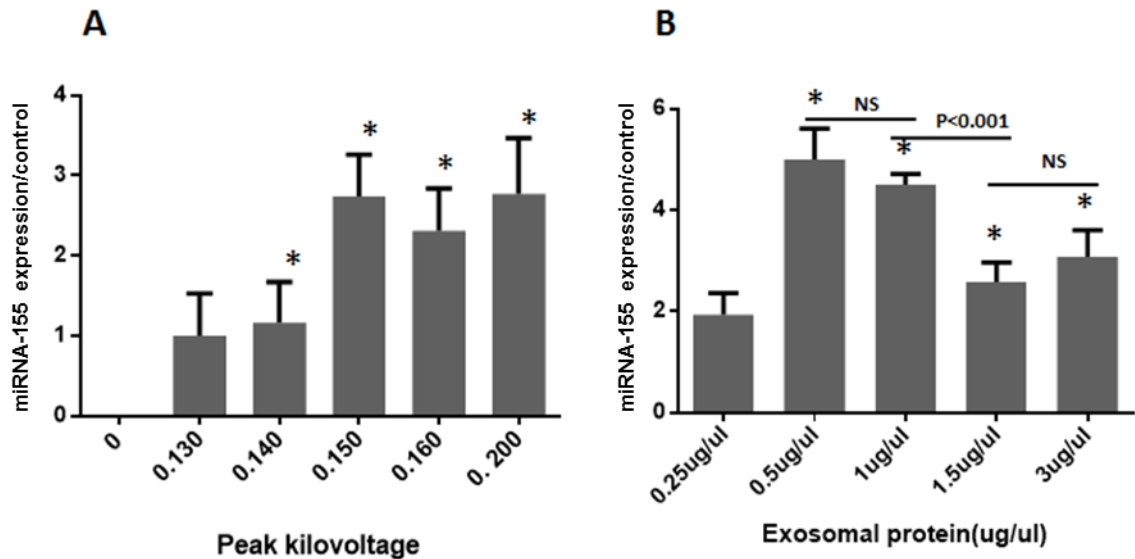
Figure 3.21: Optimization of electroporation conditions for loading of miRNA-155 mimic to exosomes. (A) Introduction of miRNA-155 to B Cell exosomes was performed using various voltages. Exosomes + miRNA-155 mimic without electroporation served as negative control. After administration of an electric pulse, exosomes were re-pelleted using Exoquick-TC™ and the encapsulation efficacy at different voltages was identified by detection of the relative amount of miRNA-155 mimic. Voltages of 0.14 kV, 0.15 kV, 0.16 kV, and 0.20 kV were more efficient compared to a lower voltage (0.130 kV) ($p<0.05$). (*indicates $p < 0.05$ compared to the lowest voltage). (B) Different concentrations of exosomal proteins were introduced to the exosomes via electroporation. All other conditions were similar. In the presence of exosomal protein concentrations of 0.5 μg/μl to 1 μg/μl loading was most efficient. The efficiency of exosome loading significantly diminished at concentration of more than 1 μg/μl ($p<0.001$). Results are obtained from three independent experiments. (*indicates $p < 0.05$ compared to the lowest concentration)

This figure is adapted from Momen-Heravi et al., 2014, Nanomedicine

3.4.4 Recovery of exosomes after miRNA-155 loading: method optimization and comparison

To compare different methods for the isolation of exosomes after electroporation and development of an optimized protocol, the same amount of exosomes was electroporated with the same amount of miRNA-155 mimic. Thus, loaded and control exosome preparations were treated with 1 unit RNase H for 1 h and re-isolated with the Exoquick™, ultracentrifugation, or immunomagnetic isolation methods and re-suspended in PBS followed by RNA isolation by Direct-zol™ RNA MiniPrep isolation kit as described in section 2.1.1 (Figure 3.22A). This study indicated Exoquick™ was the best isolation efficiency approach compared to the two other methods (Figure 3.22B); CD63

immunomagnetic selection method was also superior to ultracentrifugation for the isolation of exosomes. On the basis of applying optimized loading and isolation conditions, a miRNA-155 mimic exosome loading efficiency of 55 % with standard deviation of 3.64% was achieved.
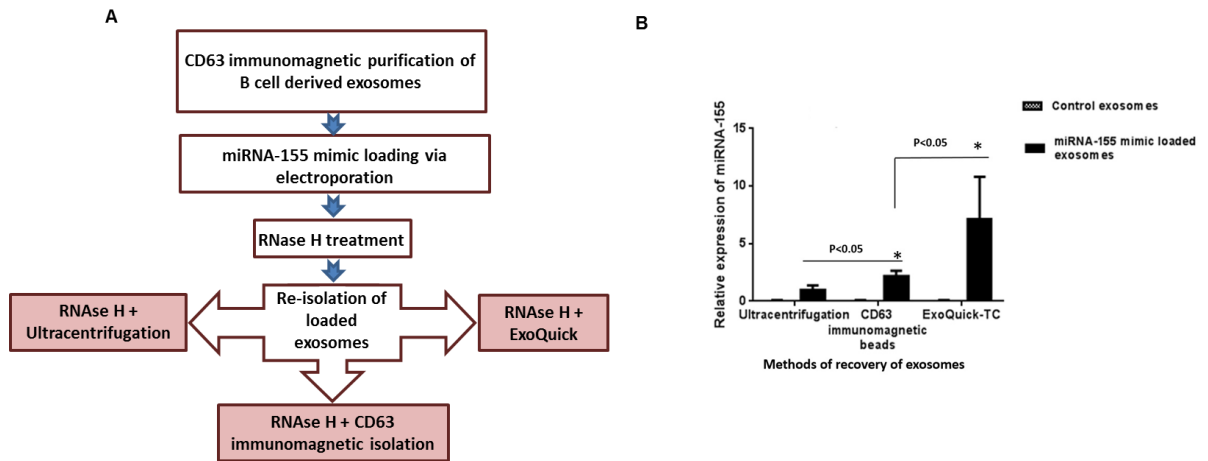
Figure 3.22: Optimization of workflow for isolation of miRNA-155 mimic loaded exosomes. (A) The schematic experimental workflow for evaluating the effect of different isolation methods on exosome recovery. (B) Identical amounts of B cell-derived exosomes isolated with CD63 immunomagnetic beads were loaded with same amount of miRNA-155 mimic by the electroporation technique and re-isolated with different methods (Exoquick-TC, ultracentrifugation, and CD63 magnetic beads). Cel-39 was spiked in the samples and served as normalizer. Exoquick outperformed ultracentrifugation and CD63 immunomagnetic isolation in vesicles recovery ($p<0.05$). Ultracentrifugation was significantly less efficient than CD63 immunomagnetic isolation ($p<0.05$). The data is represented as the mean value and SD (as error bars) of three independent experiments. (*represents $p < 0.05$ versus ultracentrifugation)*This figure is adapted from Momen-Heravi et al., 2014, Nanomedicine*

3.4.5 Exosome-mediated delivery of exogenous miRNA-155 mimic into primary mouse hepatocytes *in vitro.*

The harvested miRNA-155-loaded exosomes successfully delivered their cargo to primary mouse hepatocytes after a time course of 6 h co-culture. Delivery was evidenced by a more than 700-fold increase in intracellular miRNA-155 levels at 24 h post-exosomal transfection as measured by qRT-PCR (Figure 3.23) and was reproduced also in miRNA-155 KO mouse primary hepatocytes (Bala et al., 2015).
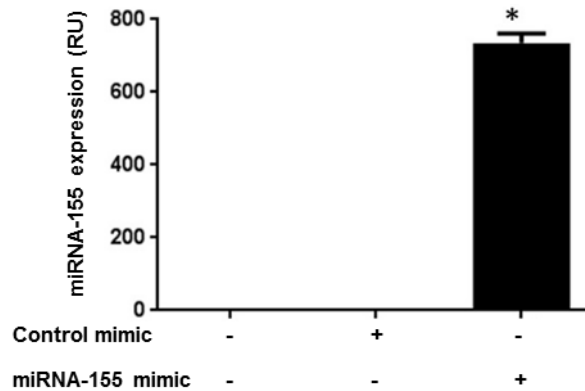
Figure 3.23: Delivery of miRNA-155 mimic to primary mouse hepatocytes via exosomes. Exosomes derived from B cells were loaded with miRNA-155 mimic utilizing optimal loading conditions. The miRNA-155 loaded exosomes and control inhibitor loaded exosomes were co-cultured with primary mouse hepatocytes (6h) followed by washing and media replacement. The levels of miRNA-155 were quantified by qPCR after 24 h. Exosomes successfully delivered miRNA-155 mimic to primary mouse hepatocytes ($p<0.001$). The PCR analysis was normalized by SnoRNA202 (internal normalizer). Results are obtained from three independent experiments. (* represents $p<0.05$ versus control cells) *This figure is adapted from Momen-Heravi et al., 2014, Nanomedicine*

Furthermore, KC were isolated from miRNA-155 KO mice and were similarly treated with exosomes loaded with miRNA-155. The protocol successfully delivered miRNA-155. The data is suggestive of increase in pro-inflammatory responses after LPS challenge as evidenced by measurement of MIP2 mRNA, MCP1 mRNA, and MCP1 protein levels (Figure 3.24). Importantly, however, these markers exhibited no inflammatory response induction in the recipient cells on account of exosome use, as evidenced by the lack of cytokine mRNA and protein increases in the cells not treated with LPS.
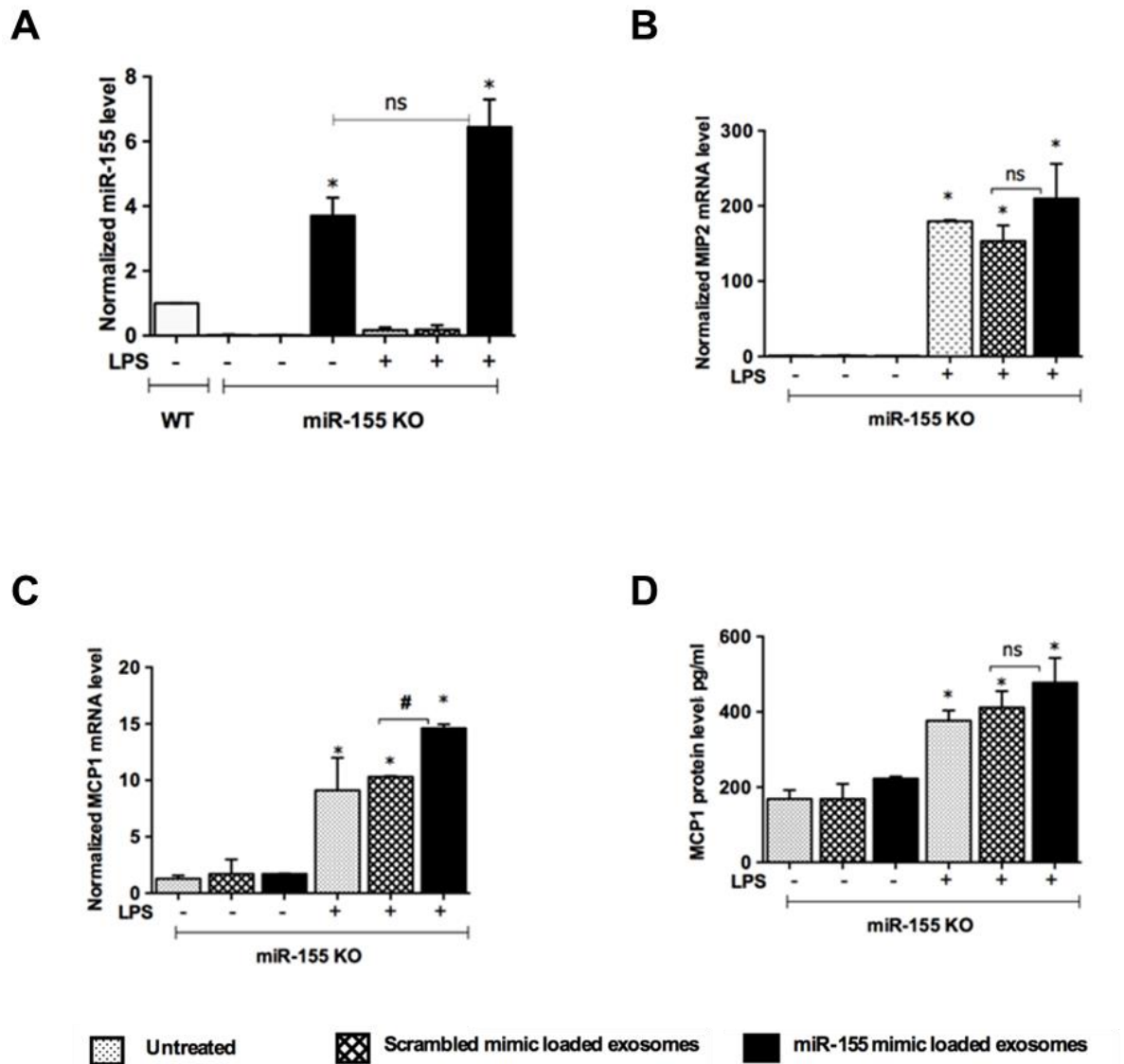
Figure 3.24: Biological function of miRNA-155 delivered via exosomes in Kupffer cells. Kupffer cells were isolated from miRNA-155 KO mice as described in Chapter 2. Exosomes were loaded with miRNA-155 or control mimic and co-cultured with cells for 6 h. The culture media was removed and cells were washed 3 times with PBS to remove free-floating exosomes. LPS (100 ng/µl for 6 h) was added to the pertinent experiment groups. (A) The expression levels of miRNA-155 were quantified in the cells. The amount of miRNA-155. SnoRNA202 was used for normalization (B&C) Levels of MIP2 and MCP1 (mRNA) were quantified using real-time qPCR and levels were normalized to untreated cells. 18S was used for normalization of mRNA to account for the technical variations between the samples. (D) MCP1 protein levels were quantified in the cell-free supernatant. Results are obtained from three independent experiments. (ns: non-significant; * $p < 0.05$ scrambled loaded exosome treated cells, # compared to scrambled loaded exosome + LPS treated cells.)

This figure is adapted from Bala et al., 2015, Scientific reports

3.4.6 Delivery of exogenous miRNA-155 inhibitor to macrophages using exosomes

To evaluate the utility of B cell-derived exosomes for anti-miRNA delivery, B cell exosomes were loaded with miRNA-155 antisense inhibitor using the loading conditions defined for miRNA mimics. These successfully delivered miRNA-155 inhibitor to RAW 264.7 macrophages as determined by qRT-PCR for miRNA-155, which is elevated in RAW264.7 cells under LPS stimulation (Bala et al., 2011). Importantly, maximal miRNA-155 inhibition appeared to be superior with exosomal delivery systems as opposed to commercial transfection reagents (P<0.05), was not (empty) exosome mediated and inhibitor sequence dependent (Figure 3.25A). However, these data evidenced only effective association of the antisense with its target after an extraction-purification procedure; conceivably, this could be on account of post-purification annealing as opposed to intracellular on-target binding. As suppressor of cytokine signaling 1 (SOCS1) is a known target of miRNA-155 implicated in the LPS-mediated response of RAW264.7 cells (Kurowska-Stolarska et al., 2011; Davey et al., 2006), the levels of this transcript were therefore assessed to determine biological significance of these findings. Thus, >5x decrease in SOCS1 mRNA induced by LPS were reduced to a 2.5x decrease in the presence of miRNA-155 exosomes (Figure 3.25B). Significantly, the effect magnitude was substantially lower with commercial transfection reagents, which at best achieved 1.4X reduction. Again, these observations were not on account of (empty) exosome use or inhibitor sequence-independent.
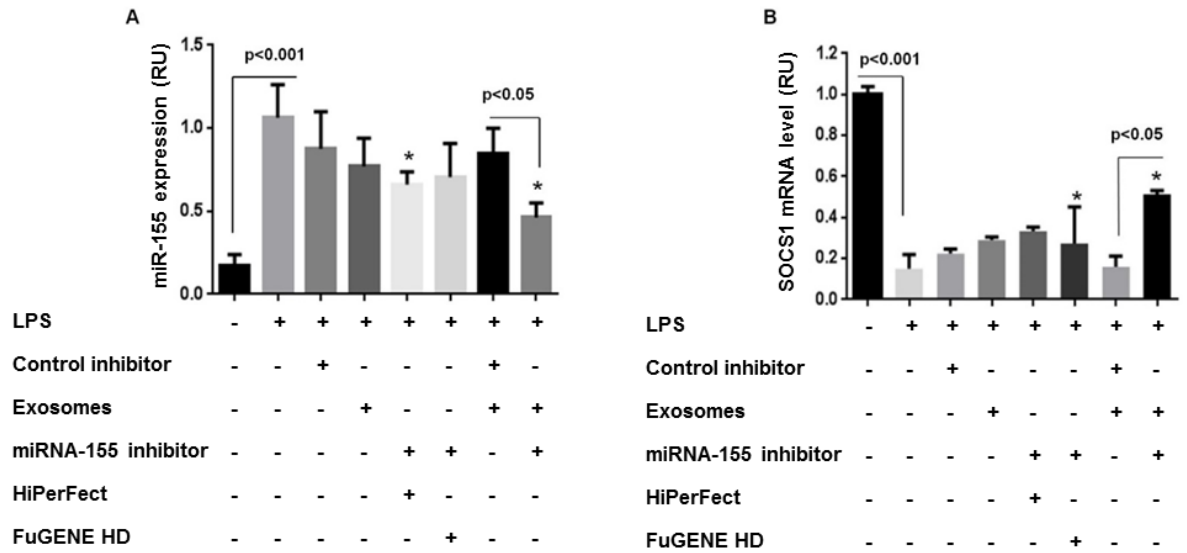
Figure 3.25: Delivery of miRNA-155 inhibitor to RAW 264.7 cells via exosomes. Raw264.7 macrophages were plated 1 day prior to the experiments and different treatment conditions and controls were administered for 24 h. LPS (100 ng/ml) was administered to the cells for 6 h as indicated. (A&B) Relative expression of miRNA-155 and SOCS 1 were measured by quantitative real-time PCR (qPCR) using a TaqMan miRNA assay and CYBR Green PCR respectively. Results are obtained from three independent experiments. (*indicates $p < 0.05$ compared to medium + LPS treated RAW264.7 macrophages).
This figure is adapted from Momen-Heravi et al., 2014, Nanomedicine

In accordance with the expected mechanistic impact of SOCS1 restoration, exosome-mediated miRNA-155 inhibition led to a significant decrease in LPS-induced TNFα protein (Figure 3.26). Significantly, the TNFα reduction achieved using exosomal miRNA-155 was statistically superior that achieved with commercial transfection reagents, not on account of (empty) exosome use and not inhibitor-sequence independent (Figure 3.26). The schematic of experiment design is depicted in Figure 3.27.
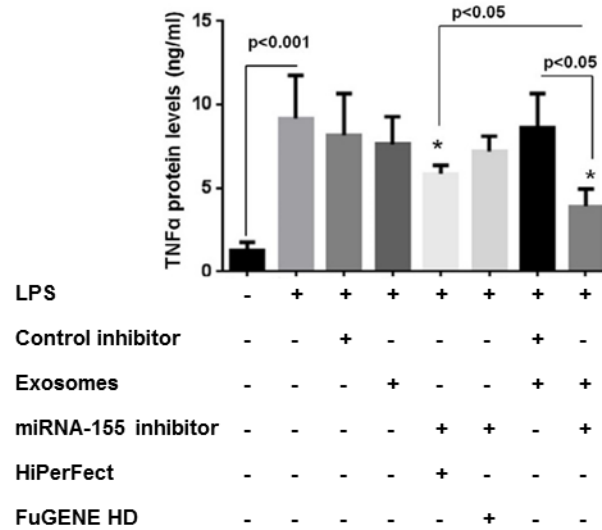
Figure 3.26: Exosome-mediate miRNA-155 delivery reduced TNFα levels in RAW264.7 cells. Raw264.7 macrophages were plated 1 day prior to the experiments and different treatment conditions and controls were administered for 24 h. LPS (100 ng/ml) was administered to the cells for 6 h as indicated. The amount of TNFα protein in the supernatants was quantified by ELISA. Data was obtained from three independent experiments. Results are obtained from three independent experiments. (*indicates $p < 0.05$ compared to medium + LPS treated RAW264.7 macrophages)*This figure is adapted from Momen-Heravi et al., 2014, Nanomedicine*
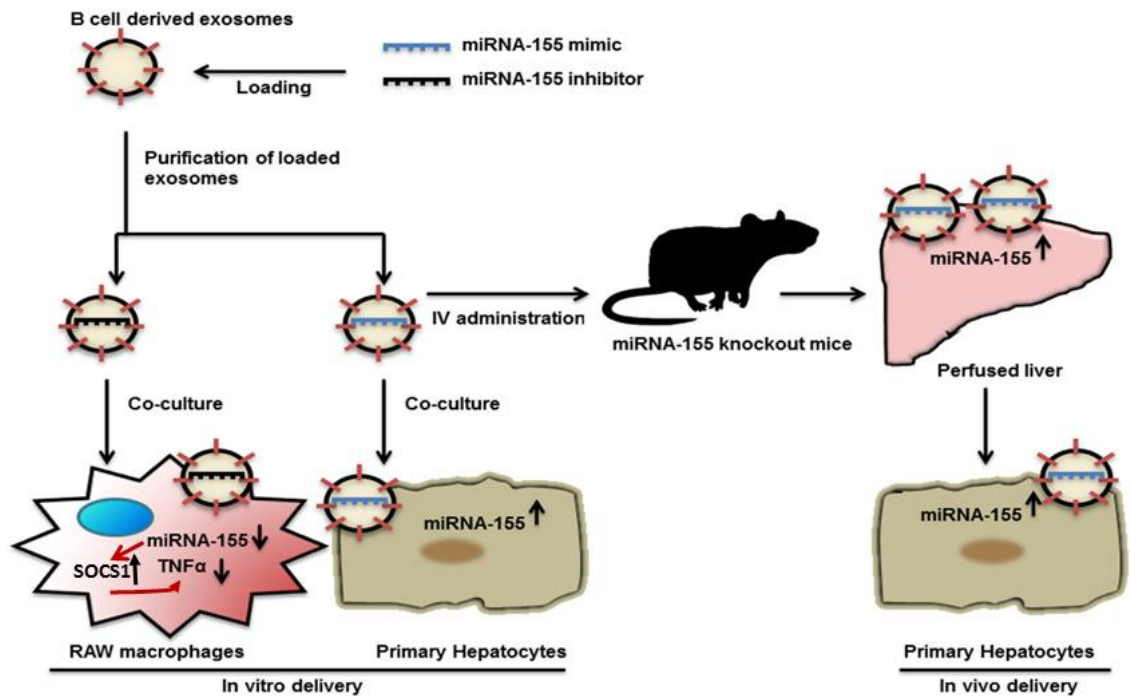
Figure 3.27: B cell-derived exosomes were used as vehicles to deliver exogenous miRNA-155 mimic or inhibitor into hepatocytes or macrophages. Exosomes loaded with a miRNA-155 mimic successfully delivered miRNA-155 mimic and significantly increased miRNA-155 levels in primary mouse hepatocytes and the liver of miRNA-155 knockout mice. Treatment of RAW264.7 macrophages with miRNA-155 inhibitor loaded exosomes resulted in a statistically significant reduction in LPS-induced TNFα production and partially prevented LPS-induced decrease in SOCS1 mRNA levels.

3.4.7 Evaluation of the cytotoxicity risk of exosome-delivered miRNA inhibitor therapies

Specially designed cationic lipids, such as the Lipofectamine have shown acute toxicity and immunogenicity after administration for nucleic acid delivery (Al-Dosari and Gao, 2009). Although viral vectors are believed to have less toxicity compared to cationic lipids, in a clinical trial for hemophilia B, an unexpected liver toxicity was observed and was attributed to a cytotoxic-T-lymphocyte response to adeno-associated virus serotype 2 (AAV-2) transduced hepatocytes (Manno et al., 2006). An ideal delivery vehicle should have high efficacy and minimal toxicity. Therefore, cytotoxic potential of exosome-delivered miRNA inhibitor therapeutics was explored alongside that of commercially available transfection reagents. To this end, the LDH release assay was used as a measure of cell lysis against known cytotoxic agents (staurosporine) (Lovborg et al., 2004). Importantly, exosome-based delivery of synthetic miRNA-155 antisense inhibitors or scrambled oligonucleotides showed no cytotoxic potential. However, in stark contrast, both of the commercially available

transfection reagents FuGENE® HD and HiPerFect showed statistically significant cytotoxicity (Figure 3.28).
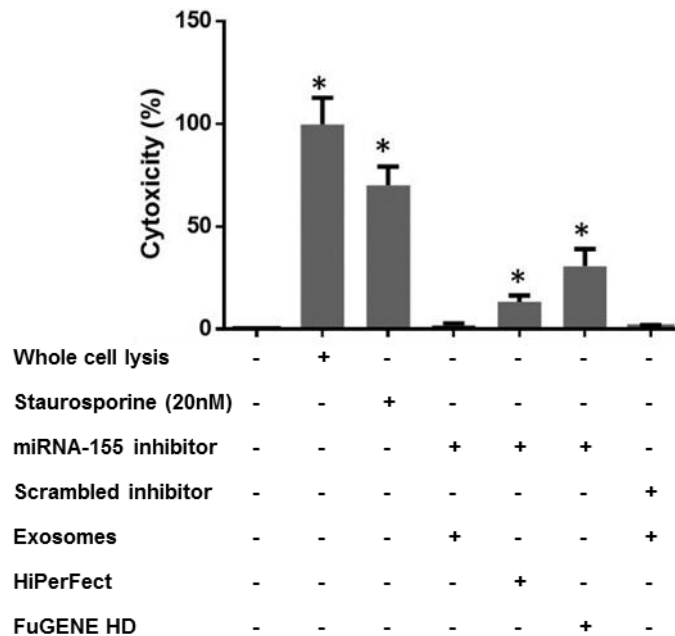
Figure 3.28: Evaluating cytotoxicty of exosome-based nucleic acid delivery and transfection reagents. LDH showed minimal cytotoxicity of exosomes compared to the transfection reagents and other controls after 36 h of co-culture. 20 nM staurosporine was used as a cytotoxic positive control. Results are obtained from three independent experiments. (*indicates $p < 0.05$ compared to non-treated macrophages)

This figure is adapted from Momen-Heravi et al., 2014, Nanomedicine

3.4.8 *In vivo* delivery and biodistribution of exogenous miRNA-155 mimic via exosomes

Several lines of evidence indicate that circulating miRNAs can be distributed into organs via the circulation (Kosaka et al., 2010; Minami et al., 2014). MicroRNAs are also receiving interest given their potential as therapeutic tools and targets in various diseases (Tiberio et al., 2015; Soifer et al., 2007). Evidences suggest that exosomes/EVs carry various molecular cargos including mRNA and non-coding RNA and can shuttle material between cells/organs (Eldh et al., 2010). MicroRNA-155 is an inflammation associated miRNA that control inflammatory responses and immune cell functions at multiple levels (O'Connell et al., 2012). We found that under a combined CpG+LPS inflammatory stimulus protocol, miRNA-155 was released into circulation and was strongly associated with EVs in the plasma of wild type mice (Figure 3.29A). We next proceeded to assess the half-life and biodistribution of ectopically produced exosomes associated with synthetic miRNA mimics *in vivo*. Thus miRNA loading of B cell exosomes generated using the optimized production

and electroporation protocols resulted in ~500x higher levels of miRNA-155 in the vesicles (Figure 3.29B). These were administered intravenously in miRNA-155 KO mice (100 µl; ~2×10^8 particles, or 100 µg exosomal protein) and their resulting bio-distribution was determined across 6 key tissues after perfusion, to focus on parenchymal tissue loading (Figure 3.29C-H).
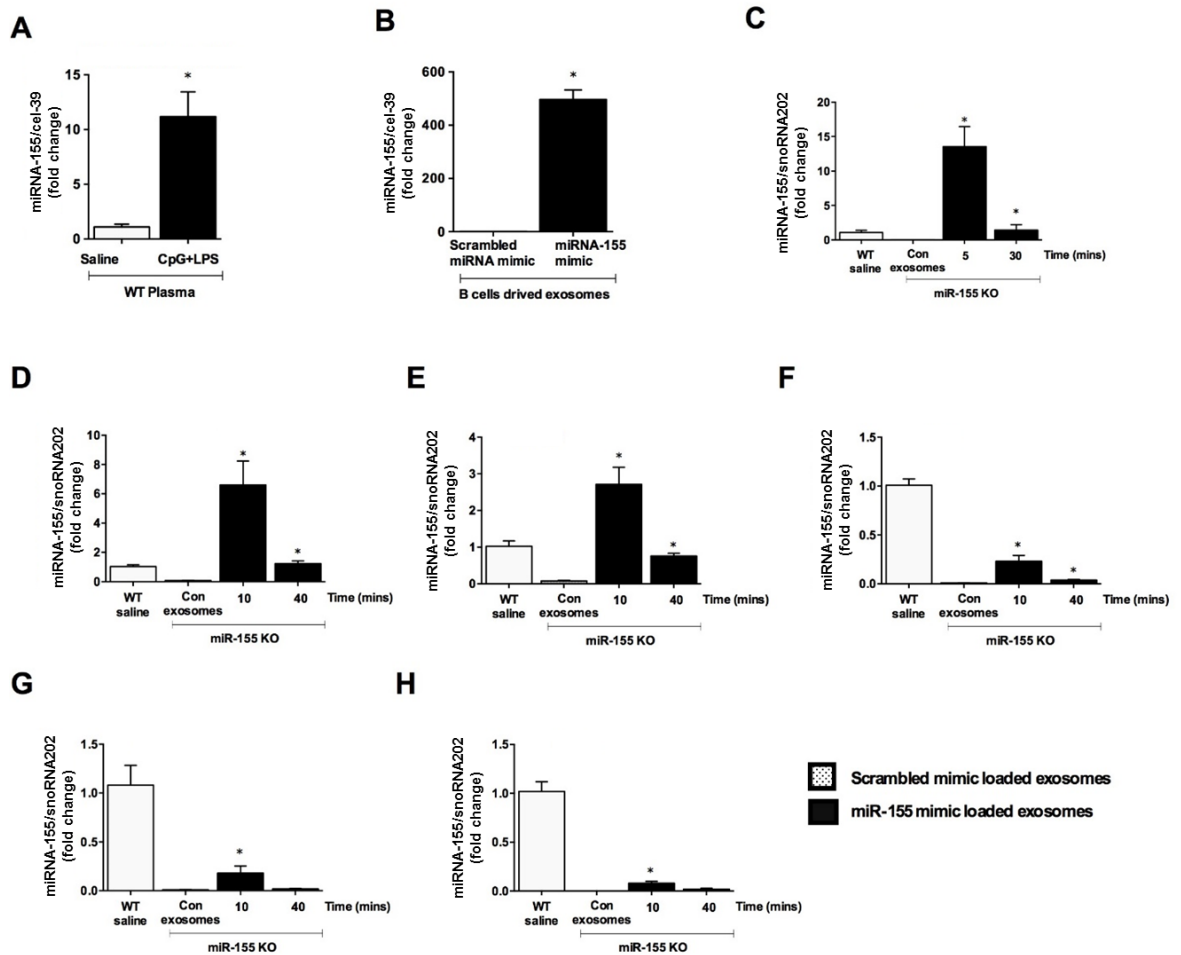
Figure 3.29: Natural and ectopic exosomal delivery of miRNA-155. (A) Saline or 2.5 mg/kg CpG DNA were injected to C57Bl/6 wild type (WT) female mice. The mice were injected (with i.p.) once a day for three days. On day 4, CpG treated mice received 0.5 mg/kg LPS for 3 h, after which blood was collected. Exosomes were purified from plasma using a filtration+ExoQuick technique as described in Chapter 2. miRNA-155 levels were determined by TaqMan qPCR. (B) B cells were stimulated with CD40 and IL-4 and exosomes were purified using CD63 magnetic beads as described Chapter 2. The exosomes were electroporated with either miRNA-155 mimic or scrambled mimic. miRNA-155 levels were quantified after RNase H treatment. 100 µl of miRNA-155 analogue-loaded exosomes was injected intravenously into miRNA-155 KO mice for the indicated times and the levels of ectopic, exosomally-derived miRNA-155 in the plasma (C), liver (D), adipose tissue (E), lung (F), muscle (G), kidney (H) were quantified using real-time qPCR. miRNA-155 levels

were expressed relative to the miRNA-155 levels in the wild type saline treated mice. Synthetic spiked cel-miRNA-39 was used to normalize the variation between samples in exosome samples before RNA extraction (A–C). SnoRNA202 was used to normalize the technical variations between the samples in different tissues (D-H). Results are obtained from three independent experiments. (*indicates $p < 0.05$ compared to scrambled mimic exosome treated KO mice)

This figure is adapted from Bala et al., 2015, Scientific reports

The protocol led to an approximately 15-fold increase in miRNA-155 levels in plasma after 5 min as compared to naturally occurring plasma miRNA-155 levels in wild type (WT) mice (Figure 3.29C) and peak tissue loading at approximately 10 min after injection. By 30 min post-injection, miRNA-155 levels had decreased substantially in plasma to match baseline miRNA-155 levels in WT mice (p=0.7) (Figure 3.29C). Notably, miR-155 kinetics were similar across plasma and the tissues assayed (Figure 3.29D-H), with accumulation being liver>adipose tissue>lung>muscle>kidney as compared to baseline miR-155 levels in WT animals. Interestingly both the liver and adipose tissue accumulated higher than baseline amounts of miRNA-155 mimic within 10 min, but regressed to the baseline WT expression levels after 40 min and disappeared after 4 h. In stark contrast, no significant increase in miRNA-155 was observed in the brain, heart, spleen, bone marrow cells or thymus. Importantly, across this study the observed miRNA-155 fluctuations were mimic-sequence specific as evidenced through use of scrambled sequence controls.

To scrutinize further the cellular distribution of exosomal miRNA-155 in the liver, the ectopic miRNA-155 was quantified in hepatocytes and liver mononuclear cells (MNCs) of KO mice. Peak levels were observed at 10 min following injection followed by a rapid decline, similar to what perfused liver observations (Figure 3.30). However, neither cell type appeared to accumulate miRNA-155 to levels comparable of those observed in WT mouse-derived cells by a factor of 2-4x.
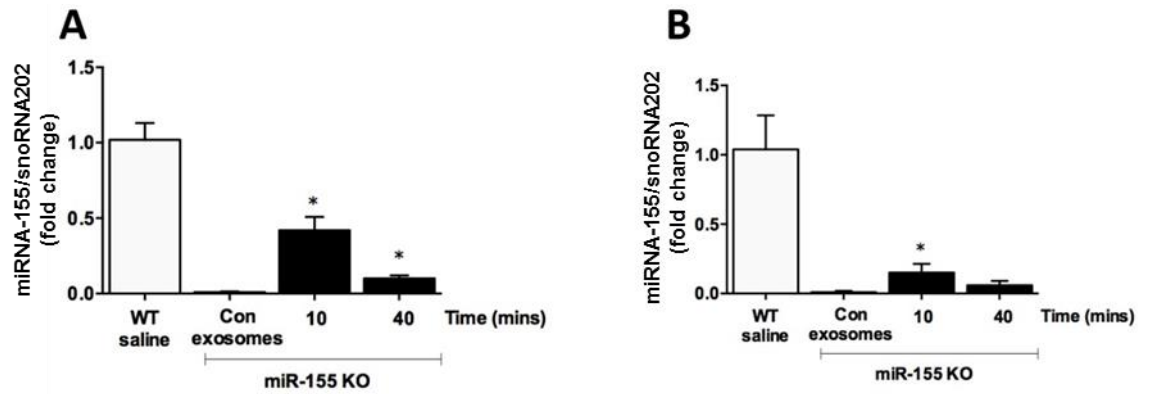
Figure 3.30: Cellular level distribution of exosome loaded miRNA-155 mimic in miRNA-155 KO mice. After *in vivo* delivery of miRNA-155, hepatocytes (A) and mononuclear cells (B) were isolated and miRNA-155 levels were determined using a real time qPCR. miRNA-155 levels were normalized to the wild type saline treated mice. SnoRNA202 was utilized to normalize the technical variations between the samples. Results are obtained from three independent experiments. (*indicates $p < 0.05$ versus scrambled mimic exosome treated KO mice; $p<0.05$ is considered statistically significant)
This figure is adapted from Bala et al., 2015, Scientific Reports

Interestingly, unlike other biological and synthetic delivery systems, miRNA exosome co-culture with liver MNCs isolated from wild type mice did not induce any pro-inflammatory cytokines in this study (TNFα, MCP1 and IL-1β) both at the mRNA and protein levels in l (Figure 3.31).
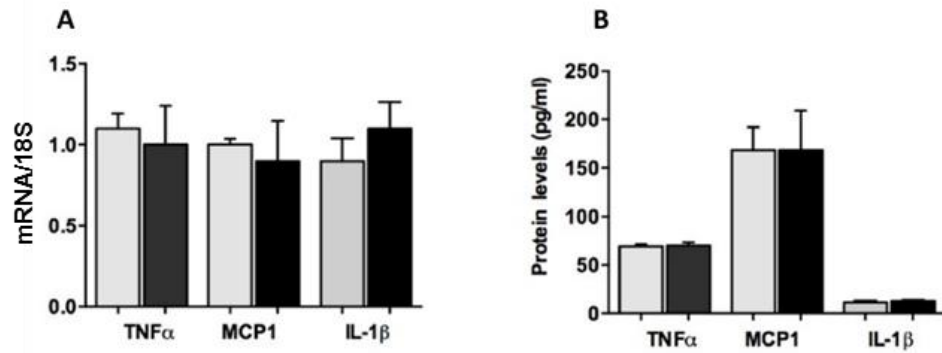
Figure 3.31: Scrambled mimic loaded exosomes do not elevate inflammatory markers in liver mononuclear cells. (A) Scrambled mimic loaded exosomes were co-cultured with the liver mononuclear cells isolated from WT mice for 6 h. Free-floating exosomes in the supernatant were removed and cells were cultured for another 6 h. The mRNA expression levels were determined by real-time PCR (B) Cell-free supernatants were used to measure protein levels of MCP1, TNFα, and IL-1β by ELISA. Results are obtained from three independent experiments. In both graphs, the dark bars demonstrate the scrambled mimic loaded exosomes and the light bars demosntrate the untreated controls.

This figure is adapted from Bala et al., 2015, Scientific Reports

Chapter 4
Discussion

Research on EVs and the role of noncoding RNA has been growing exponentially during the past few years. Exosomes are found in different biofluids and are potential sources for the discovery of novel biomarkers. Although exosome research is growing very rapidly, there remain major challenges in terms of reproducible isolation and characterization of exosomes, understanding role of exosomes in various pathological pathways, and assessing the utility of exosomes as drug delivery vehicles. My research first aimed to establish and compare methods for isolation and characterization of exosomes (Momen-Heravi et al., 2013; Momen-Heravi et al., 2012a; Momen-Heravi et al., 2012b). Secondly, my research explored the functional role of exosomes and miRNAs in the pathogenesis of different diseases including alcoholic hepatitis (Momen-Heravi et al., 2015a), hepatitis C (Bukong et al., 2014), and head and neck cancer (Momen-Heravi et al., 2014b). The result of my investigations identified pathways and new disease mechanism and introduced new diagnostic potential. Thirdly, my research explored the bio-distribution of exosomes and miRNA (Bala et al., 2015), and potentials for using exosomes as drug delivery vehicles (Momen-Heravi et al., 2014a). This resulted in an establishment of a workflow and new approaches for harnessing the delivery potential of exosomes to pursue miRNA/RNA targeted therapies in both *in vitro* and *in vivo* models. In this chapter, I will discuss some of the main findings of my research, which demonstrate a conceptual overview of my work in the field of exosomes/EVs and RNA biology. Future directions in the RNAi and exosomes/EVs field and its challenges are also considered.

4.1 Isolation and Characterization

One of the main issues in using exosomes for biomarker discovery and as drug delivery vehicles is the lack of reproducible and reliable methods of isolation and characterization. In several cases, small variation in structure or isolation techniques can lead to substantial downstream biological or analytical effect. For instance, phosphorothioate backbone modification of nucleotide-based drugs is a common modification performed to increase stability and prevent degradation of nucleic acids by plasma and intracellular nucleases. A

new reported documented unexpected effect of phosphorothioate backbone modification in triggering robust platelet activation and ROS generation (Flierl et al., 2015). In the RNAi studies, a great body of studies fail to rule out, off-target effects by employing proper negative and positive controls (Cook et al., 2014). In the exosome field, performing unadjusted protocol for rotor with lower k-factor lead to lower substantially lower yield of RNA and proteins (Cvjetkovic et al., 2014). In fact, such methods should be tailored based on the specific to the biofluid in question and the downstream (therapeutic or diagnostic) target. In addition to the necessity of method optimization, the effect of each alteration in downstream results should be fully understood and considered as part of ongoing improvement in nucleomic and exosome field.

In this domain, my research demonstrated that the viscosity of biofluids could significantly affect sedimentation efficiency after ultracentrifugation (Momen-Heravi et al., 2012b). We observed a significant difference between sedimentation efficiency of plasma, serum and culture media ($p < 0.001$) after employing identical ultracentrifugation protocol and condition. The viscosity of the plasma, serum, CM, and PBS were 1.65, 1.4, 1.1, and 1.0 cP, respectively. The Pearson correlation was -0.912 ($p < 0.001$), indicating that a greater viscosity leads to lower sedimentation efficiency (Momen-Heravi et al., 2012b). Also, we found that in more viscous biofluids, particles with larger diameters had a tendency to sediment after ultracentrifugation rather than smaller ones. These results have influenced significantly the approach taken by groups working in this area, who now incorporate normalization of viscosity in their isolation protocols of EVs (Witwer et al., 2013; Lobb et al., 2015; Taylor and Shah, 2015). Thus, this work has seeded the necessary level of standardization pertinent to clinical use of exosomes either as diagnostic or therapeutic tools.

4.2 Role of exosomes and miRNAs in the pathogenesis of alcoholic liver disease

Extracellular vesicles including exosomes exert different physiological and pathological functions that have been described extensively in the literature (Yanez-Mo et al., 2015; Yuana et al., 2013). My research resulted in novel findings revealing the role of exosomes and miRNAs in the pathogenesis of alcoholic liver disease (Momen-Heravi et al., 2015a). As with many cancer studies, this work found that the total number of exosomes was increased in an *in vitro* model of ethanol administration, in human subjects after binge alcohol drinking, as well as in murine models of chronic alcohol feeding and binge alcohol feeding. Furthermore, a significant increase in the expression level of Rab 27b was consistently observed in hepatocytes after administration of ethanol. Mechanistically, this

finding is in line with the elevation of exosome production observe, as Rab 27b is part of the family of Rab membrane bound proteins which play crucial roles in vesicular trafficking and fusion at the plasma membrane (Ostrowski et al., 2010). Thus, my work has helped corroborate the link between the cellular effects of ethanol on multivesicular body formation and exosome production, and expand understanding of the fundamental processes underpinning these phenomena.

Beside an increase in the total number of exosomes, this work also reported significantly elevated exosomal miRNA-122 levels in all *in vivo* models and in an *in vitro* setting, suggesting an alcohol-mediated activation of the exosome production machinery in hepatocytes, associated with miRNA-122 sorting into these vesicular bodies. Interestingly, it has been reported that miRNA-122 could be related to liver injury, and elevated levels were found in acetaminophen (paracetamol)-induced liver injury and Toll-like receptor (TLR) 9+ 4 ligand-induced inflammatory cell mediated liver injury (Bala et al., 2012). However, the function of exosomal miRNA-122 as the product of liver injury remained unclear.

Given the role of monocytes in acute liver injury and inflammatory disease (Zimmermann et al., 2012), my efforts focused on exploring the functional potential, if any, of hepatocyte derived exosomal miRNA-122 in these cells. These studies revealed that monocytes, which are almost devoid of miRNA-122, actively collected these exosomes (Momen-Heravi et al., 2015a) to modulate their immune function through sensitization to LPS and an increase in pro-inflammatory cytokine production through modulation of HO-1 expression and its reciprocal target, Nox2. The HO-1 pathway is a pivotal immune surveillance pathway, which is necessary for cell survival and cell plasticity after challenges with LPS and ROS (Yachie et al., 2003; Li et al., 2012b; Taille et al., 2004). Mice deficient for HO-1 show increased pro-inflammatory responses, increased cellular necrosis, and increased mortality after LPS challenge (Gozzelino et al., 2010; Poss and Tonegawa, 1997), findings aligned with the observed functional outcomes of exosomal miRNA-122 uptake by monocytes. Crucially, the observed increase in monocyte miRNA-122 levels was only due to the horizontal transfer of the mature miRNA-122: pri-miRNA-122 was undetectable in these cells suggesting no *de novo* expression and synthesis of this non-coding RNA (Momen-Heravi et al., 2015a).

Taken together, these findings demonstrate a novel mechanism of cross-talk between ethanol-exposed hepatocytes and naïve monocytes via exosomes and their small non-coding RNA contents, specifically the hepatocyte specific miRNA-122. Moreover, these

observations provide a possibly additional mechanistic basis for the previously reported pro-inflammatory phenotype or M1 phenotype in non-resident immune cells and KC; thus, production of augmented pro-inflammatory cytokines and ROS may not only be instigated by alcohol and its metabolites, but also by paracrine activity of miRNA-122 containing exosomes derived from injured hepatocytes after alcohol exposure.

In addition to well-studied direct alcohol induced damage (Gao and Bataller, 2011), immune modulation through exosome-mediated transfer of miRNA-122 and modulation of the HO-1 pathway could be another mechanism of hyper-sensitization of monocytes/macrophages to LPS, which is observed in alcoholic liver disease (Momen-Heravi et al., 2015a). Importantly, exosomes loaded with miRNA-122 inhibitors were able to therapeutically attenuate the miRNA-122 mediated pro-inflammatory phenotype in monocytes. The precise therapeutic potential of such interventions remains to be described given the promising results observed with unformulated (naked), highly modified miRNA-122 antisense in the clinic (Miravirsen)(Janssen et al., 2013) (Lee et al., 2014). Miravirsen (Santaris Pharma, Copenhagen, Denmark), showed promising results in dose dependent reduction of HCV RNA in chronic HCV genotype 1 infection levels without evidence of viral resistance in a phase 2 clinical trial (Janssen et al., 2013). Thus, whilst transient impairment of the use of miRNA-122 by Hepatitis C and in hepatocyte metabolism has been suggested, it remains to be determined if chronic attenuation of the monocyte-mediated pro-inflammatory status might offer protective functions to alcoholic liver disease or other chronic conditions characterized by inflammation-induced liver fibrosis. Significantly, whilst miravirsen targets principally hepatocytes(Gebert et al., 2014), exosomal delivery of anti-miRNA-122 might access, and potentially even specifically target the monocyte subpopulation in the future, thereby expanding the utility of such interventions and minimizing impact to the canonical role of hepatocytes. These findings therefore open a new horizon in understanding the role of exosomes and highlight the potential utility of RNA-interference-associated therapeutics in the management of alcoholic liver disease.

4.3 Exosomes play an active part in Hepatitis C transmission

Specifically within the context of HCV, this research has demonstrated that circulating exosomes isolated from sera of a) treatment-naïve, HCV-infected subjects or b) HCV treatment non-responder individuals contain replication-competent HCV virus (Bukong et al., 2014). Importantly, several steps have been taken to ensure these findings are specific to exosomes and not potentially contaminating virions in establishing that these exosomes can

transmit active HCV infection to primary human hepatocytes. Thus, a novel approach consisting of serial filtration in combination with polymer precipitation and immune magnetic CD63- positive exosome isolation has been adopted to successfully and adequately separate exosomes from viral particles. Furthermore, the resulting viral genome titres in the recipient cells is increased by up to 3 logs in primary human hepatocytes compared to the exosomal load, indicative of active replication.

In addition to the purification approach, mechanistic evidence supports the premise that HCV-containing exosomes appear to mediate virus transmission, as SR-BI, CD81, and APOE -independent mechanisms were implicated. CD81 is a member of the tetraspanin family and one of the first identified entry receptor for HCV (Pileri et al., 1998). The class B scavenger receptor (SR-BI) protein was initially identified as a high affinity low density lipoprotein (LDL) receptor; SR-BI is HCV cellular receptor and play a significant role in in the early steps of HCV infection (Sabahi, 2009). APOE is required for HCV virion infectivity and HCV virions are assembled as APOE-enriched lipoprotein particles (Chang et al., 2007). Interestingly, this might explain the potential efficacy of HCV immunotherapy in some patients. A study by Wilson et al (Wilson et al., 2011), showed that bonding of Ago2 and miRNA-122 to 5′-UTR of HCV dsRNA enhances HCV replication. Within exosomes harvested from patients and HCV-infected cultured cells, HCV RNA was associated with HSP90, miRNA-122, and Ago2. Thus, experiments were designed to analyze the therapeutic potential of miRNA-122 inhibition with respect to exosome-mediated transmission. In these studies, miRNA-122 inhibitor modulated exosome function and significantly decreased exosome-mediated HCV transmission.

Exosomes originate from the lumen of MVBs and their cellular uptake and release is associated with the endocytic pathway (Urbanelli et al., 2013). The vacuolar H^+-ATPases (V-ATPases) and proton pumps generate and maintain intra-cellular pH gradients across cell membranes. Impaired function of V-ATPases was reported to be accompanied by lysosomal dysfunction and impaired endocytosis (Jentsch et al., 2005; Vingtdeux et al., 2007). In line with these findings, the therapeutic potential of a vacuolar-type H+-ATPase inhibitor and a proton pump inhibitor was also evaluated and was shown to able to block exosome-mediated and free virus mediated transmission of HCV to Huh 7.5 hepatoma cells.

4.4 Exosome-mediated delivery, biodistribution of miRNAs, miRNA targeted therapy

4.4.1 *In vivo* biodistribution of miRNA-155

The clinical potential of any novel pharmacological approach, whether consisting of a biological, a chemical or genetic drug, pivots on absorption, distribution, metabolism and elimination kinetics *in vivo*. In line with these requirements and on the basis of the promising findings of exosomally-delivered miRNA and their antisense inhibitors, the bio-distribution and half-life profiles of this novel chemobiologic formulation was investigated (Bala et al., 2015). Intravenously-administered exosomes loaded with miRNA-155 mimic underwent rapid distribution across various, but not all of the organs of recipient mice, in what appeared to be a plasma circulation mediated fashion. Use of the miR-155 KO animals against their WT counterparts enabled comparative enumeration of the extent of tissue and cell tropism as well as some preliminary insight on the duration of tissue residence. Thus, the level of ectopically provided miRNA-155 was found to acutely exceed normal (WT) levels in the liver and adipose tissue, but also reached in appreciable quantities the lung, muscle, and kidney. In accordance with these study, other work has reported the highest concentration of fluorescently-labeled, ectopically produced exosomes to be reached in the liver, lung and spleen 1 h after i.p. administration (Sun et al., 2010; Zhuang et al., 2011). Significantly, ectopic miRNA-155 was delivered to hepatocytes and liver MNC *in vivo*, supporting the utility of these vesicles in liver-targeted RNAi modulating therapies. Likewise, in agreement with other work (Zhuang et al., 2011; Alvarez-Erviti et al., 2011), no significant accumulation of exosome-related miRNA-155 was observed in the brain, suggesting exosome modification (e.g. targeting or blood-brain-barrier relaxing moieties) could be a likely necessity for access across the blood-brain barrier. Taken together, the differential bio-distribution profile across the surveyed tissues indicates the perfusion protocol effectively eliminated circulatory exosomes to enable tissue and cell-association data to be reliably obtained.

In the contexts of both basic research and clinical practice, RNA biology has been revolutionized through the unveiling of the significant role non-coding RNAs play in physiology and disease, and by the promise of RNA-based/targeting therapeutics. These novel drugs encompass the RNAi, synthetic/*in vitro* transcribed RNA sequences, miRNA mimics and miRNA inhibitors. Beyond the miRNA-122 inhibiting Miravirsen, ALN-RSV01 (Alnylam pharmaceuticals, Cambridge, Massachusetts), which is a naked siRNA targeted against respiratory syncytial virus (RSV) nucleocapsid, showed promising results in the prevention of *bronchiolitis obliterans* syndrome respiratory syncytial virus infections in lung

transplant patients at phase 2b. (Gottlieb et al., 2016). However, the fact that most forms of RNA are prone to rapid degradation by RNases, are negatively charged, and are potentially immunogenic have repeatedly obstructed their commercial success and clinical use. Different nucleic-acid delivery modalities, including viral and non-viral vectors, and transfection reagents are already broadly used for *in vitro* and *in vivo* delivery, even onto generating genetically modified cell-based therapies (Sharpe and Mount, 2015). Nevertheless, direct treatment (i.e. not cell based) approaches with the exception of arguably only one exception (UniQure) have suffered setbacks especially when associated with repeated administration (Marcus and Leonard, 2013).

4.4.2 Exosome-mediated delivery

Exosome-mediated delivery of miRNAs and RNAi has several advantages. Firstly, exosomes can be isolated from the recipients' own biofluids and stably stored for a prolonged time, for subsequent loading of biological drugs when required (Sokolova et al., 2011). Proof of clinical and commercial principle for such an autologous biological therapy approach has been delivered through Strimvelis, however the breadth of personalized exosome biobanking, purification or ectopic modification that might be necessary to achieve maximal tissue and disease coverage remains to be determined. Secondly, based on the preliminary research presented here, exosomes do not induce any inflammatory response, either *in vitro* or *in vivo*. Although preliminary such data have delivered tremendous excitement in the past, periodically new mechanisms of immune system activation suggest caution and further work on fully dissecting the immunomodulatory potential of specific exosome preparations (Broering et al., 2014; Forsbach et al., 2008). Moreover, the evidence produced through this work indicates efficacy dissociated from the toxicity inherent to other, widely used drug delivery modalities. These data are very encouraging for processes that are routinely in use in the laboratory, but require expansion on other mechanisms of cell injury ahead of further use. Thirdly, as with viral and non-viral competition, exosomes can protect the miRNA and RNAi cargo from degradation by RNases; indeed, the comparative stability of the delivery system, the cargo and the complex, both in wet and potentially even dry formulations in the future needs to be established.

It has been shown that EVs and exosomes can naturally transfer a variety of functional macromolecules, including mRNA, miRNA, and genomic DNA and the possibility of harnessing exosomes for the delivery of bio-macromolecules is an attractive approach (Valadi et al., 2007; Crescitelli et al., 2013; Montecalvo et al., 2012; Seow and Wood, 2009). Nevertheless, the efficiency of exosome-mediated delivery must be optimized based on the

recipient cell type, target cargo and exosome type, since the exosomal cargo is selectively enriched and exosomes have different natural abilities for drug delivery (Valadi et al., 2007; Crescitelli et al., 2013). In this research, the loading conditions for B cell-derived exosomes were first optimized to explore their use for nucleic acids delivery (Momen-Heravi et al., 2014a). Upon stimulation of B cells with IL-4 and CD40, large quantities of exosomes were produced, suggesting scalability of the approach to industrial grade production. Indeed, this has been a pivotal requirement in translating antibody therapeutics from successful laboratory reagents into quality of life transforming therapies.

Thus, using optimized conditions, B cell-derived exosomes were able to effectively deliver a miRNA-155 inhibitor into RAW264.7 macrophages, causing inhibition of miRNA-155, and subsequent functional decrease of TNFα production (Momen-Heravi et al., 2014a). In comparison with conventional transfection reagents (FuGENE HD and HiPerFect) this inhibitory efficacy was not accompanied by any, even marginal degree of cytotoxicity. These results therefore support expansion of this approach to other high clinical demand / unmet need disease areas, such as neurological disorders, cancers, and autoimmune diseases where miRNA-155 is deregulated, or indeed other miRNAs and synthetic RNAi.

Pivotal to achieving these findings was the development of an optimized A to Z workflow from exosome production, purification, electroporative loading, re-isolation and *in vitro* evaluation for B cell-derived exosomes (Figure 4.1). Presently, this protocol achieves a 55 % loading efficiency for a miRNA-155 cargo, can eliminate free-floating / surface bound miRNA-155 and drug precipitation, and is the best performing approach out of three widely used solutions (ExoQuick[TM], Immunomagnetic bead-based purification and ultracentrifugation). This addresses the low efficiency bottleneck in the use of exosomes for biomarker discovery and as drug delivery vehicles (Alvarez et al., 2012; Witwer et al., 2013; Marcus and Leonard, 2013),
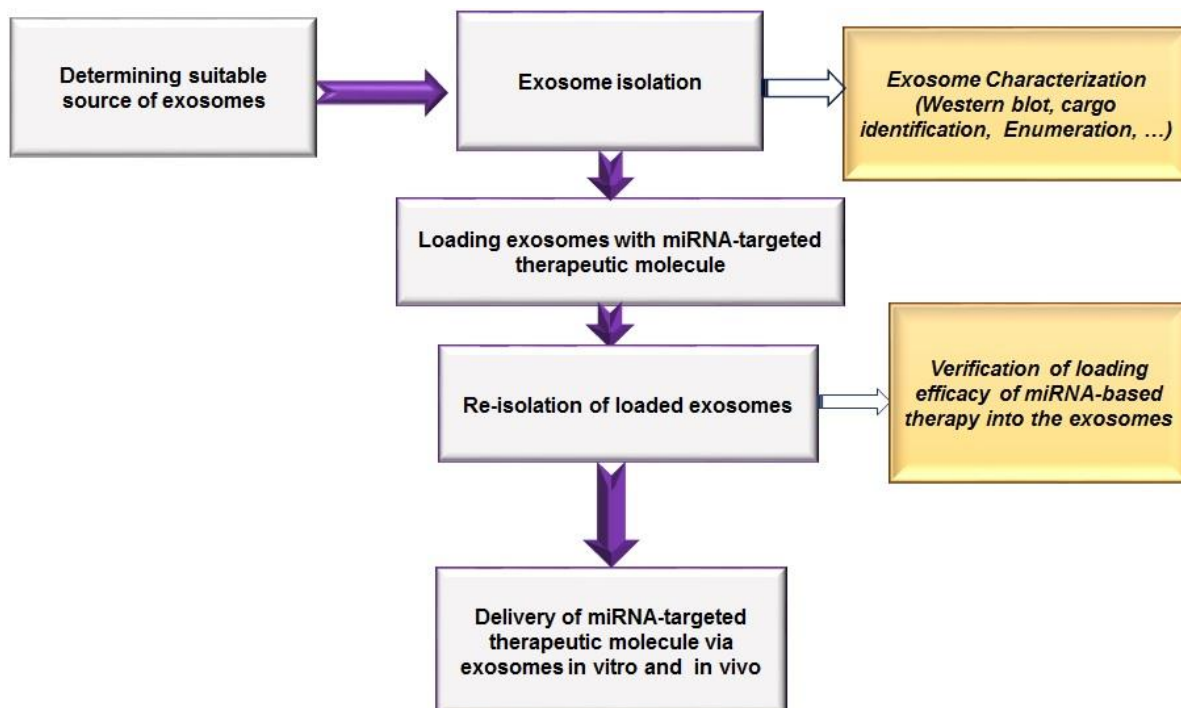
Figure 4.1: Workflow of the use of exosomes for the delivery of miRNA-targeted therapeutics

4.5 Exosomes and miRNAs as biomarkers in cancer

New advances in high-throughput technologies designed for analyzing biospecimens, coupled with the recent breakthroughs in whole genome sequencing, transcriptome and proteome profiling technologies, has led to introduction of different disease biomarkers, including transcriptomics, proteomics, lipidomics and metabolomics (de Graaf, 2013; Kulkarni et al., 2010). EVs have reignited interest in the field of biomarker discovery, as they are effective carriers of cell communication signals, and are enriched in different nucleic acids and proteins (Jia et al., 2014). Saliva in particular has been introduced as a new biomarker discovery substrate, since it can be used as a potential non-invasive approach for early detection and monitoring of different diseases.

The pivotal role of miRNAs in tumorigenesis as either tumor suppressors or oncogenes is well established (Jiang et al., 2015). In fact a high fraction of known miRNAs is located at fragile chromosomal sites or in cancer-associated genomic regions, including minimal regions of loss of heterozygosity or minimal amplicons (Calin and Croce, 2007). Based on these observations, whole genome miRNA screening was undertaken on different patient cohorts spanning OSCC, treated OSCC in remission, and oral lichen planus to find a reliable salivary biomarker for OSCC detection (Momen-Heravi et al., 2014b). The work revealed a reliable normalizer for saliva, miRNA-191, which showed the least inter group and intra

group variability. Furthermore, miRNA-27b was identified as a reliable miRNA for saliva-based diagnosis of oral cancer, as underlined by high sensitivity, high specificity, and excellent diagnostic value for patient stratification.

We also hypothesized that squamous cell carcinoma tumor amplifications might be detectable in circulation (Balaj et al., 2014). Two human tumor cell lines derived from a squamous cell carcinoma and a medulloblastoma, which had amplification for the EGFR and c-Myc genes, were implanted subcutaneously into immunocompromised mice. Transcript amplification in both groups of subcutaneous tumors was quantified and matched in circulating EVs in tumor-bearing mice, correlating well with parent gene amplification status in the tumors. This data provides further support to the notion that circulating EVs and biofluid miRNAs can serve as potential platforms for tumor biomarker identification and clinical use.

Conclusion

As exosomes and extracellular vesicles gain further attention as major players in cell communication and as potentially causal, clinically-relevant biomarkers, quality assurance and method validation has become crucial. A significant part of my research addressed that issue and led to enhancement of associated isolation methods with detailed comparative evidence over techniques relating to B cell-derived exosomes. In the context of alcoholic liver disease, my research found a novel, exosome-mediated mechanism of cross talk between ethanol-exposed hepatocytes and normal monocytes involving horizontal transfer of miRNA-122 to augment pro-inflammatory conditions in monocytes. Mechanistically, this was linked to miRNA-122-mediated suppression of the HO-1 pathway, which might consist of an alternative mechanism of sensitization of monocytes and macrophages to intestinally derived LPS in alcoholic liver disease. The activation of inflammatory pathway may also be meditated through exosomal HSP90 and which is TLR4 agonist and can exacerbate liver damage in a positive feedback loop. Experimental research to evaluate this hypothesis is needed. Crucially, these studies have evidenced the therapeutic potential of exosome-mediated RNAi modulator delivery beyond hepatocytes to the mechanistically implicated effector monocytes relevant to inflammatory liver disease. Thus, Exosomes loaded with miRNA-122 inhibitor were able to attenuate miRNA-122 mediated immune stimulation in monocytes. This is the first study to seek and evidence successful delivery to liver cell targets other than the first passage function of hepatocytes.

Furthermore, this research elucidated a mechanistic role for exosomes in promoting HCV infection. Thus, novel exosome and virus isolation/separation method were developed, to sufficiently support the evidence that a) HCV-infected hepatocyte exosomes, as opposed to HCV virions, contained APOB and no APOE; b) replication competent HCV RNA was present in these HCV-infected hepatocyte exosomes produced both by patients and infected hepatocyte cultures; c) The HCV exosomes mediated active virus transmission and replication in human hepatocytes and cell lines, even after pretreatment with a HCV virion receptor blocking antibody (anti-SR-BI, anti-CD81, anti ApoE); and d) that Ago2 and miRNA-122, both accepted enhancers of HCV replication and translation, were associated with the exosome-packaged HCV +RNA genome. We furthermore examined therapeutic approaches including vacuolar-type H+-ATPase and proton pump inhibition to show successful blockade of exosome-mediated, and even free virus mediated transmission of HCV to Huh 7.5 hepatocytes.

CONCLUSION

Collectively, this thesis puts in place the methodological basis for harnessing exosomes to deliver RNA cargos *in vitro* and *in vivo*, in a potentially non-toxic, non-immunogenic means with a broad scope of drug delivery and a robust approach to providing supporting evidence thereto. Furthermore, it has expanded evidence on the liquid biopsy promise offered through high diagnostic accuracy in the clinical setting. In order to translate EV utility from a discovery tool to a reliable clinical solution, the standardized methodology implementations presented herein can be expanded to industrial-scale applications and quality control, in line with the commercial paradigm of other autologous cell based therapeutics. Mechanistic studies focused on further elucidating EV function through high-throughput 'omic approaches in EV studies will be required to pave the way for understanding the affected pathological pathways and for developing personalized molecular therapy solutions.

Appendix: Table of primers

Primers are organized by publication, following the numbering on page 8.

Target Gene	Forward Sequence	Reverse Sequence
Publication 1		
18 S	5′-GACCTCATCCCA CCTCTCAG-3′	5′-CCATCCAATCGGTAGTAGCG-3′
human TNFα	5′-GAGTGACAAGCCTGTAGCCCATG TTGTAGCA-3′	5′-GCAATGATCCCAAAGTAGACCTG CCCAGACT-3′
human IL-1β	5′-CAGCTACGAATCTCCGACCAC-3′	5′-GGCAGGGAACCAGCATCTTC-3′
human MCP1	5′-CCCCAGTCACCTGCTGTTAT-3′	5′-TGGAATCCTGAACCCACTTC-3′
human Nox2	5′-GGGAAAAATAAAGGAATGCC-3′	5′-AGCCAGTGAGGTAGATGTTG-3′
human HO-1	5′-ACCAACTGCTTAGCACCC-3′	5′-GCAGAGAATGCTGAGTTCATG-3′
human GAPDH	5′-AGGGCTGCTTTTAACTCTGGT-3′	5′-CCCCACTTGATTTTGGAGGGA-3′
mouse HO-1	5′-CTGTGTAACCTCTGCTGTTCC-3′	5′-CCACACTACCTGAGTCTACC-3′
human Rab 27b	5′-TGCGGGACAAGAGCGGTTCCG-3′	5′-GCCAGTTCCCGAGCTTGCCGTT-3′
Publication 2		
18S	5'-GTAACCCGTTGAACCCCATT-3'	5'-CCATCCAATCGGTAGTAGCG-3'
mouse TNFα	5'-CACCACCATCAAGGACTCAA-3'	5'-AGGCAACCTGACCACTCTCC-3'
mouse IL-1β		
mouse MCP1		
Publication 4		
18S	5′-GACCTCATCCCACCTCTCAG-3′	5′-CCATCCAATCGGTAGTAGCG-3′
SOCS1	5′-GACCTCATCCCACCTCTCAG-3′	5′-ACAAGCTGCTACAACCAG GG-3′
Publication 7		
EGFR	5'-TATGTCCTCATTGCCCTCAACA-3'	5'-CTGATGATCTGCAGGTTTTCCA-3'
c-Myc	5'-CAACCCTTGCCGCATCCAC-3'	5'-AGTCGCGTCCTTGCTCGG-3'

References

Abrams, M. T., Koser, M. L., Seitzer, J., Williams, S. C., Dipietro, M. A., Wang, W., Shaw, A. W., Mao, X., Jadhav, V., Davide, J. P., Burke, P. A., Sachs, A. B., Stirdivant, S. M. and Sepp-Lorenzino, L. (2010). Evaluation of efficacy, biodistribution, and inflammation for a potent siRNA nanoparticle: effect of dexamethasone co-treatment. *Mol Ther,* 18 (1), 171-180.

Agarwal, B., Wright, G., Gatt, A., Riddell, A., Vemala, V., Mallett, S., Chowdary, P., Davenport, A., Jalan, R. and Burroughs, A. (2012). Evaluation of coagulation abnormalities in acute liver failure. *J Hepatol,* 57 (4), 780-786.

Aithal, G. P., Guha, N., Fallowfield, J., Castera, L. and Jackson, A. P. (2012). Biomarkers in liver disease: emerging methods and potential applications. *Int J Hepatol,* 2012, 437508.

Akazawa, D., Date, T., Morikawa, K., Murayama, A., Miyamoto, M., Kaga, M., Barth, H., Baumert, T. F., Dubuisson, J. and Wakita, T. (2007). CD81 expression is important for the permissiveness of Huh7 cell clones for heterogeneous hepatitis C virus infection. *J Virol,* 81 (10), 5036-5045.

Akers, J. C., Ramakrishnan, V., Kim, R., Skog, J., Nakano, I., Pingle, S., Kalinina, J., Hua, W., Kesari, S., Mao, Y., Breakefield, X. O., Hochberg, F. H., Van Meir, E. G., Carter, B. S. and Chen, C. C. (2013). MiR-21 in the extracellular vesicles (EVs) of cerebrospinal fluid (CSF): a platform for glioblastoma biomarker development. *PLoS One,* 8 (10), e78115.

Al-Dosari, M. S. and Gao, X. (2009). Nonviral gene delivery: principle, limitations, and recent progress. *AAPS J,* 11 (4), 671-681.

Allen, T. M., Austin, G. A., Chonn, A., Lin, L. and Lee, K. C. (1991). Uptake of liposomes by cultured mouse bone marrow macrophages: influence of liposome composition and size. *Biochim Biophys Acta,* 1061 (1), 56-64.

REFERENCES

Alvarez-Erviti, L., Seow, Y., Yin, H., Betts, C., Lakhal, S. and Wood, M. J. (2011). Delivery of siRNA to the mouse brain by systemic injection of targeted exosomes. *Nat Biotechnol,* 29 (4), 341-345.

Alvarez, M. L., Khosroheidari, M., Kanchi Ravi, R. and Distefano, J. K. (2012). Comparison of protein, microRNA, and mRNA yields using different methods of urinary exosome isolation for the discovery of kidney disease biomarkers. *Kidney Int,* 82 (9), 1024-1032.

Andersen, C. L., Jensen, J. L. and Orntoft, T. F. (2004). Normalization of real-time quantitative reverse transcription-PCR data: a model-based variance estimation approach to identify genes suited for normalization, applied to bladder and colon cancer data sets. *Cancer Res,* 64 (15), 5245-5250.

Andreola, G., Rivoltini, L., Castelli, C., Huber, V., Perego, P., Deho, P., Squarcina, P., Accornero, P., Lozupone, F., Lugini, L., Stringaro, A., Molinari, A., Arancia, G., Gentile, M., Parmiani, G. and Fais, S. (2002). Induction of lymphocyte apoptosis by tumor cell secretion of FasL-bearing microvesicles. *J Exp Med,* 195 (10), 1303-1316.

Arslan, F., Lai, R. C., Smeets, M. B., Akeroyd, L., Choo, A., Aguor, E. N., Timmers, L., Van Rijen, H. V., Doevendans, P. A., Pasterkamp, G., Lim, S. K. and De Kleijn, D. P. (2013). Mesenchymal stem cell-derived exosomes increase ATP levels, decrease oxidative stress and activate PI3K/Akt pathway to enhance myocardial viability and prevent adverse remodeling after myocardial ischemia/reperfusion injury. *Stem Cell Res,* 10 (3), 301-312.

Asea, A., Jean-Pierre, C., Kaur, P., Rao, P., Linhares, I. M., Skupski, D. and Witkin, S. S. (2008). Heat shock protein-containing exosomes in mid-trimester amniotic fluids. *J Reprod Immunol,* 79 (1), 12-17.

Atay, S., Gercel-Taylor, C., Kesimer, M. and Taylor, D. D. (2011). Morphologic and proteomic characterization of exosomes released by cultured extravillous trophoblast cells. *Exp Cell Res,* 317 (8), 1192-1202.

Averhoff, F. M., Glass, N. and Holtzman, D. (2012). Global burden of hepatitis C: considerations for healthcare providers in the United States. *Clin Infect Dis,* 55 Suppl 1, S10-15.

REFERENCES

Awada, A., Bondarenko, I. N., Bonneterre, J., Nowara, E., Ferrero, J. M., Bakshi, A. V., Wilke, C., Piccart, M. and Group, C. T. S. (2014). A randomized controlled phase II trial of a novel composition of paclitaxel embedded into neutral and cationic lipids targeting tumor endothelial cells in advanced triple-negative breast cancer (TNBC). *Ann Oncol,* 25 (4), 824-831.

Bae, Y. S., Oh, H., Rhee, S. G. and Yoo, Y. D. (2011). Regulation of reactive oxygen species generation in cell signaling. *Mol Cells,* 32 (6), 491-509.

Bakhshinejad, B. and Sadeghizadeh, M. (2014). Bacteriophages as vehicles for gene delivery into mammalian cells: prospects and problems. *Expert Opin Drug Deliv,* 11 (10), 1561-1574.

Bala, S., Csak, T., Momen-Heravi, F., Lippai, D., Kodys, K., Catalano, D., Satishchandran, A., Ambros, V. and Szabo, G. (2015). Biodistribution and function of extracellular miRNA-155 in mice. *Sci Rep,* 5, 10721.

Bala, S., Marcos, M., Gattu, A., Catalano, D. and Szabo, G. (2014). Acute binge drinking increases serum endotoxin and bacterial DNA levels in healthy individuals. *PLoS One,* 9 (5), e96864.

Bala, S., Marcos, M., Kodys, K., Csak, T., Catalano, D., Mandrekar, P. and Szabo, G. (2011). Up-regulation of microRNA-155 in macrophages contributes to increased tumor necrosis factor {alpha} (TNF{alpha}) production via increased mRNA half-life in alcoholic liver disease. *J Biol Chem,* 286 (2), 1436-1444.

Bala, S., Petrasek, J., Mundkur, S., Catalano, D., Levin, I., Ward, J., Alao, H., Kodys, K. and Szabo, G. (2012). Circulating microRNAs in exosomes indicate hepatocyte injury and inflammation in alcoholic, drug-induced, and inflammatory liver diseases. *Hepatology,* 56 (5), 1946-1957.

Balaj, L., Momen-Heravi, F., Chen, W., Sivaraman, S., Zhang, X., Ludwig, N., Meese, E., Wurdinger, T., Noske, D., Charest, A., Hochberg, F. H., Vandertop, P., Skog, J. and Kuo, W. P. (2014). Detection of Human c-Myc and EGFR Amplifications in Circulating Extracellular Vesicles in Mouse Tumour Models. *Journal of Circulating Biomarkers,* 3.

REFERENCES

Banizs, A. B., Huang, T., Dryden, K., Berr, S. S., Stone, J. R., Nakamoto, R. K., Shi, W. and He, J. (2014). In vitro evaluation of endothelial exosomes as carriers for small interfering ribonucleic acid delivery. *Int J Nanomedicine,* 9, 4223-4230.

Barber, R. D., Harmer, D. W., Coleman, R. A. and Clark, B. J. (2005). GAPDH as a housekeeping gene: analysis of GAPDH mRNA expression in a panel of 72 human tissues. *Physiol Genomics,* 21 (3), 389-395.

Barry, O. P., Pratico, D., Savani, R. C. and Fitzgerald, G. A. (1998). Modulation of monocyte-endothelial cell interactions by platelet microparticles. *J Clin Invest,* 102 (1), 136-144.

Bartel, D. P. (2009). MicroRNAs: target recognition and regulatory functions. *Cell,* 136 (2), 215-233.

Bartenschlager, R., Penin, F., Lohmann, V. and Andre, P. (2011). Assembly of infectious hepatitis C virus particles. *Trends Microbiol,* 19 (2), 95-103.

Bashratyan, R., Sheng, H., Regn, D., Rahman, M. J. and Dai, Y. D. (2013). Insulinoma-released exosomes activate autoreactive marginal zone-like B cells that expand endogenously in prediabetic NOD mice. *Eur J Immunol,* 43 (10), 2588-2597.

Benjamini, Y. and Hochberg, Y. (1995). Controlling the False Discovery Rate: A Practical and Powerful Approach to Multiple Testing. *Journal of the Royal Statistical Society. Series B (Methodological),* 57 (1), 289-300.

Berckmans, R. J., Nieuwland, R., Tak, P. P., Boing, A. N., Romijn, F. P., Kraan, M. C., Breedveld, F. C., Hack, C. E. and Sturk, A. (2002). Cell-derived microparticles in synovial fluid from inflamed arthritic joints support coagulation exclusively via a factor VII-dependent mechanism. *Arthritis Rheum,* 46 (11), 2857-2866.

Bergsmedh, A., Szeles, A., Henriksson, M., Bratt, A., Folkman, M. J., Spetz, A. L. and Holmgren, L. (2001). Horizontal transfer of oncogenes by uptake of apoptotic bodies. *Proc Natl Acad Sci U S A,* 98 (11), 6407-6411.

REFERENCES

Bianco, F., Perrotta, C., Novellino, L., Francolini, M., Riganti, L., Menna, E., Saglietti, L., Schuchman, E. H., Furlan, R., Clementi, E., Matteoli, M. and Verderio, C. (2009). Acid sphingomyelinase activity triggers microparticle release from glial cells. *EMBO J,* 28 (8), 1043-1054.

Biomarkers Definitions Working, G. (2001). Biomarkers and surrogate endpoints: preferred definitions and conceptual framework. *Clin Pharmacol Ther,* 69 (3), 89-95.

Blight, K. J., Mckeating, J. A. and Rice, C. M. (2002). Highly permissive cell lines for subgenomic and genomic hepatitis C virus RNA replication. *J Virol,* 76 (24), 13001-13014.

Boukouris, S. and Mathivanan, S. (2015). Exosomes in bodily fluids are a highly stable resource of disease biomarkers. *Proteomics Clin Appl,* 9 (3-4), 358-367.

Brenner, C., Galluzzi, L., Kepp, O. and Kroemer, G. (2013). Decoding cell death signals in liver inflammation. *J Hepatol,* 59 (3), 583-594.

Bretz, N. P., Ridinger, J., Rupp, A. K., Rimbach, K., Keller, S., Rupp, C., Marme, F., Umansky, L., Umansky, V., Eigenbrod, T., Sammar, M. and Altevogt, P. (2013). Body fluid exosomes promote secretion of inflammatory cytokines in monocytic cells via Toll-like receptor signaling. *J Biol Chem,* 288 (51), 36691-36702.

Brodsky, S. V., Facciuto, M. E., Heydt, D., Chen, J., Islam, H. K., Kajstura, M., Ramaswamy, G. and Aguero-Rosenfeld, M. (2008). Dynamics of circulating microparticles in liver transplant patients. *J Gastrointestin Liver Dis,* 17 (3), 261-268.

Broering, R., Real, C. I., John, M. J., Jahn-Hofmann, K., Ickenstein, L. M., Kleinehr, K., Paul, A., Gibbert, K., Dittmer, U., Gerken, G. and Schlaak, J. F. (2014). Chemical modifications on siRNAs avoid Toll-like-receptor-mediated activation of the hepatic immune system in vivo and in vitro. *Int Immunol,* 26 (1), 35-46.

Bukong, T. N., Hou, W., Kodys, K. and Szabo, G. (2013). Ethanol facilitates hepatitis C virus replication via up-regulation of GW182 and heat shock protein 90 in human hepatoma cells. *Hepatology,* 57 (1), 70-80.

REFERENCES

Bukong, T. N., Momen-Heravi, F., Kodys, K., Bala, S. and Szabo, G. (2014). Exosomes from hepatitis C infected patients transmit HCV infection and contain replication competent viral RNA in complex with Ago2-miR122-HSP90. *PLoS Pathog,* 10 (10), e1004424.

Buzas, E. I., Gyorgy, B., Nagy, G., Falus, A. and Gay, S. (2014). Emerging role of extracellular vesicles in inflammatory diseases. *Nat Rev Rheumatol,* 10 (6), 356-364.

Caby, M. P., Lankar, D., Vincendeau-Scherrer, C., Raposo, G. and Bonnerot, C. (2005). Exosomal-like vesicles are present in human blood plasma. *Int Immunol,* 17 (7), 879-887.

Calin, G. A. and Croce, C. M. (2007). Chromosomal rearrangements and microRNAs: a new cancer link with clinical implications. *J Clin Invest,* 117 (8), 2059-2066.

Candelario, K. M. and Steindler, D. A. (2014). The role of extracellular vesicles in the progression of neurodegenerative disease and cancer. *Trends Mol Med,* 20 (7), 368-374.

Carayon, K., Chaoui, K., Ronzier, E., Lazar, I., Bertrand-Michel, J., Roques, V., Balor, S., Terce, F., Lopez, A., Salome, L. and Joly, E. (2011). Proteolipidic composition of exosomes changes during reticulocyte maturation. *J Biol Chem,* 286 (39), 34426-34439.

Catanese, M. T., Uryu, K., Kopp, M., Edwards, T. J., Andrus, L., Rice, W. J., Silvestry, M., Kuhn, R. J. and Rice, C. M. (2013). Ultrastructural analysis of hepatitis C virus particles. *Proc Natl Acad Sci U S A,* 110 (23), 9505-9510.

Chang, K. S., Jiang, J., Cai, Z. and Luo, G. (2007). Human apolipoprotein e is required for infectivity and production of hepatitis C virus in cell culture. *J Virol,* 81 (24), 13783-13793.

Chargaff, E. and West, R. (1946). The biological significance of the thromboplastic protein of blood. *J Biol Chem,* 166 (1), 189-197.

Charras, G. T., Hu, C. K., Coughlin, M. and Mitchison, T. J. (2006). Reassembly of contractile actin cortex in cell blebs. *J Cell Biol,* 175 (3), 477-490.

REFERENCES

Chen, W. W., Balaj, L., Liau, L. M., Samuels, M. L., Kotsopoulos, S. K., Maguire, C. A., Loguidice, L., Soto, H., Garrett, M., Zhu, L. D., Sivaraman, S., Chen, C., Wong, E. T., Carter, B. S., Hochberg, F. H., Breakefield, X. O. and Skog, J. (2013). BEAMing and Droplet Digital PCR Analysis of Mutant IDH1 mRNA in Glioma Patient Serum and Cerebrospinal Fluid Extracellular Vesicles. *Mol Ther Nucleic Acids,* 2, e109.

Cheng, Y. S., Rees, T., Jordan, L., Oxford, L., O'brien, J., Chen, H. S. and Wong, D. (2011). Salivary endothelin-1 potential for detecting oral cancer in patients with oral lichen planus or oral cancer in remission. *Oral Oncol,* 47 (12), 1122-1126.

Cicalese, M. P., Ferrua, F., Castagnaro, L., Pajno, R., Barzaghi, F., Giannelli, S., Dionisio, F., Brigida, I., Bonopane, M., Casiraghi, M., Tabucchi, A., Carlucci, F., Grunebaum, E., Adeli, M., Bredius, R. G., Puck, J. M., Stepensky, P., Tezcan, I., Rolfe, K., De Boever, E., Reinhardt, R. R., Appleby, J., Ciceri, F., Roncarolo, M. G. and Aiuti, A. (2016). Update on the safety and efficacy of retroviral gene therapy for immunodeficiency due to adenosine deaminase deficiency. *Blood,* 128 (1), 45-54.

Clayton, A., Mitchell, J. P., Court, J., Mason, M. D. and Tabi, Z. (2007). Human tumor-derived exosomes selectively impair lymphocyte responses to interleukin-2. *Cancer Res,* 67 (15), 7458-7466.

Cohen, J. I. and Nagy, L. E. (2011). Pathogenesis of alcoholic liver disease: interactions between parenchymal and non-parenchymal cells. *J Dig Dis,* 12 (1), 3-9.

Collino, F., Deregibus, M. C., Bruno, S., Sterpone, L., Aghemo, G., Viltono, L., Tetta, C. and Camussi, G. (2010). Microvesicles derived from adult human bone marrow and tissue specific mesenchymal stem cells shuttle selected pattern of miRNAs. *PLoS One,* 5 (7), e11803.

Conde-Vancells, J., Rodriguez-Suarez, E., Gonzalez, E., Berisa, A., Gil, D., Embade, N., Valle, M., Luka, Z., Elortza, F., Wagner, C., Lu, S. C., Mato, J. M. and Falcon-Perez, M. (2010). Candidate biomarkers in exosome-like vesicles purified from rat and mouse urine samples. *Proteomics Clin Appl,* 4 (4), 416-425.

Conigliaro, A., Costa, V., Lo Dico, A., Saieva, L., Buccheri, S., Dieli, F., Manno, M., Raccosta, S., Mancone, C., Tripodi, M., De Leo, G. and Alessandro, R. (2015). CD90+

liver cancer cells modulate endothelial cell phenotype through the release of exosomes containing H19 lncRNA. *Mol Cancer,* 14, 155.

Cook, D., Brown, D., Alexander, R., March, R., Morgan, P., Satterthwaite, G. and Pangalos, M. N. (2014). Lessons learned from the fate of AstraZeneca's drug pipeline: a five-dimensional framework. *Nat Rev Drug Discov,* 13 (6), 419-431.

Costa-Silva, B., Aiello, N. M., Ocean, A. J., Singh, S., Zhang, H., Thakur, B. K., Becker, A., Hoshino, A., Mark, M. T., Molina, H., Xiang, J., Zhang, T., Theilen, T. M., Garcia-Santos, G., Williams, C., Ararso, Y., Huang, Y., Rodrigues, G., Shen, T. L., Labori, K. J., Lothe, I. M., Kure, E. H., Hernandez, J., Doussot, A., Ebbesen, S. H., Grandgenett, P. M., Hollingsworth, M. A., Jain, M., Mallya, K., Batra, S. K., Jarnagin, W. R., Schwartz, R. E., Matei, I., Peinado, H., Stanger, B. Z., Bromberg, J. and Lyden, D. (2015). Pancreatic cancer exosomes initiate pre-metastatic niche formation in the liver. *Nat Cell Biol,* 17 (6), 816-826.

Crescitelli, R., Lasser, C., Szabo, T. G., Kittel, A., Eldh, M., Dianzani, I., Buzas, E. I. and Lotvall, J. (2013). Distinct RNA profiles in subpopulations of extracellular vesicles: apoptotic bodies, microvesicles and exosomes. *J Extracell Vesicles,* 2.

Crowley, E., Di Nicolantonio, F., Loupakis, F. and Bardelli, A. (2013). Liquid biopsy: monitoring cancer-genetics in the blood. *Nat Rev Clin Oncol,* 10 (8), 472-484.

Csak, T., Ganz, M., Pespisa, J., Kodys, K., Dolganiuc, A. and Szabo, G. (2011). Fatty acid and endotoxin activate inflammasomes in mouse hepatocytes that release danger signals to stimulate immune cells. *Hepatology,* 54 (1), 133-144.

Cvjetkovic, A., Lotvall, J. and Lasser, C. (2014). The influence of rotor type and centrifugation time on the yield and purity of extracellular vesicles. *J Extracell Vesicles,* 3.

D'souza-Schorey, C. and Chavrier, P. (2006). ARF proteins: roles in membrane traffic and beyond. *Nat Rev Mol Cell Biol,* 7 (5), 347-358.

Datla, S. R., Dusting, G. J., Mori, T. A., Taylor, C. J., Croft, K. D. and Jiang, F. (2007). Induction of heme oxygenase-1 in vivo suppresses NADPH oxidase derived oxidative stress. *Hypertension,* 50 (4), 636-642.

Davey, G. M., Heath, W. R. and Starr, R. (2006). SOCS1: a potent and multifaceted regulator of cytokines and cell-mediated inflammation. *Tissue Antigens,* 67 (1), 1-9.

Dawson, D. A. (2011). Defining risk drinking. *Alcohol Res Health,* 34 (2), 144-156.

De Gassart, A., Geminard, C., Hoekstra, D. and Vidal, M. (2004). Exosome secretion: the art of reutilizing nonrecycled proteins? *Traffic,* 5 (11), 896-903.

De Graaf, D. (2013). Multi-omic biomarkers unlock the potential of diagnostic testing. *MLO Med Lab Obs,* 45 (8), 40, 42.

De Oliveria Andrade, L. J., D'oliveira, A., Melo, R. C., De Souza, E. C., Costa Silva, C. A. and Parana, R. (2009). Association between hepatitis C and hepatocellular carcinoma. *J Glob Infect Dis,* 1 (1), 33-37.

Deng, Z. B., Liu, Y., Liu, C., Xiang, X., Wang, J., Cheng, Z., Shah, S. V., Zhang, S., Zhang, L., Zhuang, X., Michalek, S., Grizzle, W. E. and Zhang, H. G. (2009). Immature myeloid cells induced by a high-fat diet contribute to liver inflammation. *Hepatology,* 50 (5), 1412-1420.

Denzer, K., Van Eijk, M., Kleijmeer, M. J., Jakobson, E., De Groot, C. and Geuze, H. J. (2000). Follicular dendritic cells carry MHC class II-expressing microvesicles at their surface. *J Immunol,* 165 (3), 1259-1265.

Deregibus, M. C., Cantaluppi, V., Calogero, R., Lo Iacono, M., Tetta, C., Biancone, L., Bruno, S., Bussolati, B. and Camussi, G. (2007). Endothelial progenitor cell derived microvesicles activate an angiogenic program in endothelial cells by a horizontal transfer of mRNA. *Blood,* 110 (7), 2440-2448.

Dragovic, R. A., Gardiner, C., Brooks, A. S., Tannetta, D. S., Ferguson, D. J., Hole, P., Carr, B., Redman, C. W., Harris, A. L., Dobson, P. J., Harrison, P. and Sargent, I. L. (2011). Sizing and phenotyping of cellular vesicles using Nanoparticle Tracking Analysis. *Nanomedicine,* 7 (6), 780-788.

REFERENCES

Drechsler, Y., Dolganiuc, A., Norkina, O., Romics, L., Li, W., Kodys, K., Bach, F. H., Mandrekar, P. and Szabo, G. (2006). Heme oxygenase-1 mediates the anti-inflammatory effects of acute alcohol on IL-10 induction involving p38 MAPK activation in monocytes. *J Immunol,* 177 (4), 2592-2600.

Drulis-Kawa, Z., Majkowska-Skrobek, G., Maciejewska, B., Delattre, A. S. and Lavigne, R. (2012). Learning from bacteriophages - advantages and limitations of phage and phage-encoded protein applications. *Curr Protein Pept Sci,* 13 (8), 699-722.

Eldh, M., Ekstrom, K., Valadi, H., Sjostrand, M., Olsson, B., Jernas, M. and Lotvall, J. (2010). Exosomes communicate protective messages during oxidative stress; possible role of exosomal shuttle RNA. *PLoS One,* 5 (12), e15353.

Ell, B., Qiu, Q., Wei, Y., Mercatali, L., Ibrahim, T., Amadori, D. and Kang, Y. (2014). The microRNA-23b/27b/24 cluster promotes breast cancer lung metastasis by targeting metastasis-suppressive gene prosaposin. *J Biol Chem,* 289 (32), 21888-21895.

Escudier, B., Dorval, T., Chaput, N., Andre, F., Caby, M. P., Novault, S., Flament, C., Leboulaire, C., Borg, C., Amigorena, S., Boccaccio, C., Bonnerot, C., Dhellin, O., Movassagh, M., Piperno, S., Robert, C., Serra, V., Valente, N., Le Pecq, J. B., Spatz, A., Lantz, O., Tursz, T., Angevin, E. and Zitvogel, L. (2005). Vaccination of metastatic melanoma patients with autologous dendritic cell (DC) derived-exosomes: results of thefirst phase I clinical trial. *J Transl Med,* 3 (1), 10.

Esteller, M. (2011). Non-coding RNAs in human disease. *Nat Rev Genet,* 12 (12), 861-874.

Fabbri, M., Calore, F., Paone, A., Galli, R. and Calin, G. A. (2013). Epigenetic regulation of miRNAs in cancer. *Adv Exp Med Biol,* 754, 137-148.

Flierl, U., Nero, T. L., Lim, B., Arthur, J. F., Yao, Y., Jung, S. M., Gitz, E., Pollitt, A. Y., Zaldivia, M. T., Jandrot-Perrus, M., Schafer, A., Nieswandt, B., Andrews, R. K., Parker, M. W., Gardiner, E. E. and Peter, K. (2015). Phosphorothioate backbone modifications of nucleotide-based drugs are potent platelet activators. *J Exp Med,* 212 (2), 129-137.

REFERENCES

Forsbach, A., Nemorin, J. G., Montino, C., Muller, C., Samulowitz, U., Vicari, A. P., Jurk, M., Mutwiri, G. K., Krieg, A. M., Lipford, G. B. and Vollmer, J. (2008). Identification of RNA sequence motifs stimulating sequence-specific TLR8-dependent immune responses. *J Immunol,* 180 (6), 3729-3738.

Galindo-Hernandez, O., Villegas-Comonfort, S., Candanedo, F., Gonzalez-Vazquez, M. C., Chavez-Ocana, S., Jimenez-Villanueva, X., Sierra-Martinez, M. and Salazar, E. P. (2013). Elevated concentration of microvesicles isolated from peripheral blood in breast cancer patients. *Arch Med Res,* 44 (3), 208-214.

Gallo, A., Tandon, M., Alevizos, I. and Illei, G. G. (2012). The majority of microRNAs detectable in serum and saliva is concentrated in exosomes. *PLoS One,* 7 (3), e30679.

Gao, B. and Bataller, R. (2011). Alcoholic liver disease: pathogenesis and new therapeutic targets. *Gastroenterology,* 141 (5), 1572-1585.

Gaudet, D., Stroes, E. S., Methot, J., Brisson, D., Tremblay, K., Bernelot Moens, S. J., Iotti, G., Rastelletti, I., Ardigo, D., Corzo, D., Meyer, C., Andersen, M., Ruszniewski, P., Deakin, M. and Bruno, M. J. (2016). A Long-Term (up to 6 years) Retrospective Analysis of Gene Therapy with Alipogene Tiparvovec and its Effect on Lipoprotein Lipase Deficiency (LPLD)-Induced Pancreatitis. *Hum Gene Ther*.

Gebert, L. F., Rebhan, M. A., Crivelli, S. E., Denzler, R., Stoffel, M. and Hall, J. (2014). Miravirsen (SPC3649) can inhibit the biogenesis of miR-122. *Nucleic Acids Res,* 42 (1), 609-621.

Gehrig, S., Sami, H. and Ogris, M. (2014). Gene therapy and imaging in preclinical and clinical oncology: recent developments in therapy and theranostics. *Ther Deliv,* 5 (12), 1275-1296.

Gibbings, D. J., Ciaudo, C., Erhardt, M. and Voinnet, O. (2009). Multivesicular bodies associate with components of miRNA effector complexes and modulate miRNA activity. *Nat Cell Biol,* 11 (9), 1143-1149.

Gottlieb, J., Zamora, M. R., Hodges, T., Musk, A. W., Sommerwerk, U., Dilling, D., Arcasoy, S., Devincenzo, J., Karsten, V., Shah, S., Bettencourt, B. R., Cehelsky, J.,

REFERENCES

Nochur, S., Gollob, J., Vaishnaw, A., Simon, A. R. and Glanville, A. R. (2016). ALN-RSV01 for prevention of bronchiolitis obliterans syndrome after respiratory syncytial virus infection in lung transplant recipients. *J Heart Lung Transplant,* 35 (2), 213-221.

Gozzelino, R., Jeney, V. and Soares, M. P. (2010). Mechanisms of cell protection by heme oxygenase-1. *Annu Rev Pharmacol Toxicol,* 50, 323-354.

Guo, F., Wang, Y., Liu, J., Mok, S. C., Xue, F. and Zhang, W. (2016). CXCL12/CXCR4: a symbiotic bridge linking cancer cells and their stromal neighbors in oncogenic communication networks. *Oncogene,* 35 (7), 816-826.

Gyorgy, B., Szabo, T. G., Pasztoi, M., Pal, Z., Misjak, P., Aradi, B., Laszlo, V., Pallinger, E., Pap, E., Kittel, A., Nagy, G., Falus, A. and Buzas, E. I. (2011). Membrane vesicles, current state-of-the-art: emerging role of extracellular vesicles. *Cell Mol Life Sci,* 68 (16), 2667-2688.

Ha, D., Yang, N. and Nadithe, V. (2016). Exosomes as therapeutic drug carriers and delivery vehicles across biological membranes: current perspectives and future challenges. *Acta Pharm Sin B,* 6 (4), 287-296.

Ha, M. and Kim, V. N. (2014). Regulation of microRNA biogenesis. *Nat Rev Mol Cell Biol,* 15 (8), 509-524.

Hajian-Tilaki, K. (2013). Receiver Operating Characteristic (ROC) Curve Analysis for Medical Diagnostic Test Evaluation. *Caspian J Intern Med,* 4 (2), 627-635.

He, L. and Hannon, G. J. (2004). MicroRNAs: small RNAs with a big role in gene regulation. *Nat Rev Genet,* 5 (7), 522-531.

He, M., Qin, H., Poon, T. C., Sze, S. C., Ding, X., Co, N. N., Ngai, S. M., Chan, T. F. and Wong, N. (2015). Hepatocellular carcinoma-derived exosomes promote motility of immortalized hepatocyte through transfer of oncogenic proteins and RNAs. *Carcinogenesis,* 36 (9), 1008-1018.

Heneghan, H. M., Miller, N. and Kerin, M. J. (2010). MiRNAs as biomarkers and therapeutic targets in cancer. *Curr Opin Pharmacol,* 10 (5), 543-550.

REFERENCES

Henke, J. I., Goergen, D., Zheng, J., Song, Y., Schuttler, C. G., Fehr, C., Junemann, C. and Niepmann, M. (2008). microRNA-122 stimulates translation of hepatitis C virus RNA. *EMBO J,* 27 (24), 3300-3310.

Hoggatt, J. (2016). Gene Therapy for "Bubble Boy" Disease. *Cell,* 166 (2), 263.

Hritz, I., Mandrekar, P., Velayudham, A., Catalano, D., Dolganiuc, A., Kodys, K., Kurt-Jones, E. and Szabo, G. (2008). The critical role of toll-like receptor (TLR) 4 in alcoholic liver disease is independent of the common TLR adapter MyD88. *Hepatology,* 48 (4), 1224-1231.

Hu, G., Yao, H., Chaudhuri, A. D., Duan, M., Yelamanchili, S. V., Wen, H., Cheney, P. D., Fox, H. S. and Buch, S. (2012). Exosome-mediated shuttling of microRNA-29 regulates HIV Tat and morphine-mediated neuronal dysfunction. *Cell Death Dis,* 3, e381.

Hu, Z., Zimmermann, B. G., Zhou, H., Wang, J., Henson, B. S., Yu, W., Elashoff, D., Krupp, G. and Wong, D. T. (2008). Exon-level expression profiling: a comprehensive transcriptome analysis of oral fluids. *Clin Chem,* 54 (5), 824-832.

Huang, X., Yuan, T., Tschannen, M., Sun, Z., Jacob, H., Du, M., Liang, M., Dittmar, R. L., Liu, Y., Liang, M., Kohli, M., Thibodeau, S. N., Boardman, L. and Wang, L. (2013). Characterization of human plasma-derived exosomal RNAs by deep sequencing. *BMC Genomics,* 14, 319.

Hurley, J. H. and Odorizzi, G. (2012). Get on the exosome bus with ALIX. *Nat Cell Biol,* 14 (7), 654-655.

Ismail, N., Wang, Y., Dakhlallah, D., Moldovan, L., Agarwal, K., Batte, K., Shah, P., Wisler, J., Eubank, T. D., Tridandapani, S., Paulaitis, M. E., Piper, M. G. and Marsh, C. B. (2013). Macrophage microvesicles induce macrophage differentiation and miR-223 transfer. *Blood,* 121 (6), 984-995.

Janssen, H. L., Reesink, H. W., Lawitz, E. J., Zeuzem, S., Rodriguez-Torres, M., Patel, K., Van Der Meer, A. J., Patick, A. K., Chen, A., Zhou, Y., Persson, R., King, B. D.,

REFERENCES

Kauppinen, S., Levin, A. A. and Hodges, M. R. (2013). Treatment of HCV infection by targeting microRNA. *N Engl J Med,* 368 (18), 1685-1694.

Jentsch, T. J., Maritzen, T. and Zdebik, A. A. (2005). Chloride channel diseases resulting from impaired transepithelial transport or vesicular function. *J Clin Invest,* 115 (8), 2039-2046.

Jepson, C. D. and March, J. B. (2004). Bacteriophage lambda is a highly stable DNA vaccine delivery vehicle. *Vaccine,* 22 (19), 2413-2419.

Jia, S., Zocco, D., Samuels, M. L., Chou, M. F., Chammas, R., Skog, J., Zarovni, N., Momen-Heravi, F. and Kuo, W. P. (2014). Emerging technologies in extracellular vesicle-based molecular diagnostics. *Expert Rev Mol Diagn,* 14 (3), 307-321.

Jiang, C., Chen, X., Alattar, M., Wei, J. and Liu, H. (2015). MicroRNAs in tumorigenesis, metastasis, diagnosis and prognosis of gastric cancer. *Cancer Gene Ther,* 22 (6), 291-301.

Jiang, H., Couto, L. B., Patarroyo-White, S., Liu, T., Nagy, D., Vargas, J. A., Zhou, S., Scallan, C. D., Sommer, J., Vijay, S., Mingozzi, F., High, K. A. and Pierce, G. F. (2006). Effects of transient immunosuppression on adenoassociated, virus-mediated, liver-directed gene transfer in rhesus macaques and implications for human gene therapy. *Blood,* 108 (10), 3321-3328.

Jopling, C. L., Yi, M., Lancaster, A. M., Lemon, S. M. and Sarnow, P. (2005). Modulation of hepatitis C virus RNA abundance by a liver-specific MicroRNA. *Science,* 309 (5740), 1577-1581.

Kalani, A., Tyagi, A. and Tyagi, N. (2014). Exosomes: mediators of neurodegeneration, neuroprotection and therapeutics. *Mol Neurobiol,* 49 (1), 590-600.

Kalra, H., Adda, C. G., Liem, M., Ang, C. S., Mechler, A., Simpson, R. J., Hulett, M. D. and Mathivanan, S. (2013). Comparative proteomics evaluation of plasma exosome isolation techniques and assessment of the stability of exosomes in normal human blood plasma. *Proteomics,* 13 (22), 3354-3364.

<center>REFERENCES</center>

Karman, J., Gumlaw, N. K., Zhang, J., Jiang, J. L., Cheng, S. H. and Zhu, Y. (2012). Proteasome inhibition is partially effective in attenuating pre-existing immunity against recombinant adeno-associated viral vectors. *PLoS One,* 7 (4), e34684.

Kim, W. R., Flamm, S. L., Di Bisceglie, A. M., Bodenheimer, H. C. and Public Policy Committee of the American Association for the Study of Liver, D. (2008). Serum activity of alanine aminotransferase (ALT) as an indicator of health and disease. *Hepatology,* 47 (4), 1363-1370.

Kogure, T., Lin, W. L., Yan, I. K., Braconi, C. and Patel, T. (2011). Intercellular nanovesicle-mediated microRNA transfer: a mechanism of environmental modulation of hepatocellular cancer cell growth. *Hepatology,* 54 (4), 1237-1248.

Kosaka, N., Iguchi, H., Yoshioka, Y., Takeshita, F., Matsuki, Y. and Ochiya, T. (2010). Secretory mechanisms and intercellular transfer of microRNAs in living cells. *J Biol Chem,* 285 (23), 17442-17452.

Kucharzewska, P., Christianson, H. C., Welch, J. E., Svensson, K. J., Fredlund, E., Ringner, M., Morgelin, M., Bourseau-Guilmain, E., Bengzon, J. and Belting, M. (2013). Exosomes reflect the hypoxic status of glioma cells and mediate hypoxia-dependent activation of vascular cells during tumor development. *Proc Natl Acad Sci U S A,* 110 (18), 7312-7317.

Kulkarni, S., Kannan, M. and Atreya, C. D. (2010). Omic approaches to quality biomarkers for stored platelets: are we there yet? *Transfus Med Rev,* 24 (3), 211-217.

Kurowska-Stolarska, M., Alivernini, S., Ballantine, L. E., Asquith, D. L., Millar, N. L., Gilchrist, D. S., Reilly, J., Ierna, M., Fraser, A. R., Stolarski, B., Mcsharry, C., Hueber, A. J., Baxter, D., Hunter, J., Gay, S., Liew, F. Y. and Mcinnes, I. B. (2011). MicroRNA-155 as a proinflammatory regulator in clinical and experimental arthritis. *Proc Natl Acad Sci U S A,* 108 (27), 11193-11198.

Lagos-Quintana, M., Rauhut, R., Yalcin, A., Meyer, J., Lendeckel, W. and Tuschl, T. (2002). Identification of tissue-specific microRNAs from mouse. *Curr Biol,* 12 (9), 735-739.

REFERENCES

Lambertz, U., Oviedo Ovando, M. E., Vasconcelos, E. J., Unrau, P. J., Myler, P. J. and Reiner, N. E. (2015). Small RNAs derived from tRNAs and rRNAs are highly enriched in exosomes from both old and new world Leishmania providing evidence for conserved exosomal RNA Packaging. *BMC Genomics,* 16, 151.

Lasser, C., Alikhani, V. S., Ekstrom, K., Eldh, M., Paredes, P. T., Bossios, A., Sjostrand, M., Gabrielsson, S., Lotvall, J. and Valadi, H. (2011). Human saliva, plasma and breast milk exosomes contain RNA: uptake by macrophages. *J Transl Med,* 9, 9.

Laulagnier, K., Motta, C., Hamdi, S., Roy, S., Fauvelle, F., Pageaux, J. F., Kobayashi, T., Salles, J. P., Perret, B., Bonnerot, C. and Record, M. (2004). Mast cell- and dendritic cell-derived exosomes display a specific lipid composition and an unusual membrane organization. *Biochem J,* 380 (Pt 1), 161-171.

Lavanchy, D. (2011). Evolving epidemiology of hepatitis C virus. *Clin Microbiol Infect,* 17 (2), 107-115.

Lee, C. H., Kim, J. H. and Lee, S. W. (2014). The role of microRNAs in hepatitis C virus replication and related liver diseases. *J Microbiol,* 52 (6), 445-451.

Leichter, A. L., Purcell, R. V., Sullivan, M. J., Eccles, M. R. and Chatterjee, A. (2015). Multi-platform microRNA profiling of hepatoblastoma patients using formalin fixed paraffin embedded archival samples. *Gigascience,* 4, 54.

Li, B., Antonyak, M. A., Zhang, J. and Cerione, R. A. (2012a). RhoA triggers a specific signaling pathway that generates transforming microvesicles in cancer cells. *Oncogene,* 31 (45), 4740-4749.

Li, B., Lee, D. S., Choi, H. G., Kim, K. S., Jeong, G. S., An, R. B. and Kim, Y. C. (2012b). Involvement of Heme Oxygenase-1 Induction in the Cytoprotective and Immunomodulatory Activities of Viola patrinii in Murine Hippocampal and Microglia Cells. *Evid Based Complement Alternat Med,* 2012, 128019.

Li, J., Liu, K., Liu, Y., Xu, Y., Zhang, F., Yang, H., Liu, J., Pan, T., Chen, J., Wu, M., Zhou, X. and Yuan, Z. (2013). Exosomes mediate the cell-to-cell transmission of IFN-alpha-induced antiviral activity. *Nat Immunol,* 14 (8), 793-803.

Lin, X., Lo, H. C., Wong, D. T. and Xiao, X. (2015). Noncoding RNAs in human saliva as potential disease biomarkers. *Front Genet,* 6, 175.

Lindenbach, B. D., Evans, M. J., Syder, A. J., Wolk, B., Tellinghuisen, T. L., Liu, C. C., Maruyama, T., Hynes, R. O., Burton, D. R., Mckeating, J. A. and Rice, C. M. (2005). Complete replication of hepatitis C virus in cell culture. *Science,* 309 (5734), 623-626.

Lindenbach, B. D. and Rice, C. M. (2013). The ins and outs of hepatitis C virus entry and assembly. *Nat Rev Microbiol,* 11 (10), 688-700.

Liu, Y., Luo, F., Wang, B., Li, H., Xu, Y., Liu, X., Shi, L., Lu, X., Xu, W., Lu, L., Qin, Y., Xiang, Q. and Liu, Q. (2015). STAT3-regulated exosomal miR-21 promotes angiogenesis and is involved in neoplastic processes of transformed human bronchial epithelial cells. *Cancer Lett*.

Livak, K. J. and Schmittgen, T. D. (2001). Analysis of relative gene expression data using real-time quantitative PCR and the 2(-Delta Delta C(T)) Method. *Methods,* 25 (4), 402-408.

Lobb, R. J., Becker, M., Wen, S. W., Wong, C. S., Wiegmans, A. P., Leimgruber, A. and Moller, A. (2015). Optimized exosome isolation protocol for cell culture supernatant and human plasma. *J Extracell Vesicles,* 4, 27031.

Logozzi, M., De Milito, A., Lugini, L., Borghi, M., Calabro, L., Spada, M., Perdicchio, M., Marino, M. L., Federici, C., Iessi, E., Brambilla, D., Venturi, G., Lozupone, F., Santinami, M., Huber, V., Maio, M., Rivoltini, L. and Fais, S. (2009). High levels of exosomes expressing CD63 and caveolin-1 in plasma of melanoma patients. *PLoS One,* 4 (4), e5219.

Lotvall, J., Hill, A. F., Hochberg, F., Buzas, E. I., Di Vizio, D., Gardiner, C., Gho, Y. S., Kurochkin, I. V., Mathivanan, S., Quesenberry, P., Sahoo, S., Tahara, H., Wauben, M. H., Witwer, K. W. and Thery, C. (2014). Minimal experimental requirements for definition of extracellular vesicles and their functions: a position statement from the International Society for Extracellular Vesicles. *J Extracell Vesicles,* 3, 26913.

REFERENCES

Lovborg, H., Nygren, P. and Larsson, R. (2004). Multiparametric evaluation of apoptosis: effects of standard cytotoxic agents and the cyanoguanidine CHS 828. *Mol Cancer Ther,* 3 (5), 521-526.

Machida, T., Tomofuji, T., Ekuni, D., Maruyama, T., Yoneda, T., Kawabata, Y., Mizuno, H., Miyai, H., Kunitomo, M. and Morita, M. (2015). MicroRNAs in Salivary Exosome as Potential Biomarkers of Aging. *Int J Mol Sci,* 16 (9), 21294-21309.

Madhavan, B., Yue, S., Galli, U., Rana, S., Gross, W., Muller, M., Giese, N. A., Kalthoff, H., Becker, T., Buchler, M. W. and Zoller, M. (2015). Combined evaluation of a panel of protein and miRNA serum-exosome biomarkers for pancreatic cancer diagnosis increases sensitivity and specificity. *Int J Cancer,* 136 (11), 2616-2627.

Manno, C. S., Pierce, G. F., Arruda, V. R., Glader, B., Ragni, M., Rasko, J. J., Ozelo, M. C., Hoots, K., Blatt, P., Konkle, B., Dake, M., Kaye, R., Razavi, M., Zajko, A., Zehnder, J., Rustagi, P. K., Nakai, H., Chew, A., Leonard, D., Wright, J. F., Lessard, R. R., Sommer, J. M., Tigges, M., Sabatino, D., Luk, A., Jiang, H., Mingozzi, F., Couto, L., Ertl, H. C., High, K. A. and Kay, M. A. (2006). Successful transduction of liver in hemophilia by AAV-Factor IX and limitations imposed by the host immune response. *Nat Med,* 12 (3), 342-347.

Mantel, P. Y., Hoang, A. N., Goldowitz, I., Potashnikova, D., Hamza, B., Vorobjev, I., Ghiran, I., Toner, M., Irimia, D., Ivanov, A. R., Barteneva, N. and Marti, M. (2013). Malaria-infected erythrocyte-derived microvesicles mediate cellular communication within the parasite population and with the host immune system. *Cell Host Microbe,* 13 (5), 521-534.

Marcilla, A., Trelis, M., Cortes, A., Sotillo, J., Cantalapiedra, F., Minguez, M. T., Valero, M. L., Sanchez Del Pino, M. M., Munoz-Antoli, C., Toledo, R. and Bernal, D. (2012). Extracellular vesicles from parasitic helminths contain specific excretory/secretory proteins and are internalized in intestinal host cells. *PLoS One,* 7 (9), e45974.

Marcus, M. E. and Leonard, J. N. (2013). FedExosomes: Engineering Therapeutic Biological Nanoparticles that Truly Deliver. *Pharmaceuticals (Basel),* 6 (5), 659-680.

REFERENCES

Martinez-Lorenzo, M. J., Anel, A., Gamen, S., Monle N, I., Lasierra, P., Larrad, L., Pineiro, A., Alava, M. A. and Naval, J. (1999). Activated human T cells release bioactive Fas ligand and APO2 ligand in microvesicles. *J Immunol,* 163 (3), 1274-1281.

Martinez, M. C., Larbret, F., Zobairi, F., Coulombe, J., Debili, N., Vainchenker, W., Ruat, M. and Freyssinet, J. M. (2006). Transfer of differentiation signal by membrane microvesicles harboring hedgehog morphogens. *Blood,* 108 (9), 3012-3020.

Masat, E., Pavani, G. and Mingozzi, F. (2013). Humoral immunity to AAV vectors in gene therapy: challenges and potential solutions. *Discov Med,* 15 (85), 379-389.

Masyuk, A. I., Huang, B. Q., Ward, C. J., Gradilone, S. A., Banales, J. M., Masyuk, T. V., Radtke, B., Splinter, P. L. and Larusso, N. F. (2010). Biliary exosomes influence cholangiocyte regulatory mechanisms and proliferation through interaction with primary cilia. *Am J Physiol Gastrointest Liver Physiol,* 299 (4), G990-999.

Matsui, M., Chu, Y., Zhang, H., Gagnon, K. T., Shaikh, S., Kuchimanchi, S., Manoharan, M., Corey, D. R. and Janowski, B. A. (2013). Promoter RNA links transcriptional regulation of inflammatory pathway genes. *Nucleic Acids Res,* 41 (22), 10086-10109.

Mcintosh, J. H., Cochrane, M., Cobbold, S., Waldmann, H., Nathwani, S. A., Davidoff, A. M. and Nathwani, A. C. (2012). Successful attenuation of humoral immunity to viral capsid and transgenic protein following AAV-mediated gene transfer with a non-depleting CD4 antibody and cyclosporine. *Gene Ther,* 19 (1), 78-85.

Meckes, D. G., Jr., Gunawardena, H. P., Dekroon, R. M., Heaton, P. R., Edwards, R. H., Ozgur, S., Griffith, J. D., Damania, B. and Raab-Traub, N. (2013). Modulation of B-cell exosome proteins by gamma herpesvirus infection. *Proc Natl Acad Sci U S A,* 110 (31), E2925-2933.

Metz, C. E. (1978). Basic principles of ROC analysis. *Semin Nucl Med,* 8 (4), 283-298.

Meuleman, P., Hesselgesser, J., Paulson, M., Vanwolleghem, T., Desombere, I., Reiser, H. and Leroux-Roels, G. (2008). Anti-CD81 antibodies can prevent a hepatitis C virus infection in vivo. *Hepatology,* 48 (6), 1761-1768.

REFERENCES

Millimaggi, D., Mari, M., D'ascenzo, S., Carosa, E., Jannini, E. A., Zucker, S., Carta, G., Pavan, A. and Dolo, V. (2007). Tumor vesicle-associated CD147 modulates the angiogenic capability of endothelial cells. *Neoplasia,* 9 (4), 349-357.

Min, J. J., Nguyen, V. H. and Gambhir, S. S. (2010). Molecular imaging of biological gene delivery vehicles for targeted cancer therapy: beyond viral vectors. *Nucl Med Mol Imaging,* 44 (1), 15-24.

Minami, K., Uehara, T., Morikawa, Y., Omura, K., Kanki, M., Horinouchi, A., Ono, A., Yamada, H., Ohno, Y. and Urushidani, T. (2014). miRNA expression atlas in male rat. *Sci Data,* 1, 140005.

Mohankumar, S. and Patel, T. (2015). Extracellular vesicle long noncoding RNA as potential biomarkers of liver cancer. *Brief Funct Genomics*.

Mohd-Ismail, N. K., Deng, L., Sukumaran, S. K., Yu, V. C., Hotta, H. and Tan, Y. J. (2009). The hepatitis C virus core protein contains a BH3 domain that regulates apoptosis through specific interaction with human Mcl-1. *J Virol,* 83 (19), 9993-10006.

Molenaar, T. J., Michon, I., De Haas, S. A., Van Berkel, T. J., Kuiper, J. and Biessen, E. A. (2002). Uptake and processing of modified bacteriophage M13 in mice: implications for phage display. *Virology,* 293 (1), 182-191.

Momen-Heravi, F., Bala, S., Bukong, T. and Szabo, G. (2014a). Exosome-mediated delivery of functionally active miRNA-155 inhibitor to macrophages. *Nanomedicine,* 10 (7), 1517-1527.

Momen-Heravi, F., Bala, S., Kodys, K. and Szabo, G. (2015a). Exosomes derived from alcohol-treated hepatocytes horizontally transfer liver specific miRNA-122 and sensitize monocytes to LPS. *Sci Rep,* 5, 9991.

Momen-Heravi, F., Balaj, L., Alian, S., Mantel, P. Y., Halleck, A. E., Trachtenberg, A. J., Soria, C. E., Oquin, S., Bonebreak, C. M., Saracoglu, E., Skog, J. and Kuo, W. P. (2013). Current methods for the isolation of extracellular vesicles. *Biol Chem,* 394 (10), 1253-1262.

REFERENCES

Momen-Heravi, F., Balaj, L., Alian, S., Tigges, J., Toxavidis, V., Ericsson, M., Distel, R. J., Ivanov, A. R., Skog, J. and Kuo, W. P. (2012a). Alternative methods for characterization of extracellular vesicles. *Front Physiol,* 3, 354.

Momen-Heravi, F., Balaj, L., Alian, S., Trachtenberg, A. J., Hochberg, F. H., Skog, J. and Kuo, W. P. (2012b). Impact of biofluid viscosity on size and sedimentation efficiency of the isolated microvesicles. *Front Physiol,* 3, 162.

Momen-Heravi, F., Saha, B., Kodys, K., Catalano, D., Satishchandran, A. and Szabo, G. (2015b). Increased number of circulating exosomes and their microRNA cargos are potential novel biomarkers in alcoholic hepatitis. *J Transl Med,* 13, 261.

Momen-Heravi, F., Trachtenberg, A. J., Kuo, W. P. and Cheng, Y. S. (2014b). Genomewide Study of Salivary MicroRNAs for Detection of Oral Cancer. *J Dent Res,* 93 (7 Suppl), 86S-93S.

Montecalvo, A., Larregina, A. T., Shufesky, W. J., Stolz, D. B., Sullivan, M. L., Karlsson, J. M., Baty, C. J., Gibson, G. A., Erdos, G., Wang, Z., Milosevic, J., Tkacheva, O. A., Divito, S. J., Jordan, R., Lyons-Weiler, J., Watkins, S. C. and Morelli, A. E. (2012). Mechanism of transfer of functional microRNAs between mouse dendritic cells via exosomes. *Blood,* 119 (3), 756-766.

Moratti, E., Vezzalini, M., Tomasello, L., Giavarina, D. and Sorio, C. (2015). Identification of protein tyrosine phosphatase receptor gamma extracellular domain (sPTPRG) as a natural soluble protein in plasma. *PLoS One,* 10 (3), e0119110.

Morelli, A. E., Larregina, A. T., Shufesky, W. J., Sullivan, M. L., Stolz, D. B., Papworth, G. D., Zahorchak, A. F., Logar, A. J., Wang, Z., Watkins, S. C., Falo, L. D., Jr. and Thomson, A. W. (2004). Endocytosis, intracellular sorting, and processing of exosomes by dendritic cells. *Blood,* 104 (10), 3257-3266.

Morin, T. J., Broering, T. J., Leav, B. A., Blair, B. M., Rowley, K. J., Boucher, E. N., Wang, Y., Cheslock, P. S., Knauber, M., Olsen, D. B., Ludmerer, S. W., Szabo, G., Finberg, R. W., Purcell, R. H., Lanford, R. E., Ambrosino, D. M., Molrine, D. C. and Babcock, G. J. (2012). Human monoclonal antibody HCV1 effectively prevents and treats HCV infection in chimpanzees. *PLoS Pathog,* 8 (8), e1002895.

Moschos, S. A. (2013). CHAPTER 7 MicroRNA Biotherapeutics: Key Challenges from a Drug Development Perspective in *Biotherapeutics: Recent Developments using Chemical and Molecular Biology*, The Royal Society of Chemistry, 176-223.

Mulcahy, L. A., Pink, R. C. and Carter, D. R. (2014). Routes and mechanisms of extracellular vesicle uptake. *J Extracell Vesicles,* 3.

Murakami, Y., Toyoda, H., Tanahashi, T., Tanaka, J., Kumada, T., Yoshioka, Y., Kosaka, N., Ochiya, T. and Taguchi, Y. H. (2012). Comprehensive miRNA expression analysis in peripheral blood can diagnose liver disease. *PLoS One,* 7 (10), e48366.

Nabhan, J. F., Hu, R., Oh, R. S., Cohen, S. N. and Lu, Q. (2012). Formation and release of arrestin domain-containing protein 1-mediated microvesicles (ARMMs) at plasma membrane by recruitment of TSG101 protein. *Proc Natl Acad Sci U S A,* 109 (11), 4146-4151.

Nagy, L. E. (2015). The Role of Innate Immunity in Alcoholic Liver Disease. *Alcohol Res,* 37 (2), 237-250.

Narayanan, A., Iordanskiy, S., Das, R., Van Duyne, R., Santos, S., Jaworski, E., Guendel, I., Sampey, G., Dalby, E., Iglesias-Ussel, M., Popratiloff, A., Hakami, R., Kehn-Hall, K., Young, M., Subra, C., Gilbert, C., Bailey, C., Romerio, F. and Kashanchi, F. (2013). Exosomes derived from HIV-1-infected cells contain trans-activation response element RNA. *J Biol Chem,* 288 (27), 20014-20033.

Narayanan, G., Cossu, G., Galli, M. C., Flory, E., Ovelgonne, H., Salmikangas, P., Schneider, C. K. and Trouvin, J. H. (2014). Clinical development of gene therapy needs a tailored approach: a regulatory perspective from the European Union. *Hum Gene Ther Clin Dev,* 25 (1), 1-6.

Nawaz, M., Camussi, G., Valadi, H., Nazarenko, I., Ekstrom, K., Wang, X., Principe, S., Shah, N., Ashraf, N. M., Fatima, F., Neder, L. and Kislinger, T. (2014). The emerging role of extracellular vesicles as biomarkers for urogenital cancers. *Nat Rev Urol,* 11 (12), 688-701.

REFERENCES

Nicolaides, N. C., Sass, P. M. and Grasso, L. (2010). Advances in targeted therapeutic agents. *Expert Opin Drug Discov,* 5 (11), 1123-1140.

Njock, M. S., Cheng, H. S., Dang, L. T., Nazari-Jahantigh, M., Lau, A. C., Boudreau, E., Roufaiel, M., Cybulsky, M. I., Schober, A. and Fish, J. E. (2015). Endothelial cells suppress monocyte activation through secretion of extracellular vesicles containing antiinflammatory microRNAs. *Blood,* 125 (20), 3202-3212.

Nojima, H., Freeman, C. M., Schuster, R. M., Japtok, L., Kleuser, B., Edwards, M. J., Gulbins, E. and Lentsch, A. B. (2016). Hepatocyte exosomes mediate liver repair and regeneration via sphingosine-1-phosphate. *J Hepatol,* 64 (1), 60-68.

Nseir, W., Hellou, E. and Assy, N. (2014). Role of diet and lifestyle changes in nonalcoholic fatty liver disease. *World J Gastroenterol,* 20 (28), 9338-9344.

O'connell, R. M., Rao, D. S. and Baltimore, D. (2012). microRNA regulation of inflammatory responses. *Annu Rev Immunol,* 30, 295-312.

Ogata-Kawata, H., Izumiya, M., Kurioka, D., Honma, Y., Yamada, Y., Furuta, K., Gunji, T., Ohta, H., Okamoto, H., Sonoda, H., Watanabe, M., Nakagama, H., Yokota, J., Kohno, T. and Tsuchiya, N. (2014). Circulating exosomal microRNAs as biomarkers of colon cancer. *PLoS One,* 9 (4), e92921.

Ogawa, Y., Kanai-Azuma, M., Akimoto, Y., Kawakami, H. and Yanoshita, R. (2008). Exosome-like vesicles with dipeptidyl peptidase IV in human saliva. *Biol Pharm Bull,* 31 (6), 1059-1062.

Ohno, S., Takanashi, M., Sudo, K., Ueda, S., Ishikawa, A., Matsuyama, N., Fujita, K., Mizutani, T., Ohgi, T., Ochiya, T., Gotoh, N. and Kuroda, M. (2013). Systemically injected exosomes targeted to EGFR deliver antitumor microRNA to breast cancer cells. *Mol Ther,* 21 (1), 185-191.

Ostrowski, M., Carmo, N. B., Krumeich, S., Fanget, I., Raposo, G., Savina, A., Moita, C. F., Schauer, K., Hume, A. N., Freitas, R. P., Goud, B., Benaroch, P., Hacohen, N., Fukuda, M., Desnos, C., Seabra, M. C., Darchen, F., Amigorena, S., Moita, L. F. and Thery, C.

(2010). Rab27a and Rab27b control different steps of the exosome secretion pathway. *Nat Cell Biol,* 12 (1), 19-30; sup pp 11-13.

Parolini, I., Federici, C., Raggi, C., Lugini, L., Palleschi, S., De Milito, A., Coscia, C., Iessi, E., Logozzi, M., Molinari, A., Colone, M., Tatti, M., Sargiacomo, M. and Fais, S. (2009). Microenvironmental pH is a key factor for exosome traffic in tumor cells. *J Biol Chem,* 284 (49), 34211-34222.

Pecot, C. V., Calin, G. A., Coleman, R. L., Lopez-Berestein, G. and Sood, A. K. (2011). RNA interference in the clinic: challenges and future directions. *Nat Rev Cancer,* 11 (1), 59-67.

Pegtel, D. M., Cosmopoulos, K., Thorley-Lawson, D. A., Van Eijndhoven, M. A., Hopmans, E. S., Lindenberg, J. L., De Gruijl, T. D., Wurdinger, T. and Middeldorp, J. M. (2010). Functional delivery of viral miRNAs via exosomes. *Proc Natl Acad Sci U S A,* 107 (14), 6328-6333.

Peinado, H., Aleckovic, M., Lavotshkin, S., Matei, I., Costa-Silva, B., Moreno-Bueno, G., Hergueta-Redondo, M., Williams, C., Garcia-Santos, G., Ghajar, C., Nitadori-Hoshino, A., Hoffman, C., Badal, K., Garcia, B. A., Callahan, M. K., Yuan, J., Martins, V. R., Skog, J., Kaplan, R. N., Brady, M. S., Wolchok, J. D., Chapman, P. B., Kang, Y., Bromberg, J. and Lyden, D. (2012). Melanoma exosomes educate bone marrow progenitor cells toward a pro-metastatic phenotype through MET. *Nat Med,* 18 (6), 883-891.

Petrasek, J., Dolganiuc, A., Csak, T., Kurt-Jones, E. A. and Szabo, G. (2011). Type I interferons protect from Toll-like receptor 9-associated liver injury and regulate IL-1 receptor antagonist in mice. *Gastroenterology,* 140 (2), 697-708 e694.

Pileri, P., Uematsu, Y., Campagnoli, S., Galli, G., Falugi, F., Petracca, R., Weiner, A. J., Houghton, M., Rosa, D., Grandi, G. and Abrignani, S. (1998). Binding of hepatitis C virus to CD81. *Science,* 282 (5390), 938-941.

Pisitkun, T., Shen, R. F. and Knepper, M. A. (2004). Identification and proteomic profiling of exosomes in human urine. *Proc Natl Acad Sci U S A,* 101 (36), 13368-13373.

REFERENCES

Poss, K. D. and Tonegawa, S. (1997). Reduced stress defense in heme oxygenase 1-deficient cells. *Proc Natl Acad Sci U S A,* 94 (20), 10925-10930.

Properzi, F., Logozzi, M. and Fais, S. (2013). Exosomes: the future of biomarkers in medicine. *Biomark Med,* 7 (5), 769-778.

Quesenberry, P. J., Aliotta, J., Deregibus, M. C. and Camussi, G. (2015). Role of extracellular RNA-carrying vesicles in cell differentiation and reprogramming. *Stem Cell Res Ther,* 6, 153.

Racicot, K., Schmitt, A. and Ott, T. (2012). The myxovirus-resistance protein, MX1, is a component of exosomes secreted by uterine epithelial cells. *Am J Reprod Immunol,* 67 (6), 498-505.

Raiborg, C. and Stenmark, H. (2009). The ESCRT machinery in endosomal sorting of ubiquitylated membrane proteins. *Nature,* 458 (7237), 445-452.

Raj, D. A., Fiume, I., Capasso, G. and Pocsfalvi, G. (2012). A multiplex quantitative proteomics strategy for protein biomarker studies in urinary exosomes. *Kidney Int,* 81 (12), 1263-1272.

Ramakrishnaiah, V., Thumann, C., Fofana, I., Habersetzer, F., Pan, Q., De Ruiter, P. E., Willemsen, R., Demmers, J. A., Stalin Raj, V., Jenster, G., Kwekkeboom, J., Tilanus, H. W., Haagmans, B. L., Baumert, T. F. and Van Der Laan, L. J. (2013). Exosome-mediated transmission of hepatitis C virus between human hepatoma Huh7.5 cells. *Proc Natl Acad Sci U S A,* 110 (32), 13109-13113.

Rana, S., Malinowska, K. and Zoller, M. (2013). Exosomal tumor microRNA modulates premetastatic organ cells. *Neoplasia,* 15 (3), 281-295.

Raposo, G. and Stoorvogel, W. (2013). Extracellular vesicles: exosomes, microvesicles, and friends. *J Cell Biol,* 200 (4), 373-383.

Redzic, J. S., Balaj, L., Van Der Vos, K. E. and Breakefield, X. O. (2014). Extracellular RNA mediates and marks cancer progression. *Semin Cancer Biol,* 28, 14-23.

REFERENCES

Rice, C. M. (2011). New insights into HCV replication: potential antiviral targets. *Top Antivir Med,* 19 (3), 117-120.

Roberts, T. C. (2014). The MicroRNA Biology of the Mammalian Nucleus. *Mol Ther Nucleic Acids,* 3, e188.

Robertson, B., Dalby, A. B., Karpilow, J., Khvorova, A., Leake, D. and Vermeulen, A. (2010). Specificity and functionality of microRNA inhibitors. *Silence,* 1 (1), 10.

Ruijter, J. M., Ramakers, C., Hoogaars, W. M., Karlen, Y., Bakker, O., Van Den Hoff, M. J. and Moorman, A. F. (2009). Amplification efficiency: linking baseline and bias in the analysis of quantitative PCR data. *Nucleic Acids Res,* 37 (6), e45.

Saa, P., Yakovleva, O., De Castro, J., Vasilyeva, I., De Paoli, S. H., Simak, J. and Cervenakova, L. (2014). First demonstration of transmissible spongiform encephalopathy-associated prion protein (PrPTSE) in extracellular vesicles from plasma of mice infected with mouse-adapted variant Creutzfeldt-Jakob disease by in vitro amplification. *J Biol Chem,* 289 (42), 29247-29260.

Sabahi, A. (2009). Hepatitis C Virus entry: the early steps in the viral replication cycle. *Virol J,* 6, 117.

Sadovska, L., Eglitis, J. and Line, A. (2015). Extracellular Vesicles as Biomarkers and Therapeutic Targets in Breast Cancer. *Anticancer Res,* 35 (12), 6379-6390.

Saha, B., Momen-Heravi, F., Kodys, K. and Szabo, G. (2015). MicroRNA Cargo of Extracellular Vesicles from Alcohol-Exposed Monocytes Signals Naive Monocytes to Differentiate into M2 Macrophages. *J Biol Chem*.

San Lucas, F. A., Allenson, K., Bernard, V., Castillo, J., Kim, D., Ellis, K., Ehli, E. A., Davies, G. E., Petersen, J. L., Li, D., Wolff, R., Katz, M., Varadhachary, G., Wistuba, I., Maitra, A. and Alvarez, H. (2015). Minimally invasive genomic and transcriptomic profiling of visceral cancers by next-generation sequencing of circulating exosomes. *Ann Oncol*.

REFERENCES

Saunderson, S. C., Schuberth, P. C., Dunn, A. C., Miller, L., Hock, B. D., Mackay, P. A., Koch, N., Jack, R. W. and Mclellan, A. D. (2008). Induction of exosome release in primary B cells stimulated via CD40 and the IL-4 receptor. *J Immunol,* 180 (12), 8146-8152.

Schmittgen, T. D., Lee, E. J., Jiang, J., Sarkar, A., Yang, L., Elton, T. S. and Chen, C. (2008). Real-time PCR quantification of precursor and mature microRNA. *Methods,* 44 (1), 31-38.

Seow, Y. and Wood, M. J. (2009). Biological gene delivery vehicles: beyond viral vectors. *Mol Ther,* 17 (5), 767-777.

Serguera, C. and Bemelmans, A. P. (2014). Gene therapy of the central nervous system: general considerations on viral vectors for gene transfer into the brain. *Rev Neurol (Paris),* 170 (12), 727-738.

Shan, Y., Zheng, J., Lambrecht, R. W. and Bonkovsky, H. L. (2007). Reciprocal effects of micro-RNA-122 on expression of heme oxygenase-1 and hepatitis C virus genes in human hepatocytes. *Gastroenterology,* 133 (4), 1166-1174.

Sharpe, M. and Mount, N. (2015). Genetically modified T cells in cancer therapy: opportunities and challenges. *Dis Model Mech,* 8 (4), 337-350.

Sivadasan, P., Gupta, M. K., Sathe, G. J., Balakrishnan, L., Palit, P., Gowda, H., Suresh, A., Kuriakose, M. A. and Sirdeshmukh, R. (2015). Human salivary proteome - a resource of potential biomarkers for oral cancer. *J Proteomics,* 127 (Pt A), 89-95.

Sohn, W., Kim, J., Kang, S. H., Yang, S. R., Cho, J. Y., Cho, H. C., Shim, S. G. and Paik, Y. H. (2015). Serum exosomal microRNAs as novel biomarkers for hepatocellular carcinoma. *Exp Mol Med,* 47, e184.

Soifer, H. S., Rossi, J. J. and Saetrom, P. (2007). MicroRNAs in disease and potential therapeutic applications. *Mol Ther,* 15 (12), 2070-2079.

Sokolova, V., Ludwig, A. K., Hornung, S., Rotan, O., Horn, P. A., Epple, M. and Giebel, B. (2011). Characterisation of exosomes derived from human cells by nanoparticle

tracking analysis and scanning electron microscopy. *Colloids Surf B Biointerfaces,* 87 (1), 146-150.

Sonoda, H., Yokota-Ikeda, N., Oshikawa, S., Kanno, Y., Yoshinaga, K., Uchida, K., Ueda, Y., Kimiya, K., Uezono, S., Ueda, A., Ito, K. and Ikeda, M. (2009). Decreased abundance of urinary exosomal aquaporin-1 in renal ischemia-reperfusion injury. *Am J Physiol Renal Physiol,* 297 (4), F1006-1016.

Soucy-Faulkner, A., Mukawera, E., Fink, K., Martel, A., Jouan, L., Nzengue, Y., Lamarre, D., Vande Velde, C. and Grandvaux, N. (2010). Requirement of NOX2 and reactive oxygen species for efficient RIG-I-mediated antiviral response through regulation of MAVS expression. *PLoS Pathog,* 6 (6), e1000930.

Soutschek, J., Akinc, A., Bramlage, B., Charisse, K., Constien, R., Donoghue, M., Elbashir, S., Geick, A., Hadwiger, P., Harborth, J., John, M., Kesavan, V., Lavine, G., Pandey, R. K., Racie, T., Rajeev, K. G., Rohl, I., Toudjarska, I., Wang, G., Wuschko, S., Bumcrot, D., Koteliansky, V., Limmer, S., Manoharan, M. and Vornlocher, H. P. (2004). Therapeutic silencing of an endogenous gene by systemic administration of modified siRNAs. *Nature,* 432 (7014), 173-178.

Street, J. M., Barran, P. E., Mackay, C. L., Weidt, S., Balmforth, C., Walsh, T. S., Chalmers, R. T., Webb, D. J. and Dear, J. W. (2012). Identification and proteomic profiling of exosomes in human cerebrospinal fluid. *J Transl Med,* 10, 5.

Sugimachi, K., Matsumura, T., Hirata, H., Uchi, R., Ueda, M., Ueo, H., Shinden, Y., Iguchi, T., Eguchi, H., Shirabe, K., Ochiya, T., Maehara, Y. and Mimori, K. (2015). Identification of a bona fide microRNA biomarker in serum exosomes that predicts hepatocellular carcinoma recurrence after liver transplantation. *Br J Cancer,* 112 (3), 532-538.

Sun, D., Zhuang, X., Xiang, X., Liu, Y., Zhang, S., Liu, C., Barnes, S., Grizzle, W., Miller, D. and Zhang, H. G. (2010). A novel nanoparticle drug delivery system: the anti-inflammatory activity of curcumin is enhanced when encapsulated in exosomes. *Mol Ther,* 18 (9), 1606-1614.

REFERENCES

Suzuki, T., Higgins, P. J. and Crawford, D. R. (2000). Control selection for RNA quantitation. *Biotechniques,* 29 (2), 332-337.

Szabo, G. and Bala, S. (2010). Alcoholic liver disease and the gut-liver axis. *World J Gastroenterol,* 16 (11), 1321-1329.

Szabo, G. and Bala, S. (2013). MicroRNAs in liver disease. *Nat Rev Gastroenterol Hepatol,* 10 (9), 542-552.

Szajnik, M., Czystowska, M., Szczepanski, M. J., Mandapathil, M. and Whiteside, T. L. (2010). Tumor-derived microvesicles induce, expand and up-regulate biological activities of human regulatory T cells (Treg). *PLoS One,* 5 (7), e11469.

Taille, C., El-Benna, J., Lanone, S., Dang, M. C., Ogier-Denis, E., Aubier, M. and Boczkowski, J. (2004). Induction of heme oxygenase-1 inhibits NAD(P)H oxidase activity by down-regulating cytochrome b558 expression via the reduction of heme availability. *J Biol Chem,* 279 (27), 28681-28688.

Takakura, Y., Nishikawa, M., Yamashita, F. and Hashida, M. (2001). Development of gene drug delivery systems based on pharmacokinetic studies. *Eur J Pharm Sci,* 13 (1), 71-76.

Takata, K., Matsuzaki, T., Tajika, Y., Ablimit, A. and Hasegawa, T. (2008). Localization and trafficking of aquaporin 2 in the kidney. *Histochem Cell Biol,* 130 (2), 197-209.

Tanaka, K., Miyata, H., Sugimura, K., Fukuda, S., Kanemura, T., Yamashita, K., Miyazaki, Y., Takahashi, T., Kurokawa, Y., Yamasaki, M., Wada, H., Nakajima, K., Takiguchi, S., Mori, M. and Doki, Y. (2015). miR-27 is associated with chemoresistance in esophageal cancer through transformation of normal fibroblasts to cancer-associated fibroblasts. *Carcinogenesis,* 36 (8), 894-903.

Taylor, D. D. and Gercel-Taylor, C. (2008). MicroRNA signatures of tumor-derived exosomes as diagnostic biomarkers of ovarian cancer. *Gynecol Oncol,* 110 (1), 13-21.

Taylor, D. D. and Shah, S. (2015). Methods of isolating extracellular vesicles impact down-stream analyses of their cargoes. *Methods,* 87, 3-10.

REFERENCES

Thery, C., Amigorena, S., Raposo, G. and Clayton, A. (2006). Isolation and characterization of exosomes from cell culture supernatants and biological fluids. *Curr Protoc Cell Biol,* Chapter 3, Unit 3 22.

Tiberio, P., Callari, M., Angeloni, V., Daidone, M. G. and Appierto, V. (2015). Challenges in using circulating miRNAs as cancer biomarkers. *Biomed Res Int,* 2015, 731479.

Tickner, J. A., Urquhart, A. J., Stephenson, S. A., Richard, D. J. and O'byrne, K. J. (2014). Functions and therapeutic roles of exosomes in cancer. *Front Oncol,* 4, 127.

Timpe, J. M., Stamataki, Z., Jennings, A., Hu, K., Farquhar, M. J., Harris, H. J., Schwarz, A., Desombere, I., Roels, G. L., Balfe, P. and Mckeating, J. A. (2008). Hepatitis C virus cell-cell transmission in hepatoma cells in the presence of neutralizing antibodies. *Hepatology,* 47 (1), 17-24.

Tomiyama, T., Yang, G. X., Zhao, M., Zhang, W., Tanaka, H., Wang, J., Leung, P. S., Okazaki, K., He, X. S., Lu, Q., Coppel, R. L., Bowlus, C. L. and Gershwin, M. E. (2015). The modulation of co-stimulatory molecules by circulating exosomes in primary biliary cirrhosis. *Cell Mol Immunol*.

Tscherne, D. M., Jones, C. T., Evans, M. J., Lindenbach, B. D., Mckeating, J. A. and Rice, C. M. (2006). Time- and temperature-dependent activation of hepatitis C virus for low-pH-triggered entry. *J Virol,* 80 (4), 1734-1741.

Turchinovich, A., Weiz, L., Langheinz, A. and Burwinkel, B. (2011). Characterization of extracellular circulating microRNA. *Nucleic Acids Res,* 39 (16), 7223-7233.

Turturici, G., Tinnirello, R., Sconzo, G. and Geraci, F. (2014). Extracellular membrane vesicles as a mechanism of cell-to-cell communication: advantages and disadvantages. *Am J Physiol Cell Physiol,* 306 (7), C621-633.

Urbanelli, L., Magini, A., Buratta, S., Brozzi, A., Sagini, K., Polchi, A., Tancini, B. and Emiliani, C. (2013). Signaling pathways in exosomes biogenesis, secretion and fate. *Genes (Basel),* 4 (2), 152-170.

REFERENCES

Valadi, H., Ekstrom, K., Bossios, A., Sjostrand, M., Lee, J. J. and Lotvall, J. O. (2007). Exosome-mediated transfer of mRNAs and microRNAs is a novel mechanism of genetic exchange between cells. *Nat Cell Biol,* 9 (6), 654-659.

Van Der Pol, E., Boing, A. N., Harrison, P., Sturk, A. and Nieuwland, R. (2012). Classification, functions, and clinical relevance of extracellular vesicles. *Pharmacol Rev,* 64 (3), 676-705.

Van Niel, G., Mallegol, J., Bevilacqua, C., Candalh, C., Brugiere, S., Tomaskovic-Crook, E., Heath, J. K., Cerf-Bensussan, N. and Heyman, M. (2003). Intestinal epithelial exosomes carry MHC class II/peptides able to inform the immune system in mice. *Gut,* 52 (12), 1690-1697.

Van Niel, G., Raposo, G., Candalh, C., Boussac, M., Hershberg, R., Cerf-Bensussan, N. and Heyman, M. (2001). Intestinal epithelial cells secrete exosome-like vesicles. *Gastroenterology,* 121 (2), 337-349.

Vanlandingham, P. A. and Ceresa, B. P. (2009). Rab7 regulates late endocytic trafficking downstream of multivesicular body biogenesis and cargo sequestration. *J Biol Chem,* 284 (18), 12110-12124.

Verma, M., Lam, T. K., Hebert, E. and Divi, R. L. (2015). Extracellular vesicles: potential applications in cancer diagnosis, prognosis, and epidemiology. *BMC Clin Pathol,* 15, 6.

Vinaixa, C., Rubin, A., Aguilera, V. and Berenguer, M. (2013). Recurrence of hepatitis C after liver transplantation. *Ann Gastroenterol,* 26 (4), 304-313.

Vingtdeux, V., Hamdane, M., Loyens, A., Gele, P., Drobeck, H., Begard, S., Galas, M. C., Delacourte, A., Beauvillain, J. C., Buee, L. and Sergeant, N. (2007). Alkalizing drugs induce accumulation of amyloid precursor protein by-products in luminal vesicles of multivesicular bodies. *J Biol Chem,* 282 (25), 18197-18205.

Vojtech, L., Woo, S., Hughes, S., Levy, C., Ballweber, L., Sauteraud, R. P., Strobl, J., Westerberg, K., Gottardo, R., Tewari, M. and Hladik, F. (2014). Exosomes in human semen carry a distinctive repertoire of small non-coding RNAs with potential regulatory functions. *Nucleic Acids Res,* 42 (11), 7290-7304.

REFERENCES

Wahlgren, J., De, L. K. T., Brisslert, M., Vaziri Sani, F., Telemo, E., Sunnerhagen, P. and Valadi, H. (2012). Plasma exosomes can deliver exogenous short interfering RNA to monocytes and lymphocytes. *Nucleic Acids Res,* 40 (17), e130.

Wang, H., Hou, L., Li, A., Duan, Y., Gao, H. and Song, X. (2014). Expression of serum exosomal microRNA-21 in human hepatocellular carcinoma. *Biomed Res Int,* 2014, 864894.

Wang, X., Ding, X., Nan, L., Wang, Y., Wang, J., Yan, Z., Zhang, W., Sun, J., Zhu, W., Ni, B., Dong, S. and Yu, L. (2015). Investigation of the roles of exosomes in colorectal cancer liver metastasis. *Oncol Rep,* 33 (5), 2445-2453.

Wang, Z., Kuhr, C. S., Allen, J. M., Blankinship, M., Gregorevic, P., Chamberlain, J. S., Tapscott, S. J. and Storb, R. (2007). Sustained AAV-mediated dystrophin expression in a canine model of Duchenne muscular dystrophy with a brief course of immunosuppression. *Mol Ther,* 15 (6), 1160-1166.

Webber, J., Steadman, R., Mason, M. D., Tabi, Z. and Clayton, A. (2010). Cancer exosomes trigger fibroblast to myofibroblast differentiation. *Cancer Res,* 70 (23), 9621-9630.

Wei, J. X., Lv, L. H., Wan, Y. L., Cao, Y., Li, G. L., Lin, H. M., Zhou, R., Shang, C. Z., Cao, J., He, H., Han, Q. F., Liu, P. Q., Zhou, G. and Min, J. (2015). Vps4A functions as a tumor suppressor by regulating the secretion and uptake of exosomal microRNAs in human hepatoma cells. *Hepatology,* 61 (4), 1284-1294.

Welker, M. W., Reichert, D., Susser, S., Sarrazin, C., Martinez, Y., Herrmann, E., Zeuzem, S., Piiper, A. and Kronenberger, B. (2012). Soluble serum CD81 is elevated in patients with chronic hepatitis C and correlates with alanine aminotransferase serum activity. *PLoS One,* 7 (2), e30796.

Wenzel, P., Rossmann, H., Muller, C., Kossmann, S., Oelze, M., Schulz, A., Arnold, N., Simsek, C., Lagrange, J., Klemz, R., Schonfelder, T., Brandt, M., Karbach, S. H., Knorr, M., Finger, S., Neukirch, C., Hauser, F., Beutel, M. E., Kroller-Schon, S., Schulz, E., Schnabel, R. B., Lackner, K., Wild, P. S., Zeller, T., Daiber, A., Blankenberg, S. and

REFERENCES

Munzel, T. (2015). Heme oxygenase-1 suppresses a pro-inflammatory phenotype in monocytes and determines endothelial function and arterial hypertension in mice and humans. *Eur Heart J,* 36 (48), 3437-3446.

Wiley, R. D. and Gummuluru, S. (2006). Immature dendritic cell-derived exosomes can mediate HIV-1 trans infection. *Proc Natl Acad Sci U S A,* 103 (3), 738-743.

Willis, J. C. and Lord, G. M. (2015). Immune biomarkers: the promises and pitfalls of personalized medicine. *Nat Rev Immunol,* 15 (5), 323-329.

Wilson, J. A., Zhang, C., Huys, A. and Richardson, C. D. (2011). Human Ago2 is required for efficient microRNA 122 regulation of hepatitis C virus RNA accumulation and translation. *J Virol,* 85 (5), 2342-2350.

Witek, R. P., Yang, L., Liu, R., Jung, Y., Omenetti, A., Syn, W. K., Choi, S. S., Cheong, Y., Fearing, C. M., Agboola, K. M., Chen, W. and Diehl, A. M. (2009). Liver cell-derived microparticles activate hedgehog signaling and alter gene expression in hepatic endothelial cells. *Gastroenterology,* 136 (1), 320-330 e322.

Witwer, K. W., Buzas, E. I., Bemis, L. T., Bora, A., Lasser, C., Lotvall, J., Nolte-'T Hoen, E. N., Piper, M. G., Sivaraman, S., Skog, J., Thery, C., Wauben, M. H. and Hochberg, F. (2013). Standardization of sample collection, isolation and analysis methods in extracellular vesicle research. *J Extracell Vesicles,* 2.

Xiao, X., Li, J. and Samulski, R. J. (1996). Efficient long-term gene transfer into muscle tissue of immunocompetent mice by adeno-associated virus vector. *J Virol,* 70 (11), 8098-8108.

Xie, Z., Yin, X., Gong, B., Nie, W., Wu, B., Zhang, X., Huang, J., Zhang, P., Zhou, Z. and Li, Z. (2015). Salivary microRNAs show potential as a noninvasive biomarker for detecting resectable pancreatic cancer. *Cancer Prev Res (Phila),* 8 (2), 165-173.

Yachie, A., Toma, T., Mizuno, K., Okamoto, H., Shimura, S., Ohta, K., Kasahara, Y. and Koizumi, S. (2003). Heme oxygenase-1 production by peripheral blood monocytes during acute inflammatory illnesses of children. *Exp Biol Med (Maywood),* 228 (5), 550-556.

REFERENCES

Yanez-Mo, M., Siljander, P. R., Andreu, Z., Zavec, A. B., Borras, F. E., Buzas, E. I., Buzas, K., Casal, E., Cappello, F., Carvalho, J., Colas, E., Cordeiro-Da Silva, A., Fais, S., Falcon-Perez, J. M., Ghobrial, I. M., Giebel, B., Gimona, M., Graner, M., Gursel, I., Gursel, M., Heegaard, N. H., Hendrix, A., Kierulf, P., Kokubun, K., Kosanovic, M., Kralj-Iglic, V., Kramer-Albers, E. M., Laitinen, S., Lasser, C., Lener, T., Ligeti, E., Line, A., Lipps, G., Llorente, A., Lotvall, J., Mancek-Keber, M., Marcilla, A., Mittelbrunn, M., Nazarenko, I., Nolte-'T Hoen, E. N., Nyman, T. A., O'driscoll, L., Olivan, M., Oliveira, C., Pallinger, E., Del Portillo, H. A., Reventos, J., Rigau, M., Rohde, E., Sammar, M., Sanchez-Madrid, F., Santarem, N., Schallmoser, K., Ostenfeld, M. S., Stoorvogel, W., Stukelj, R., Van Der Grein, S. G., Vasconcelos, M. H., Wauben, M. H. and De Wever, O. (2015). Biological properties of extracellular vesicles and their physiological functions. *J Extracell Vesicles,* 4, 27066.

Yang, P., Wang, G., Huo, H., Li, Q., Zhao, Y. and Liu, Y. (2015). SDF-1/CXCR4 signaling up-regulates survivin to regulate human sacral chondrosarcoma cell cycle and epithelial-mesenchymal transition via ERK and PI3K/AKT pathway. *Med Oncol,* 32 (1), 377.

Yuana, Y., Sturk, A. and Nieuwland, R. (2013). Extracellular vesicles in physiological and pathological conditions. *Blood Rev,* 27 (1), 31-39.

Zhang, J. S., Liu, F. and Huang, L. (2005). Implications of pharmacokinetic behavior of lipoplex for its inflammatory toxicity. *Adv Drug Deliv Rev,* 57 (5), 689-698.

Zhang, Y., Liu, D., Chen, X., Li, J., Li, L., Bian, Z., Sun, F., Lu, J., Yin, Y., Cai, X., Sun, Q., Wang, K., Ba, Y., Wang, Q., Wang, D., Yang, J., Liu, P., Xu, T., Yan, Q., Zhang, J., Zen, K. and Zhang, C. Y. (2010). Secreted monocytic miR-150 enhances targeted endothelial cell migration. *Mol Cell,* 39 (1), 133-144.

Zhang, Y., Shi, L., Mei, H., Zhang, J., Zhu, Y., Han, X. and Zhu, D. (2015). Inflamed macrophage microvesicles induce insulin resistance in human adipocytes. *Nutr Metab (Lond),* 12, 21.

Zhuang, X., Xiang, X., Grizzle, W., Sun, D., Zhang, S., Axtell, R. C., Ju, S., Mu, J., Zhang, L., Steinman, L., Miller, D. and Zhang, H. G. (2011). Treatment of brain inflammatory

diseases by delivering exosome encapsulated anti-inflammatory drugs from the nasal region to the brain. *Mol Ther,* 19 (10), 1769-1779.

Zimmermann, H. W., Trautwein, C. and Tacke, F. (2012). Functional role of monocytes and macrophages for the inflammatory response in acute liver injury. *Front Physiol,* 3, 56.

Zocco, D., Ferruzzi, P., Cappello, F., Kuo, W. P. and Fais, S. (2014). Extracellular vesicles as shuttles of tumor biomarkers and anti-tumor drugs. *Front Oncol,* 4, 267.